

1601
1)

PROJECT ADMINISTRATION DATA SHEET

ORIGINAL REVISION NO. _____

Project No. G-35-633 GTRI/GIT DATE 6 / 27 / 84

Project Director: Dr. Justus School XXX Geo. Sci.

Sponsor: U. S. Department of Energy
Golden, Colorado

Type Agreement: Grant No. DE-FG02-84CH10200

Award Period: From 6/15/84 To 12/14/85 (Performance) 7/14/85 (Reports)

Sponsor Amount: This Change 6-15-87 Total to Date

Estimated: \$ 94,139 \$ 94,139

Funded: \$ 94,139 \$ 94,139

Cost Sharing Amount: \$ _____ Cost Sharing No: _____

Title: Satellite Techniques of Solar Resource Assessment for Focusing and
Non-focusing Solar Collector Systems

ADMINISTRATIVE DATA

OCA Contact Brian J. Lindberg x-4820

1) Sponsor Technical Contact:

~~Stephen Sargent See Rev. #1~~
~~U. S. Department of Energy~~
~~SERI Site Office~~
~~1617 Cole Boulevard~~
~~Golden, Colorado 80401~~
~~(303) 231-1366~~

2) Sponsor Admin/Contractual Matters:

Charles M. Skinner, Contracting Officer
U. S. Department of Energy
SERI Site Office
1617 Cole Boulevard
Golden, Colorado 80401
(303) 231-1495

Defense Priority Rating: N/A Military Security Classification: N/A

(or) Company/Industrial Proprietary: N/A

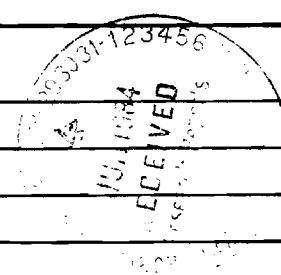
RESTRICTIONS

See Attached N/A Supplemental Information Sheet for Additional Requirements.

Travel: Foreign travel must have prior approval - Contact OCA in each case. Domestic travel requires sponsor approval where total will exceed greater of \$500 or 125% of approved proposal budget category.

Equipment: Title vests with None proposed or anticipated

COMMENTS:



COPIES TO:

Sponsor I.D. #02,141.009,84,001.

Project Director
Research Administrative Network
Research Property Management
Accounting

Procurement/EES Supply Services
Research Security Services
Reports Coordinator (OCA)
Research Communications (2)

GTRI
Library
Project File
Other I. Newton

SPONSORED PROJECT TERMINATION/CLOSEOUT SHEET

2-
SR-781

Date November 4, 1987

Project No. G-35-633

School/~~dept~~ Geophysical Sciences

Includes Subproject No.(s) N/A

Project Director(s) Dr. Jerry Justus GTRC / ~~XXX~~

Sponsor U. S. Department of Energy / Golden, Colorado

Title Satellite Techniques of Solar Resource Assessment for Focusing and Non-Focusing
Solar Collector Systems

Effective Completion Date: 6/15/87 (Performance) 9/15/87 (Reports)

Grant/Contract Closeout Actions Remaining:

- None
- Final Invoice or Final Fiscal Report - already submitted
- Closing Documents
- Final Report of Inventions - already submitted
- Govt. Property Inventory & Related Certificate
- Classified Material Certificate
- Other _____

Continues Project No. _____ Continued by Project No. _____

COPIES TO:

Project Director
 Research Administrative Network
 Research Property Management
 Accounting
 Procurement/GTRI Supply Services
 Research Security Services
 Reports Coordinator (OCA) ✓
 Legal Services

Library
 GTRC
 Research Communications (2)
 Project File
 Other Russ Embry
Angela DuBose
Duane Hutchison

**Satellite Techniques of Solar
Resource Assessment for
Focusing and Non-Focusing
Solar Collector Systems**

C. B. Justus

**School of Geophysical Sciences
Georgia Institute of Technology
Atlanta, GA 30332**

Technical Progress Report

March, 1985

**Prepared by the
GEORGIA INSTITUTE OF TECHNOLOGY
for the
U. S. DEPARTMENT OF ENERGY
SOLERAS PROGRAM**

Grant Number DE-FB02-B4CH10200

Mr. Jim Williamson, Midwest Research Institute, Technical Monitor

Georgia Tech Project G-35-633

PROGRESS REPORT

Following is a statement of the accomplishments and significant results obtained on the project to date:

1. A Solar Energy Resource Report from Current Satellite Insolation Data

The Satellite Applications Laboratory of the National Oceanic and Atmospheric Administration (NOAA), under the AgRISTARS program, currently uses GOES satellite data to produce daily estimates of global horizontal insolation for the entire continental United States, Mexico, and parts of South America. These insolation estimates, available on computer tape from NOAA at a spatial resolution of $1^\circ \times 1^\circ$ in latitude-longitude, have been summarized into monthly mean values, standard deviations about the monthly mean, and root-mean-square (rms) deviations across 1° of latitude or longitude. A report outlining the NOAA insolation methodology and giving in atlas form the monthly statistical results has been prepared. An abstract of this report, "Atlas of Satellite-Measured Insolation in the United States, Mexico, and South America", is attached. Figure 1 shows a comparison of the monthly mean daily total values derived from the NOAA satellite estimates with monthly means of surface-measured insolation at the Georgia Tech insolation monitoring site. The rms difference between the satellite-estimated and ground-observed monthly mean daily total values shown in Figure 1 is 0.77 MJ/m^2 , or 5.2% of the mean value of 14.8 MJ/m^2 . Figure 2 gives a sample of the maps of monthly mean data which are shown in the atlas report. This figure shows the annual mean daily total global horizontal insolation for the continental United States for the year 1983.

2. Development of a Satellite Technique for Direct Beam Insolation Estimates

The current insolation estimates being done by NOAA are only for global horizontal irradiance. Although this is adequate to meet the needs of their agriculturally oriented program, solar energy researchers and systems designers would find estimates for direct normal (for focusing collectors) and global irradiance on tilted surfaces (non-focusing collectors) of considerable additional benefit. A 16-month set of surface-measured data has been used together with GOES satellite brightness information from NOAA, to produce a regression model for hourly total global horizontal irradiance, and for hourly total direct normal irradiance. These two estimates can be combined, using a relation by Klutcher (Solar Energy, 23, 111-114, 1979), to produce an estimate of global irradiance on a tilted surface (estimates have been compared here to measurements taken on a latitude tilt). Results for observed versus satellite-estimated daily total global horizontal irradiance are shown in Figure 3, for 1982-1983 Georgia-Tech data. The rms difference between satellite estimates and observed data in this figure is 1.3 MJ/m^2 , or 8.4% of the mean value of 15.8 MJ/m^2 . This accuracy is somewhat better than from a similar comparison against the operational NOAA estimates, interpolated to the Atlanta, Georgia Tech site, which, for the same observation period, showed an rms difference between satellite estimates and observed data of 1.9 MJ/m^2 , or 12.8% of the mean value of 14.9 MJ/m^2 . The comparison with the operational data contains somewhat more days, since it required only a valid global horizontal data value for comparison, whereas the current model comparison additionally requires a valid direct normal and global tilted value. Similar comparisons between surface observations and the new satellite methods for estimating daily totals of direct normal and global latitude-tilted irradiances are shown in Figures 4 and 5. The direct normal values

cannot be estimated as accurately as the global horizontal, giving an rms difference of 3.1 MJ/m^2 , or 21.3% of the mean value of 14.4 MJ/m^2 . Because it relies in part on the direct normal estimate, the estimated global tilted values are also slightly less accurate than the global horizontal values, with the data in Figure 5 having an rms difference of 1.9 MJ/m^2 , or 11.1% of the mean value of 17.2 MJ/m^2 . This error estimate for the global tilted irradiance is, however, comparable to the estimated accuracy in the current NOAA operational estimates of global horizontal irradiance.

3. Development of a Satellite Insolation Estimation Technique for Photovoltaic Systems

In addition to the highly accurate Eppley radiometers used as surface observation data to develop the methods for satellite estimation of the global horizontal, direct normal, and global tilted, the Georgia Tech solar radiation monitoring site also includes Licor photocell radiometers, operated both on the horizontal and on a latitude tilt angle. Figure 6 shows a comparison of the spectral response curve of the Licor photocell radiometer to that for typical crystalline silicon photocell material (Bird, SERI/TR-215-1598, 1982). Georgia Tech surface measurements during 1982 and 1983 have also been used to develop a method for using the satellite data to estimate global horizontal or tilted irradiance as measured by these Licor photocell radiometers. The results of comparison of these estimates with the photocell radiometer measurements are shown in Figures 7 and 8. These comparisons indicate comparable accuracies for the photocell irradiance measurements as for the Eppley instruments, giving rms differences of 8.8% for the global horizontal and 11.0% for the global tilted values. Although the Licor radiometers are normally calibrated in terms of equivalent full solar spectrum irradiance, comparisons with spectral irradiance model results and between the curves in

Figure 6, indicate that values of photocell collector system short circuit current in amps per square meter of collector can be estimated as 0.32 times the Licor photocell radiometer reading in W/m^2 .

4. Development of a Technique for Satellite Insolation Estimation with Snow Cover on the Ground

The current NOAA operational method for satellite estimation of insolation does not automatically distinguish between high brightness values produced by clouds and by snow cover on the ground. Consequently, clear conditions with snow on the ground will be interpreted as cloudy conditions and the insolation will be significantly underestimated. A set of SOLMET station data for the last part of 1980 has been merged with the NOAA GOES satellite brightness data for use in developing a technique to handle the snow cases. These data also include the GOES infrared brightnesses, which can be used to distinguish between cold, bright clouds and (relatively) warm, snow covered ground surfaces. A total of 685 hourly observations with snow cover have been identified in the data set from 8 SOLMET sites. Of these, 98 occurred in clear conditions, 365 occurred in overcast conditions, and the remainder were under various degrees of partial cloud cover.

5. Investigation of Error Reduction if Precipitable Water is Included

Figure 9 shows a scatter plot of observed global transmittance (ratio of global to extraterrestrial horizontal) versus cosine of solar zenith angle for clear skies and low precipitable water (<1.7 cm), with x's showing observations which have less than average observed satellite brightness values, and +'s having higher than average brightness. Figure 10 shows comparable results for the clear

cases with high precipitable water (>1.7 cm). These figures illustrate the sensitivity of clear global transmittance both to precipitable water amount and to satellite brightness value (presumably an indication of aerosol turbidity in the atmosphere). Most of the improvement in accuracy (8.4% versus 12.8%, as discussed above) between the new method and the NOAA operational method for insolation estimates from satellites is due to the inclusion of precipitable water value in the new estimation algorithm.

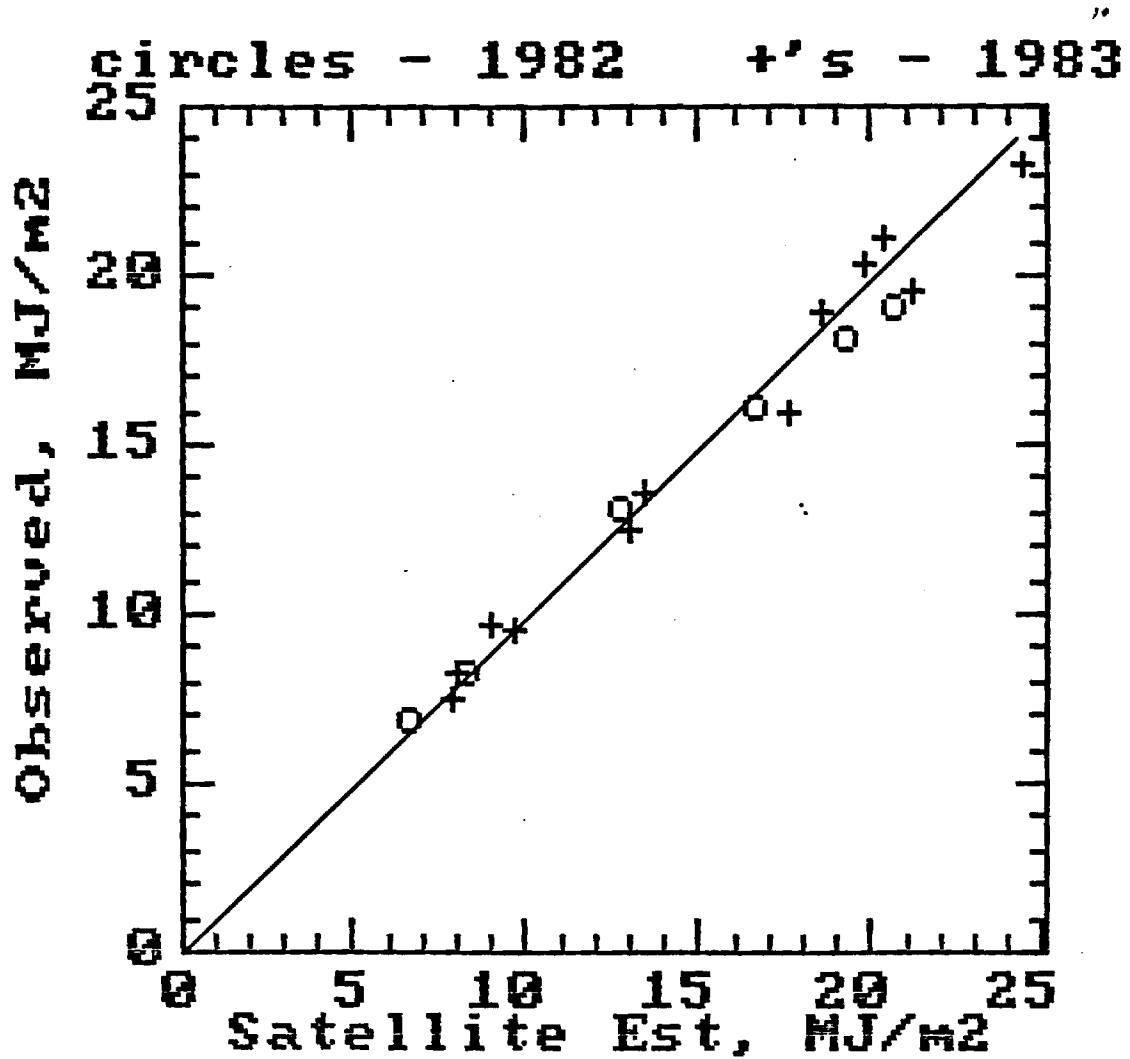


Figure 1. Observed Monthly Mean Insolation at Georgia Tech versus GOES Satellite Estimates for 1982 and 1983.

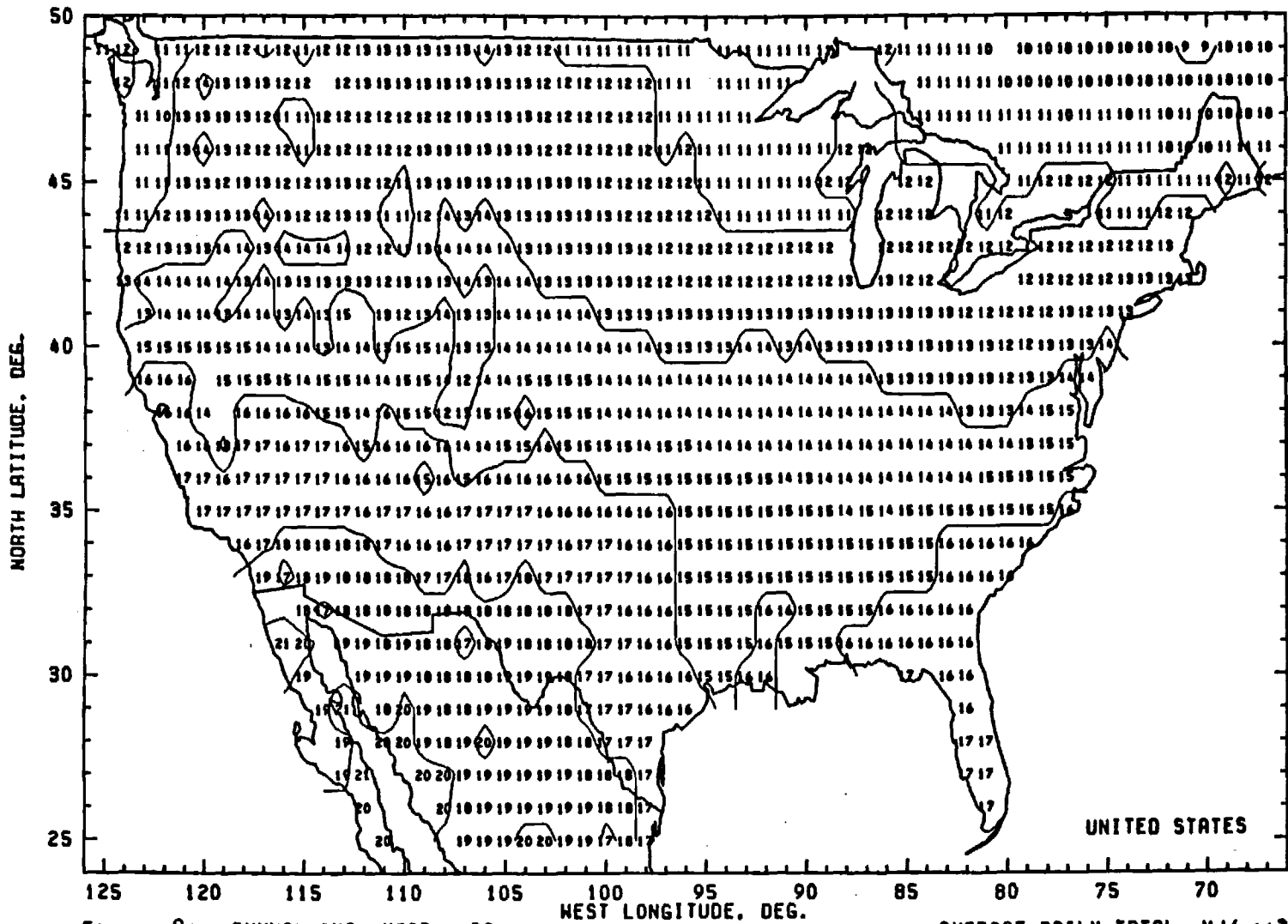


Figure 2: ANNUAL AVG. YEAR = 83

AVERAGE DAILY TOTAL, MJ/m²

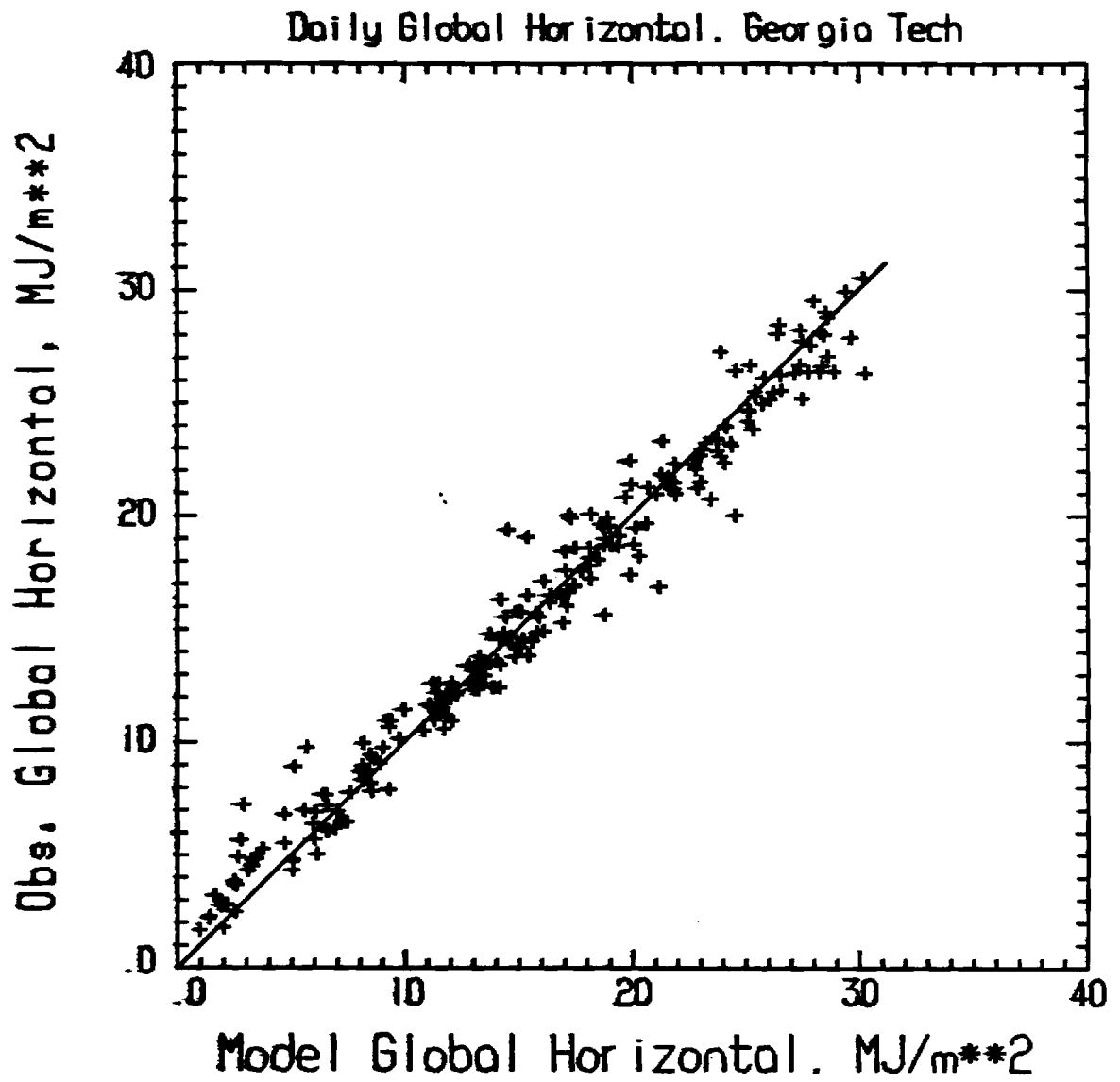


Fig. 3: Observed Daily Total Global Horizontal Irradiance Versus Satellite Estimated, Georgia Tech Site, 1982-1983.

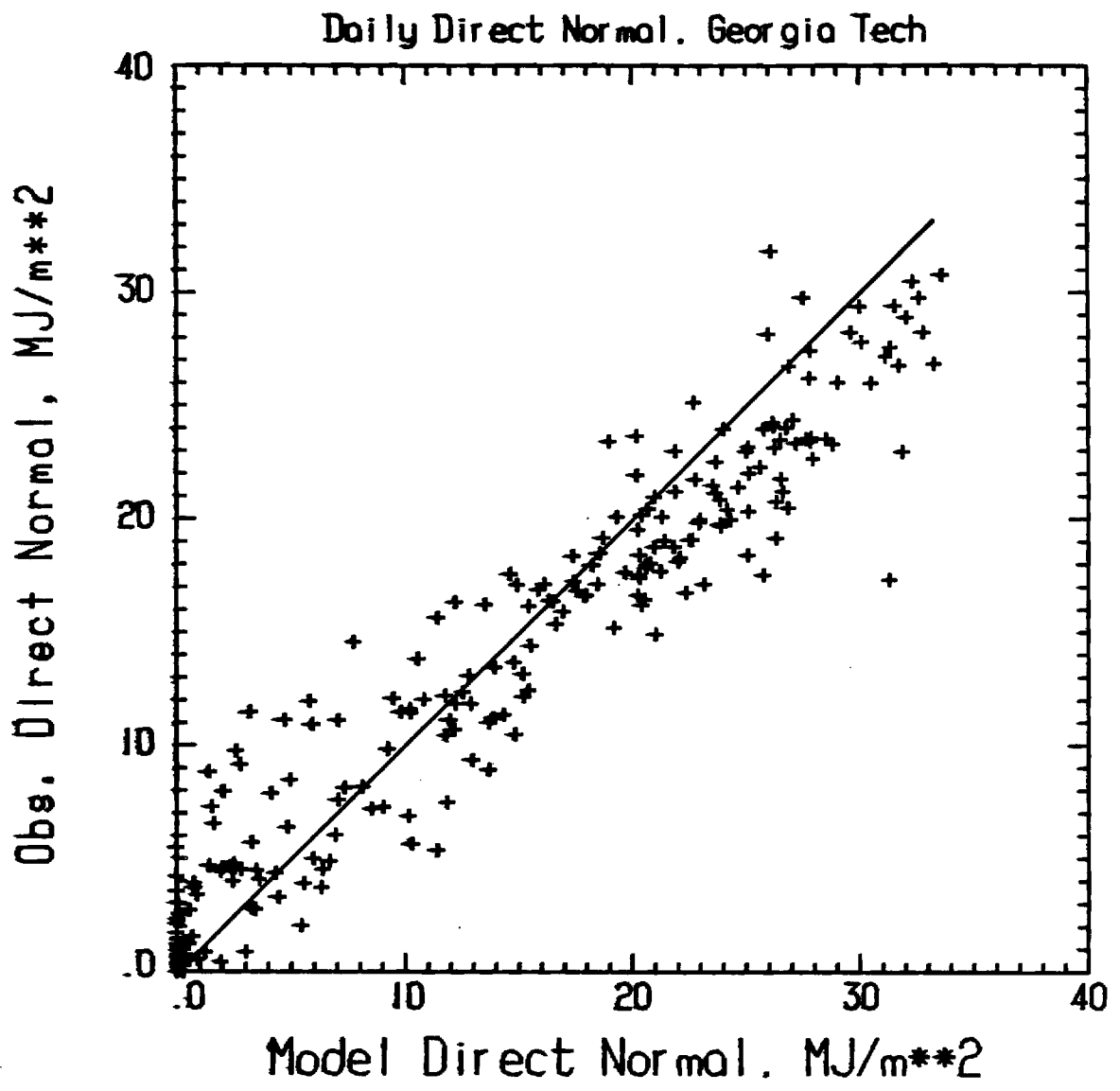


Fig. 4: As in Figure 3 for Direct Normal.

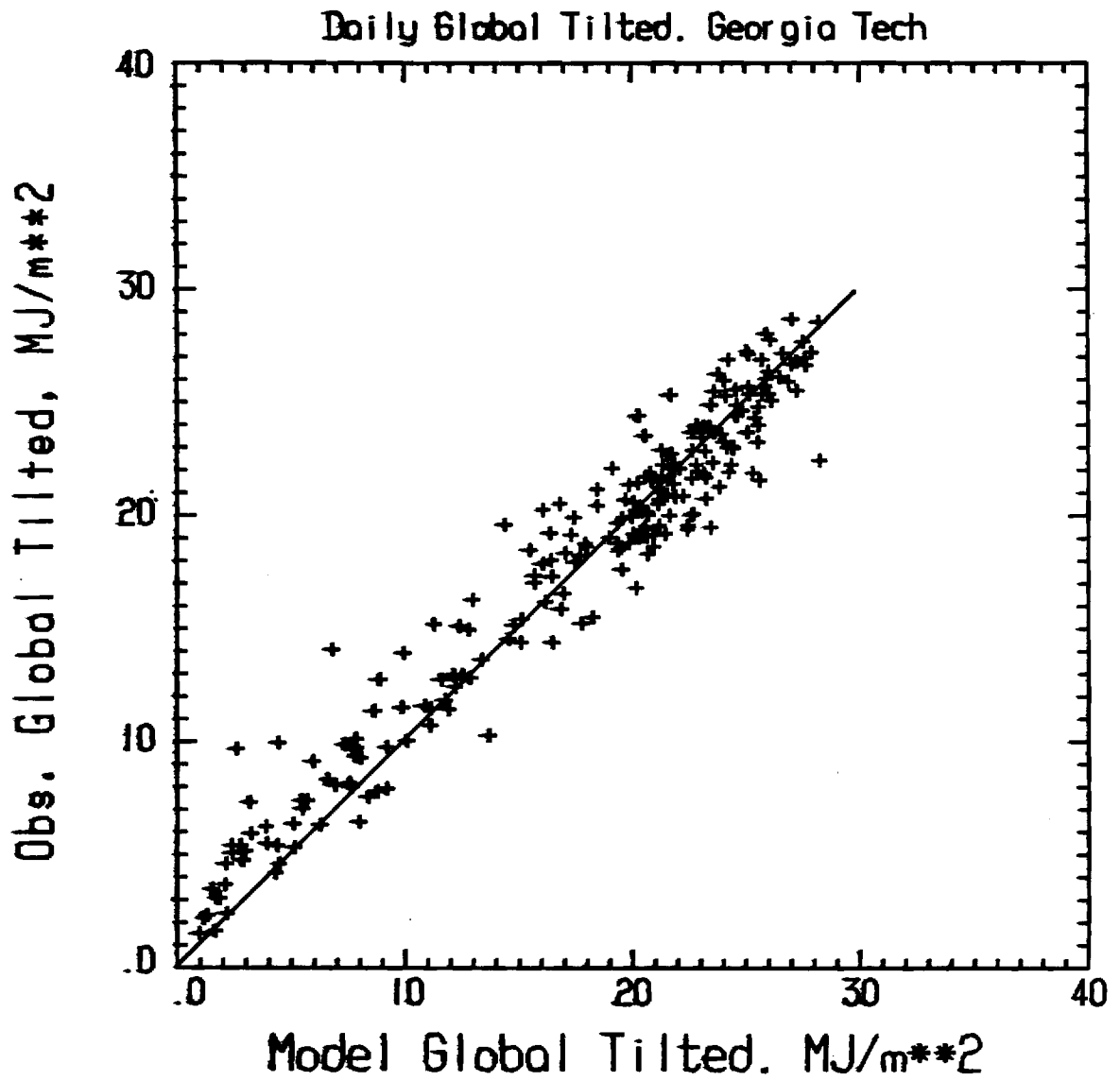


Fig. 5: As in Figure 3 for Global Irradiance on a Latitude Tilted Surface.

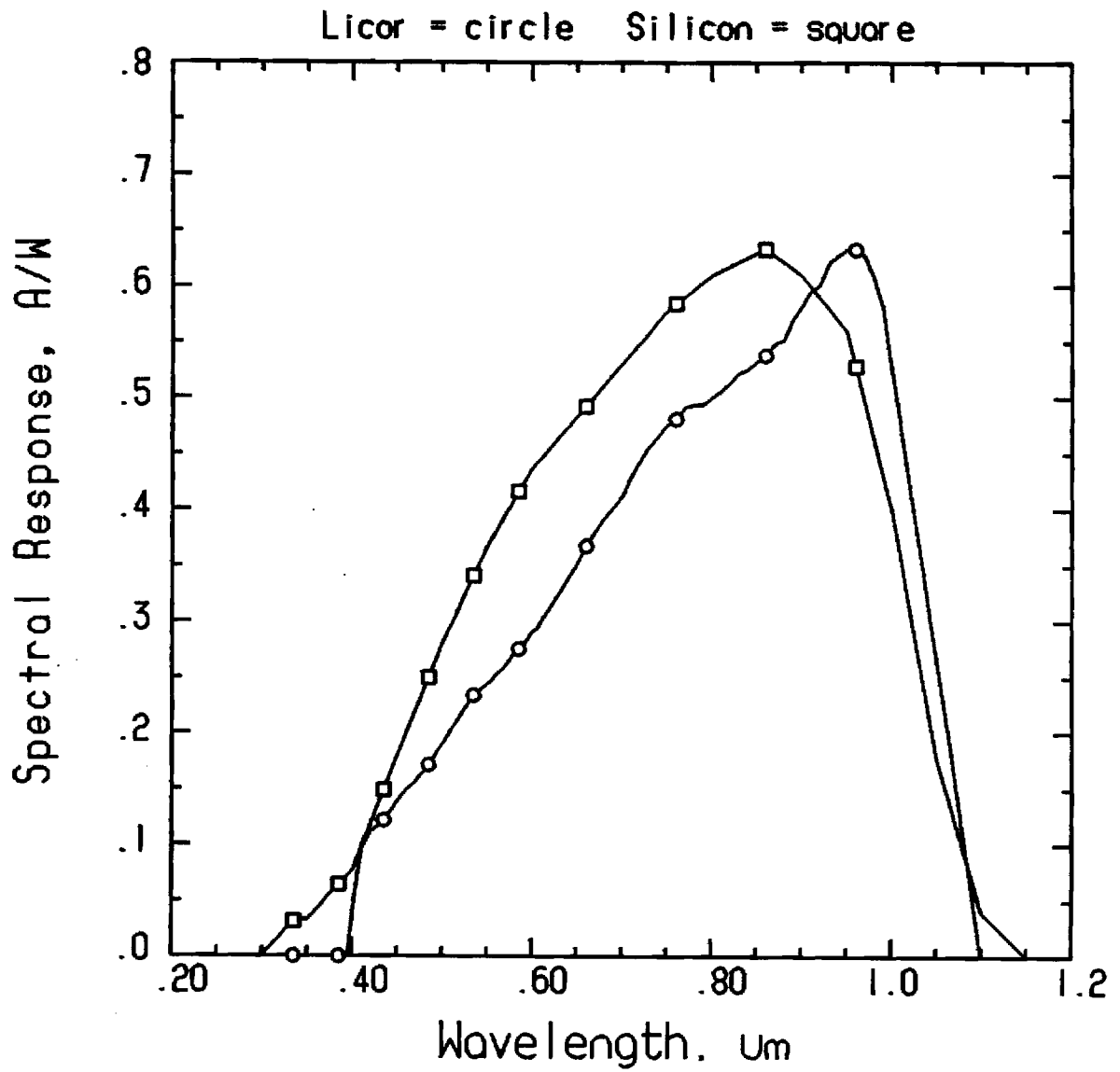


Fig. 6: Comparison of Filter Curve of Licor Photocell Radiometer (Normalized to 0.63 peak) with Spectral Response Curve (in amps/watt) for Crystalline Silicon Photocell Material (Bird, SERI/TR-215-1598, 1982).

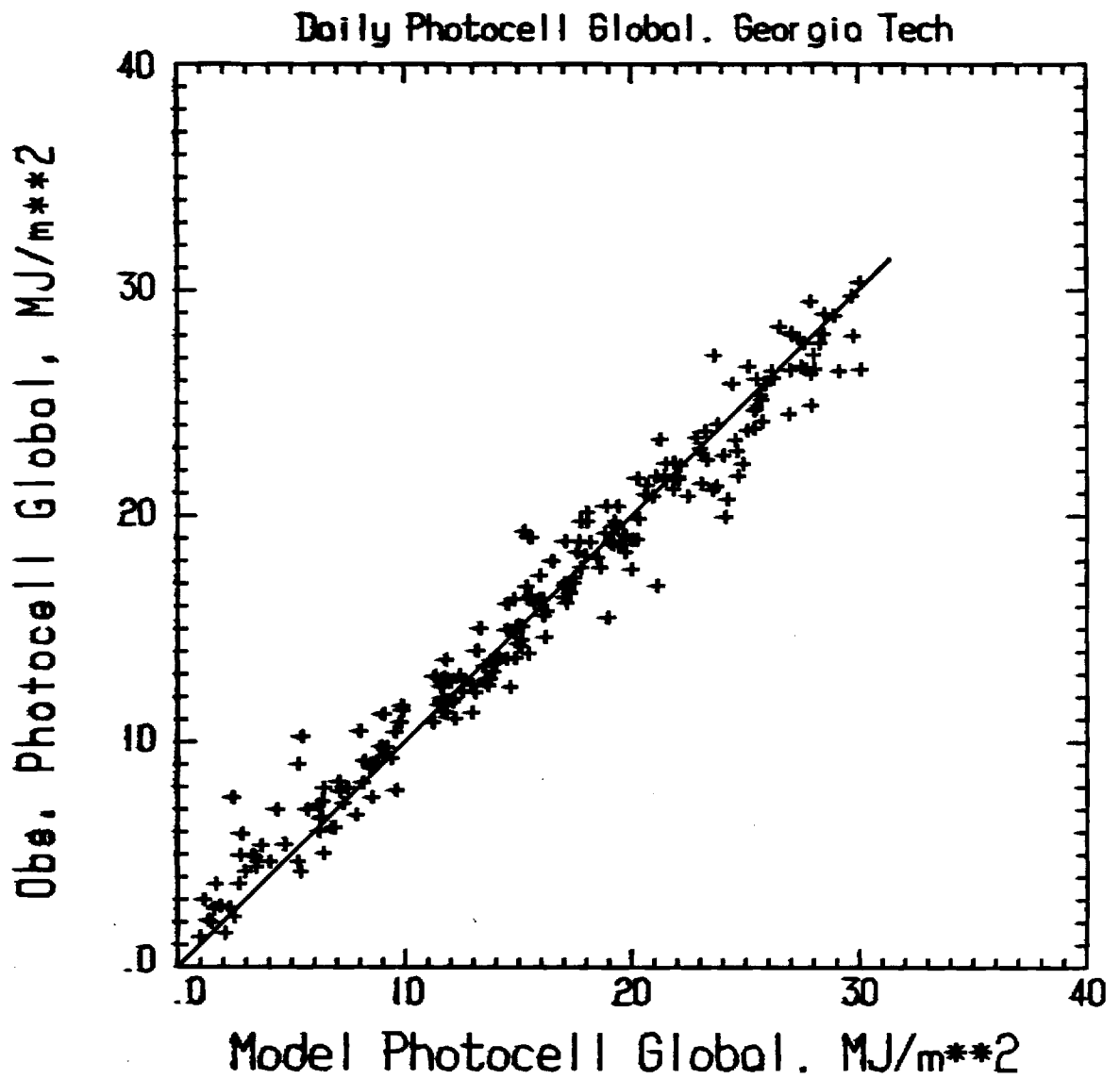


Fig. 7: Photocell Radiometer Observed Daily Total Global Horizontal Irradiance versus Satellite Estimated, Georgia Tech Site, 1982-83.

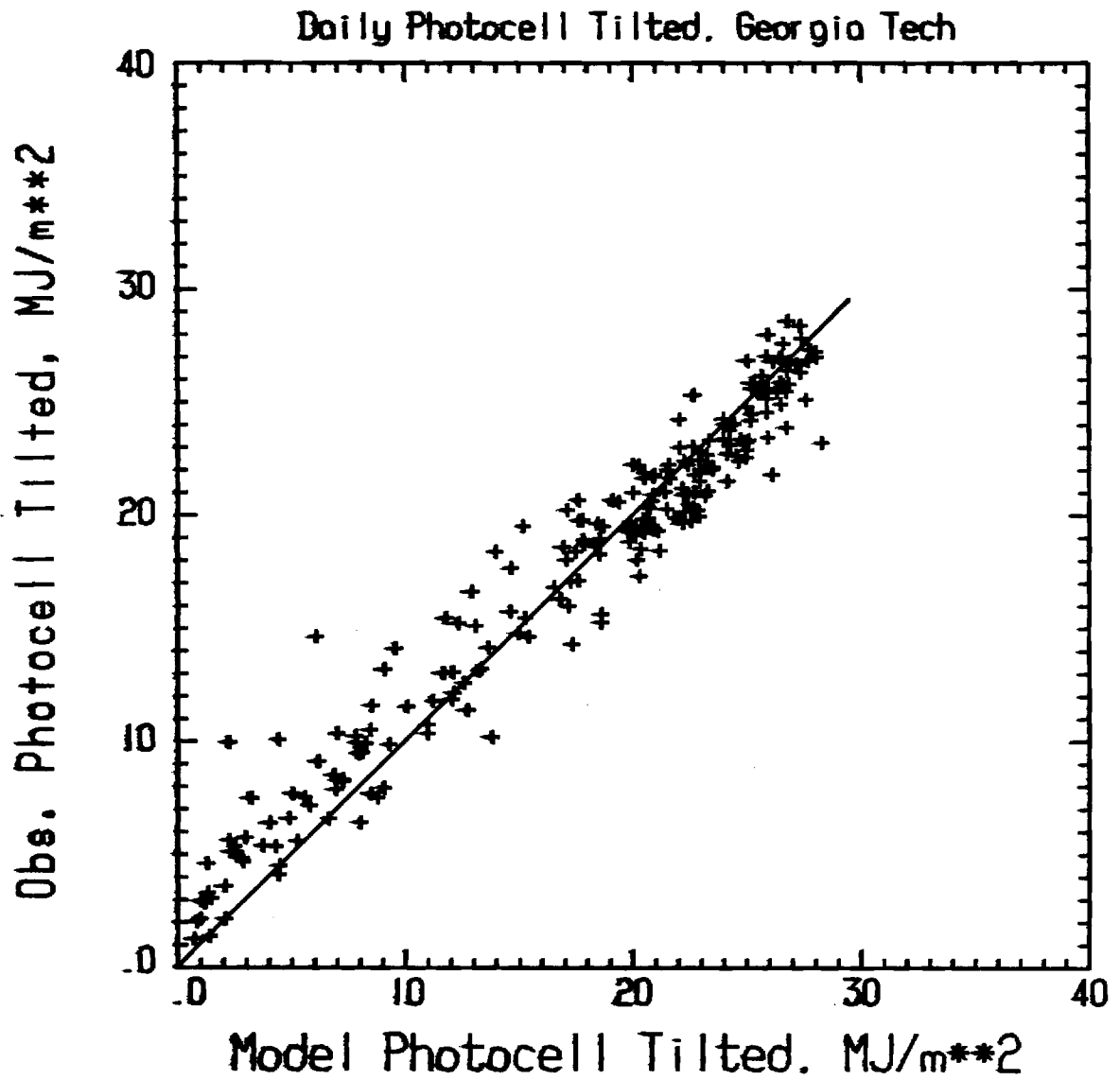


Fig. 8: As in Figure 7 for Photocell Radiometer on Latitude-Tilted Surface.

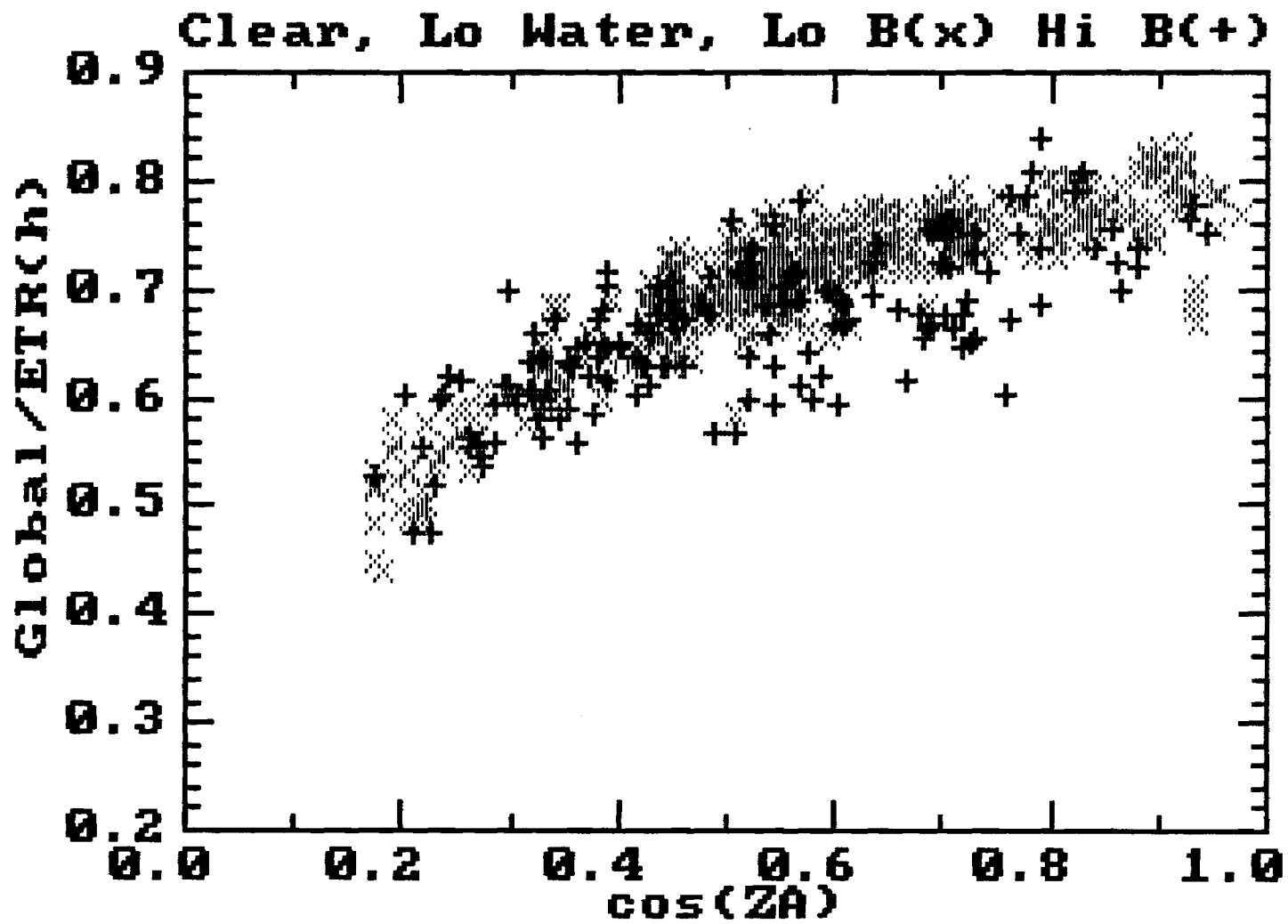


Fig. 9: Observed Ratio of Global to Extraterrestrial Horizontal under Clear Conditions and Low Precipitable water, versus cosine of solar zenith angle for low and high satellite brightness ranges.

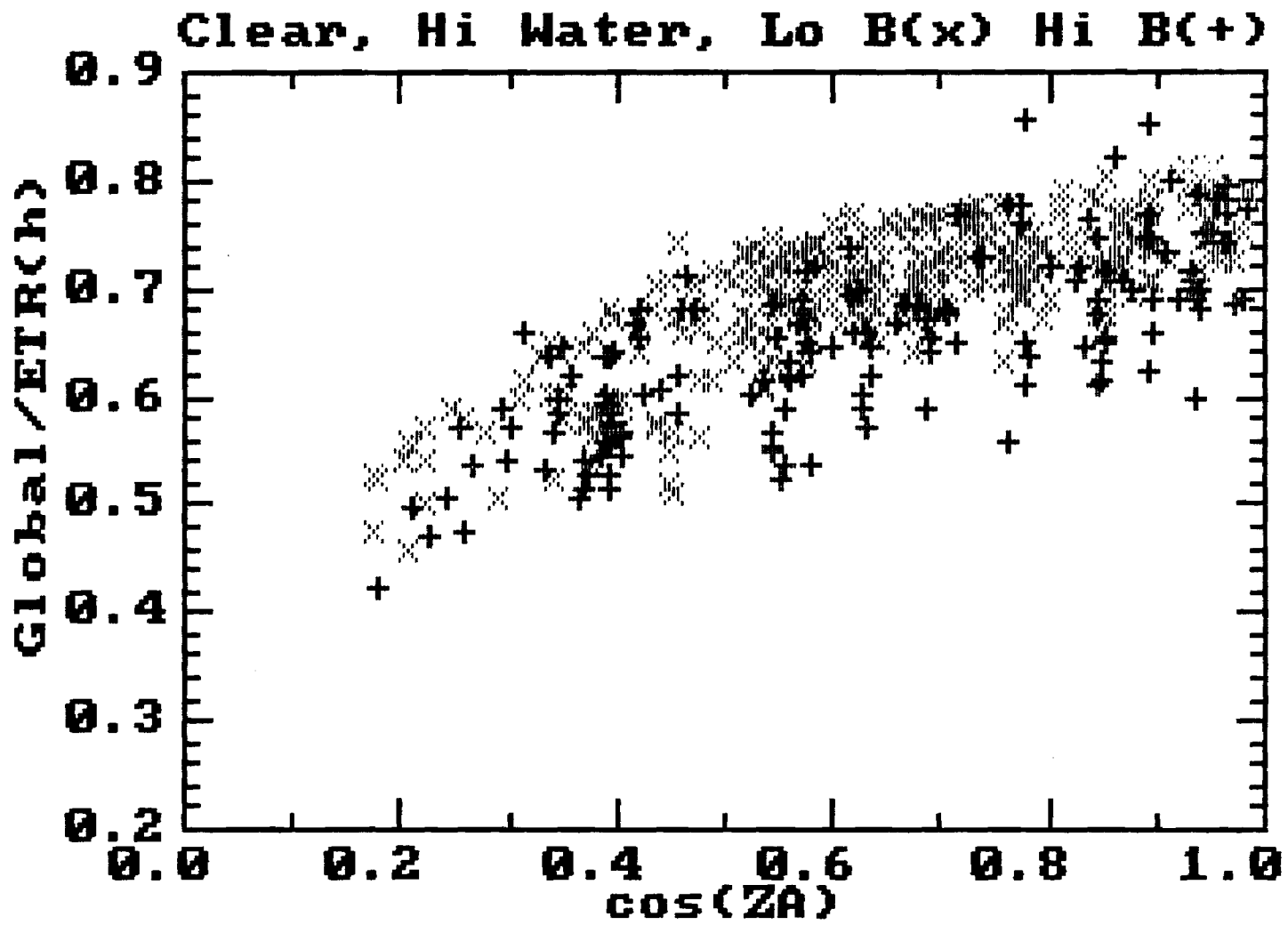


Fig. 10: As in Figure 9 for high precipitable water range.

ATLAS OF SATELLITE-MEASURED INSOLATION IN THE
UNITED STATES, MEXICO, AND SOUTH AMERICA

Abstract

A summary is given of the development, testing and applications of the satellite insolation estimation project of the National Oceanic and Atmospheric Administration (NOAA) Agriculture and Resources Inventory Surveys through Aerospace Remote Sensing (AgRISTARS) program. The NOAA/AgRISTARS procedure uses data from the Geostationary Operational Environmental Satellite (GOES) to estimate daily total insolation (on a horizontal surface) at an array of $1^{\circ} \times 1^{\circ}$ latitude-longitude locations throughout the continental United States, Mexico, and parts of South America. This methodology is compared with some other satellite techniques in terms of accuracy and applicability. Summary maps of monthly average daily total insolation for the period July, 1982 through December, 1983, as well as annual total maps for 1983, are presented for all three geographic coverage areas. As measures of temporal and spatial variability, monthly and annual data are also presented for the standard deviation of the daily insolation values about the monthly mean, and for root-mean-square values of both north-south and east-west differences over 1° latitude or longitude spacing. From the estimated error analysis the monthly mean values appear to be accurate to about 5% of the mean value, except for the western part of the United States when GOES-1 was put back into temporary service as the western GOES satellite. Compared to long-term surface-measured insolation in the United States, the satellite-derived means for the reported period are somewhat low, especially in the central and southwestern United States. Lowest standard deviation areas tend to be associated with areas where the mean insolation is high, e.g. desert regions where high values tend to persist from day to day. Some of the areas with high mean insolation also exhibit low spatial variability, with nearby areas of higher-than-average spatial variability where the insolation regime changes to one of lower mean value. An area of exceptionally large spatial variability is found in the mountainous areas of Bolivia and Argentina. Areas of somewhat higher-than-average spatial variability are also found throughout the southern and central Rocky Mountains of the United States. The rms spatial variability, which has not been reported before for such extensive geographic regions, is important in assessing the reliability of interpolations or extrapolations from sites with measured insolation to other locations where insolation values are desired.

Satellite Techniques of Solar
Resource Assessment for
Focusing and Non-Focusing
Solar Collector Systems

C. G. Justus

School of Geophysical Sciences
Georgia Institute of Technology
Atlanta, GA 30332

Technical Progress Report

March, 1986

Prepared by the
GEORGIA INSTITUTE OF TECHNOLOGY
for the
U. S. DEPARTMENT OF ENERGY
SOLERAS PROGRAM

Grant Number DE-FG02-84CH10200

Mr. Jim Williamson, Midwest Research Institute, Technical Monitor

Georgia Tech Project G-35-633

PROGRESS REPORT

Tests of Suitability of METEOSAT Data for Insolation Estimation in Saudi Arabia

Since the GOES satellites used in the first phase of this work do not provide coverage of the area of the world which includes Saudi Arabia, data from the European Space Agency (ESA) METEOSAT satellite had to be used for the studies of insolation estimation over Saudi Arabia. Since Saudi Arabia is somewhat near the edge of the usable area of coverage of METEOSAT, and since much of the area consists of bright sandy soil (which reduces the contrasting signal between clear and cloud-cover conditions), these factors must be examined. Figure 1 shows simulated results for a variety of cloud conditions (optical depths 1, 2, 16, and 64) and for a surface assumed to be sand with a surface albedo of 0.45. This figure plots the irradiance reduction from clear-sky value versus the increase in METEOSAT visible-band sensor counts from clear-sky counts. Surface and top-of-atmosphere irradiances were computed by a spectral model which treats clear layers above and below a cloud layer which is modeled by a delta-Eddington radiative transfer process (Justus and Paris, 1985; Paris, 1985). Modeled top-of-atmosphere METEOSAT visible-band radiances were converted to sensor counts by assuming the calibration of Koepke (1982). The current satellite insolation algorithms assume essentially a linear relationship between the variables plotted in Figure 1. The best-fit straight line shown in Figure 1 has a slope of $7.208 \text{ W m}^{-2} \text{ count}^{-1}$, and yields a standard error of 36 W/m^2 , with an r^2 of 0.985. Since the detailed model results shown confirm the linear relationship expected, this lends additional credence to the applicability of

our model studies to verify the use of METEOSAT in insolation estimation techniques.

Data from the Riyadh insolation monitoring site have been obtained for several days, and corresponding days of METEOSAT data for four of these days were ordered. Figures 2 and 3 show the surface-monitored direct and global insolation for Day 167 in years 1982, 1983 and 1984. A variety of amounts of reduction in the afternoon direct normal insolation is noted. The large variations in direct normal are not reflected in variations of the global insolation, however. This is to be expected, since scattering out of the direct beam by aerosols and dust is largely restored to the global insolation in the form of the diffuse component.

Figures 4 and 5 show the measured and modeled direct and global insolation for Day 167, 1983. The large drop in direct normal insolation in the afternoon is reproduced by assuming a change from an absorbing (urban, 80%RH) aerosol of optical depth 0.8 in the morning and a relatively non-absorbing (rural 0%RH) aerosol of optical depth 1.8 in the afternoon. The global insolation is relatively insensitive to the changes in aerosol properties. Figures 6 and 7 show similar results for Day 348, 1982, with the variation during the day represented by urban 80%RH aerosol with optical depth changing from 0.3 in the morning to 0.4 in the afternoon.

Process Surface Insolation Data and METEOSAT Data and Develop and Test Algorithms

METEOSAT data from four clear days (Day 167, for years 1982, 1983 and 1984, and Day 348 for 1982) were ordered. These days exhibit a range of aerosol and dust effects, allowing sensitivity to this effect to be studied. Seven visible images for each day were ordered. Images were processed on the recently acquired

ERDAS image processing system. Areal mean counts and standard deviation for an approximately 40 km x 40 km area around the Riyadh monitoring site were measured and are shown in Figure 8. These results show that the satellite-observed count values are fairly insensitive to the various aerosol and dust levels on the three years of Day 167 results. Figure 9 indicates that the radiation transfer model, using the Koepke calibration, is able to reproduce the main features of the daily variation in METEOSAT visible counts on the Day 167 and Day 348 data. Discrepancies in the details between measured and modeled counts are thought to be due to the non-uniform directional surface reflectance. Although a non-Lambertian surface directional surface reflectance was assumed in the model, the actual surface directional reflectance properties for sand in the 0.4-1.0 micrometer wavelength range are not well known.

If the satellite counts and surface insolation measurements for the 3 Day 167 data sets are plotted in the same manner as in Figure 1, the results are as shown by the circles in Figure 10. For reference, the modeled values for optical depth 1 and 2 clouds from Figure 1 are also shown in Figure 10 (as the x's). These results indicate that the details of the hour-to-hour variations in direct and global insolation due to variable aerosol and dust optical depths will not be easily measured by using the METEOSAT visible sensor alone. However the results of the previous year's study with a large number of days of GOES data indicate that the METEOSAT data should produce comparably accurate daily and monthly totals. Some preliminary studies with both visible and infrared images from the AVHRR sensor on the NOAA 7 polar orbiting satellite indicate that additional information about the large optical depth dust cloud cases may be obtained if METEOSAT infrared data is analyzed along with the visible data. It is suggested that this idea be explored further during a proposed follow-on study period.

References

- Justus, C. G., and M. V. Paris (1985): "A Model for Solar Spectral Irradiance and Radiance at the Bottom and Top of a Cloudless Atmosphere", J. Clim. Appl. Meteorol., 24, 193-205.
- Koepke, P. (1982): "Vicarious Satellite Calibration in the Solar Spectral Range by Means of Calculated Radiances and its Application to Meteosat", Appl. Optics, 21, 2845-2854.
- Paris, M. V. (1985): "Model Studies of Solar Spectral Irradiance at the Bottom and Top of a Cloudy Atmosphere", Ph.D. Thesis, Georgia Institute of Technology, December.

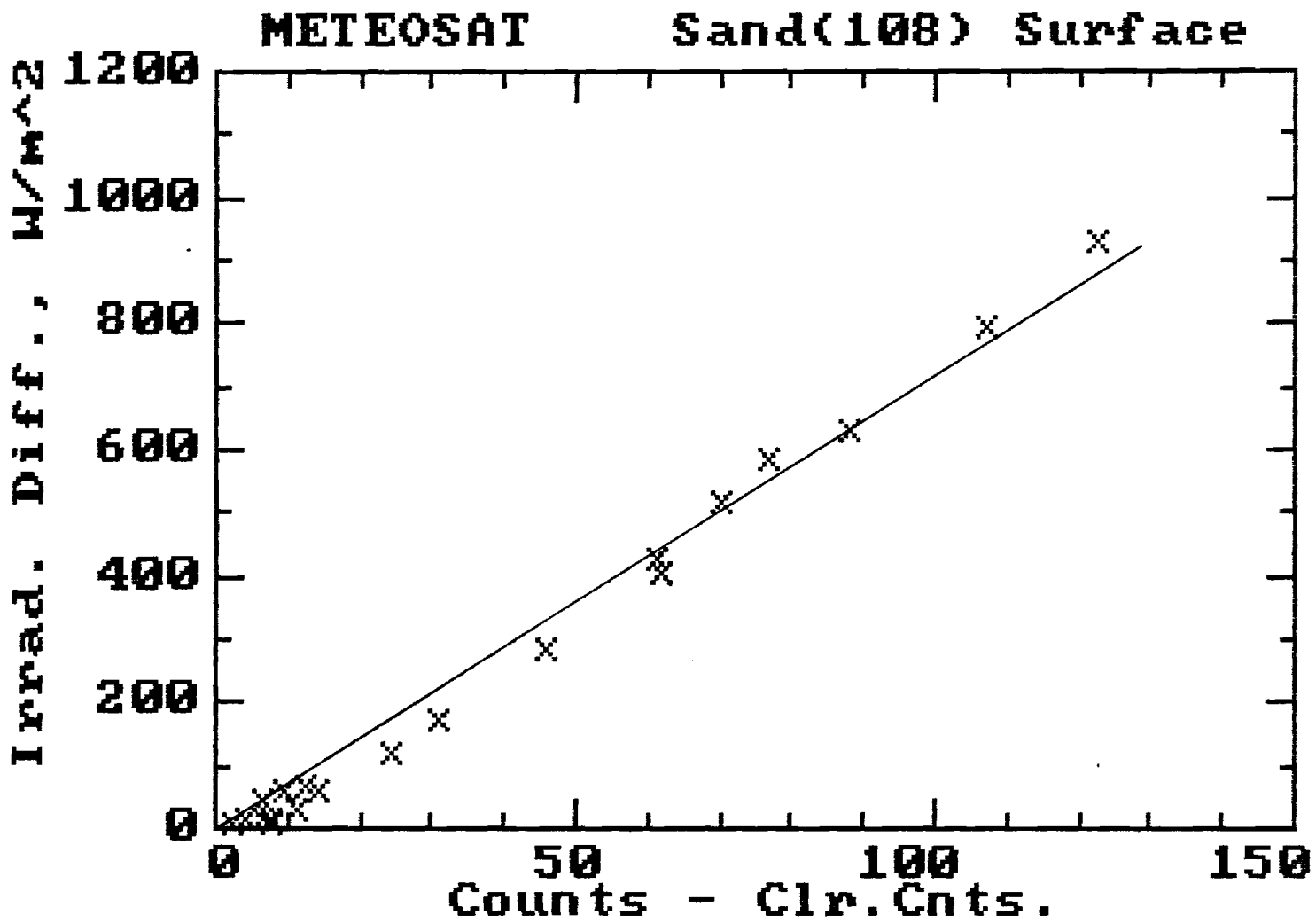


Fig. 1. Model reduction in surface irradiance from clear-sky value versus increase in METEOSAT count from clear-sky counts. Simulations are for cloud optical depths 1, 2, 16 and 64.

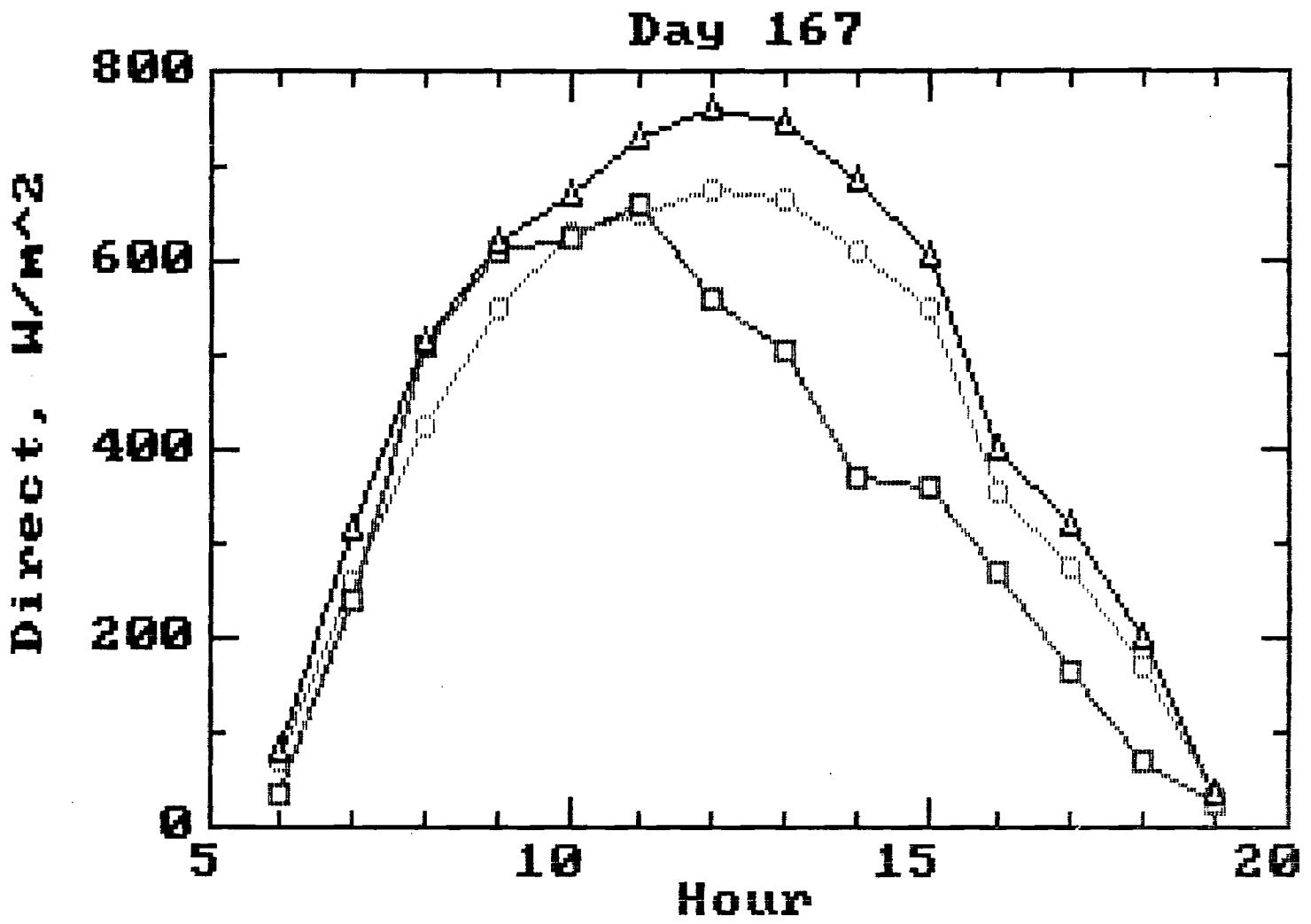


Fig. 2. Direct normal insolation for Day 167, years 1982 (circle), 1983 (squares) and 1984 (triangles).

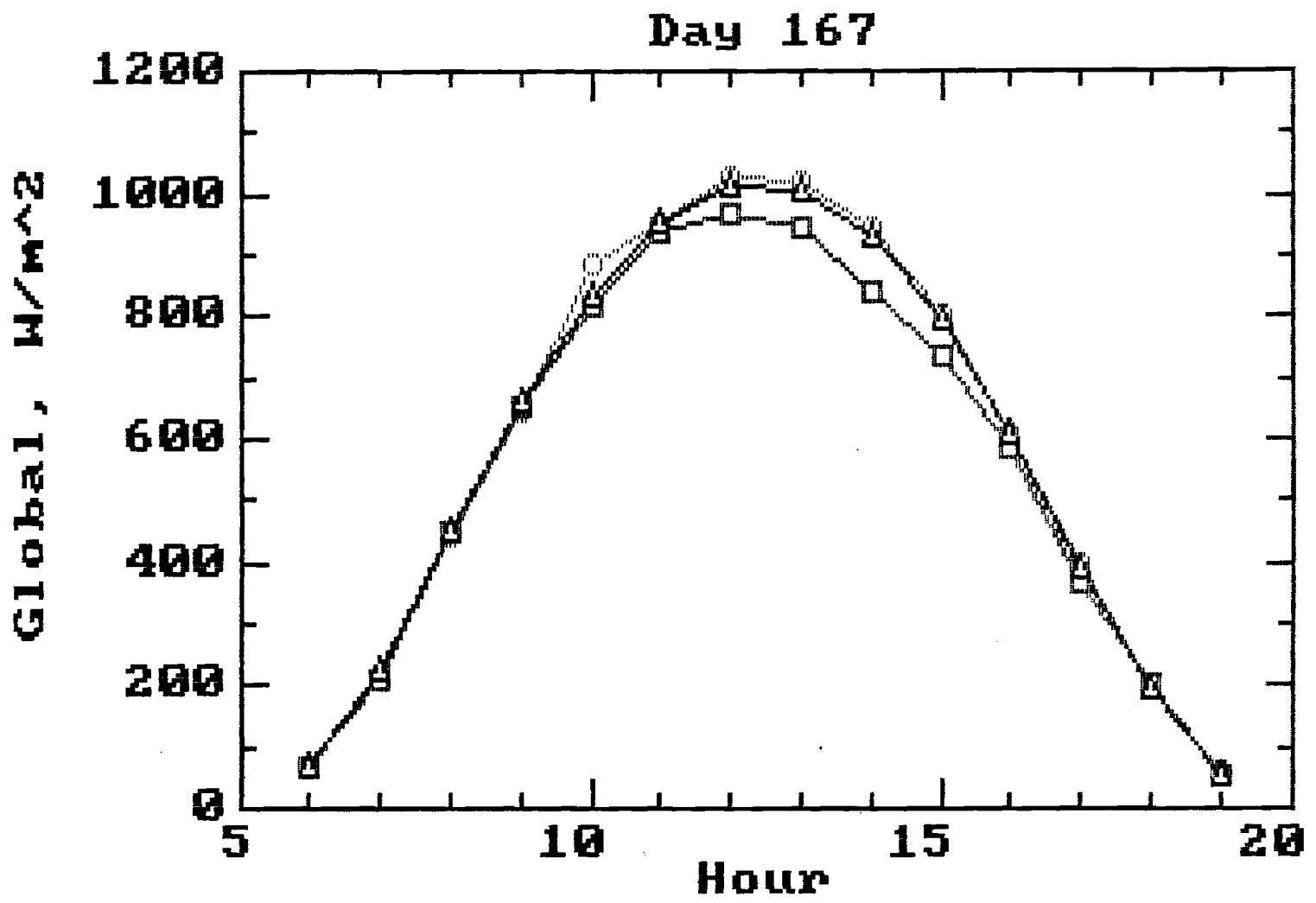


Fig. 3. As in Figure 2 for global insolation.

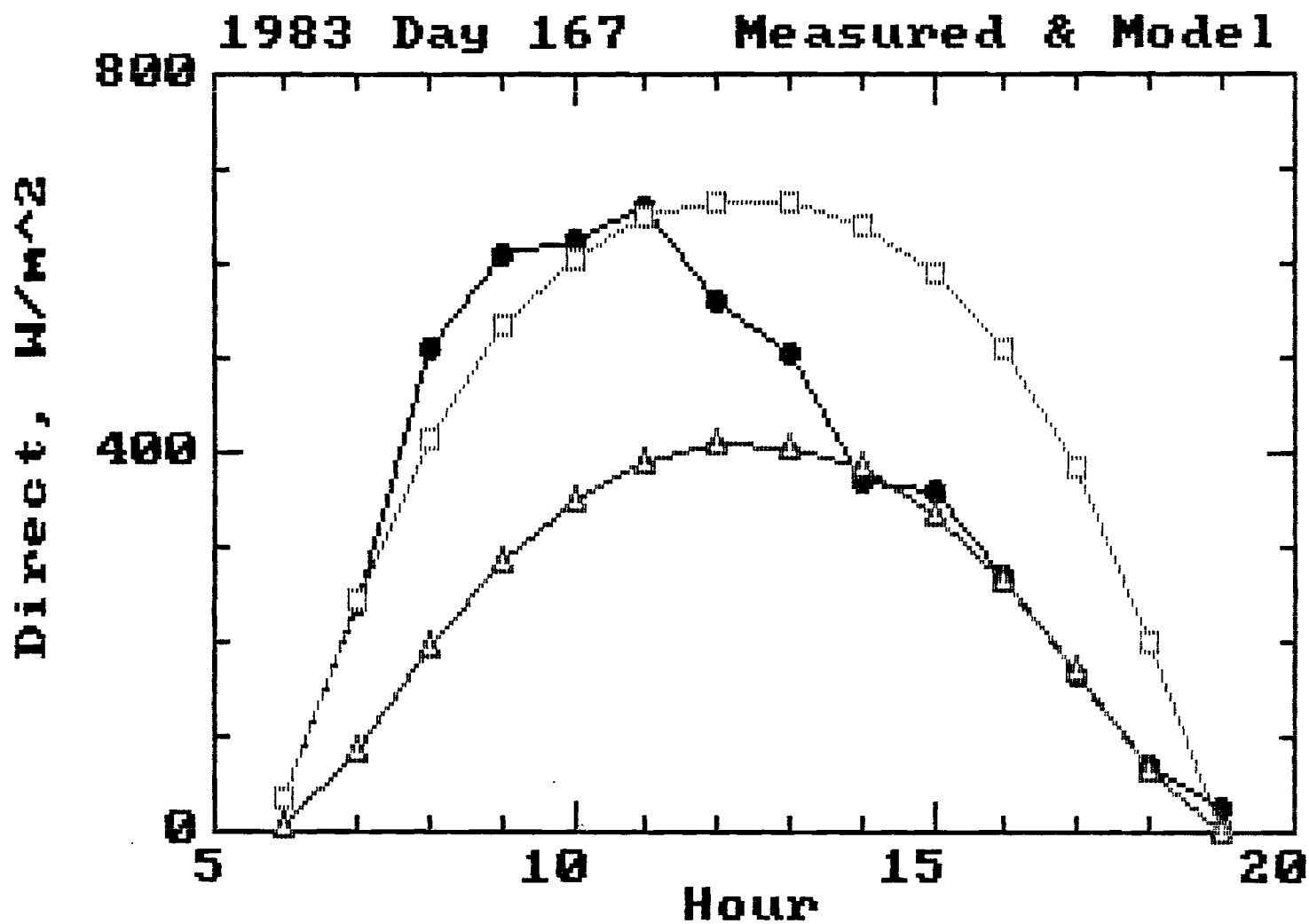


Fig. 4. Measured and modeled direct insolation for Day 167, 1983.
 Modeled optical depths are 0.8 (squares) and 1.8 (triangles).

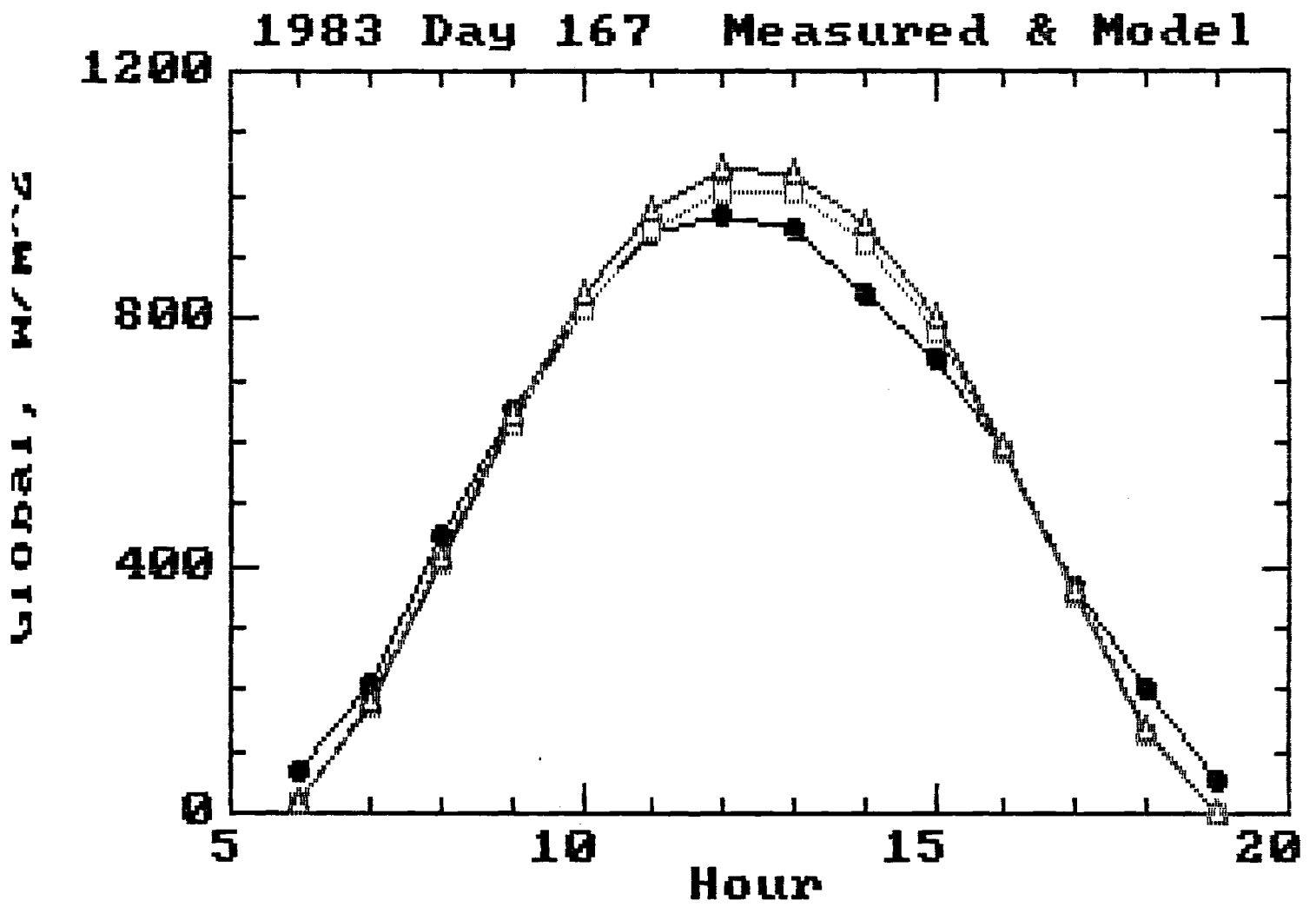


Fig. 5. As in Figure 4 for global insolation.

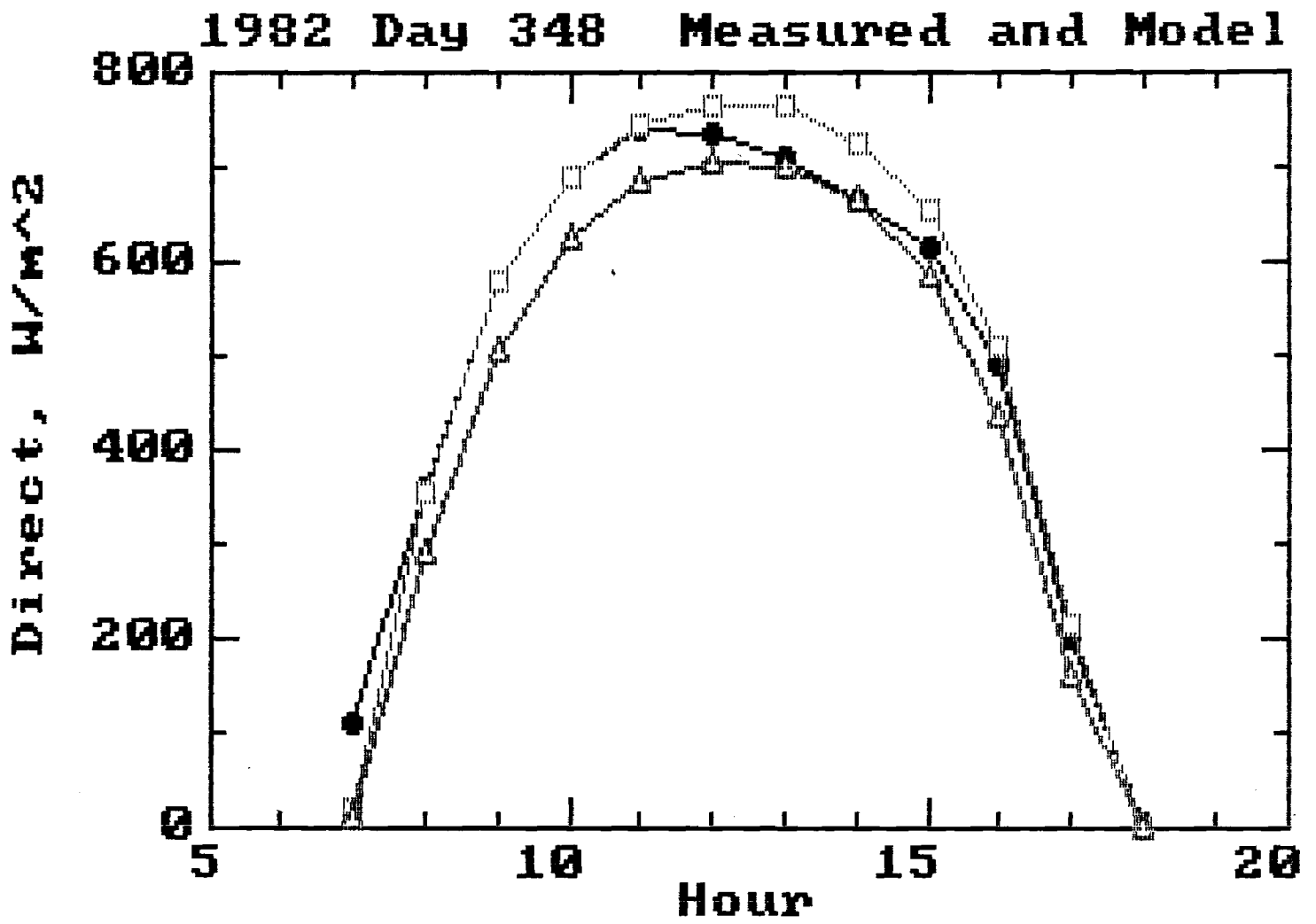


Fig. 6. Measured and modeled direct insolation for Day 348, 1982. Modeled optical depths are 0.3 (squares) and 0.4 (triangles).

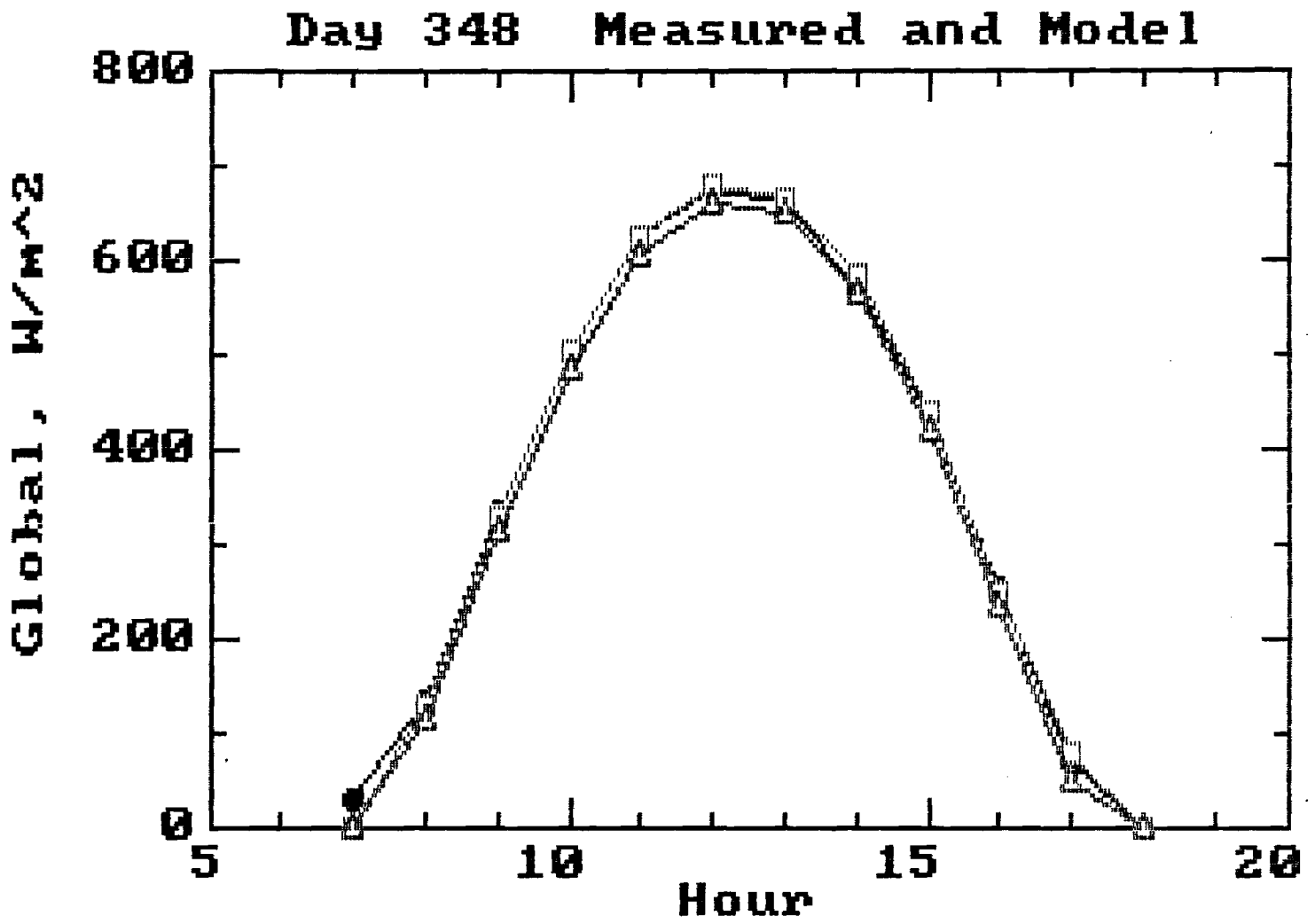


Fig. 7. As in Figure 6 for global insolation.

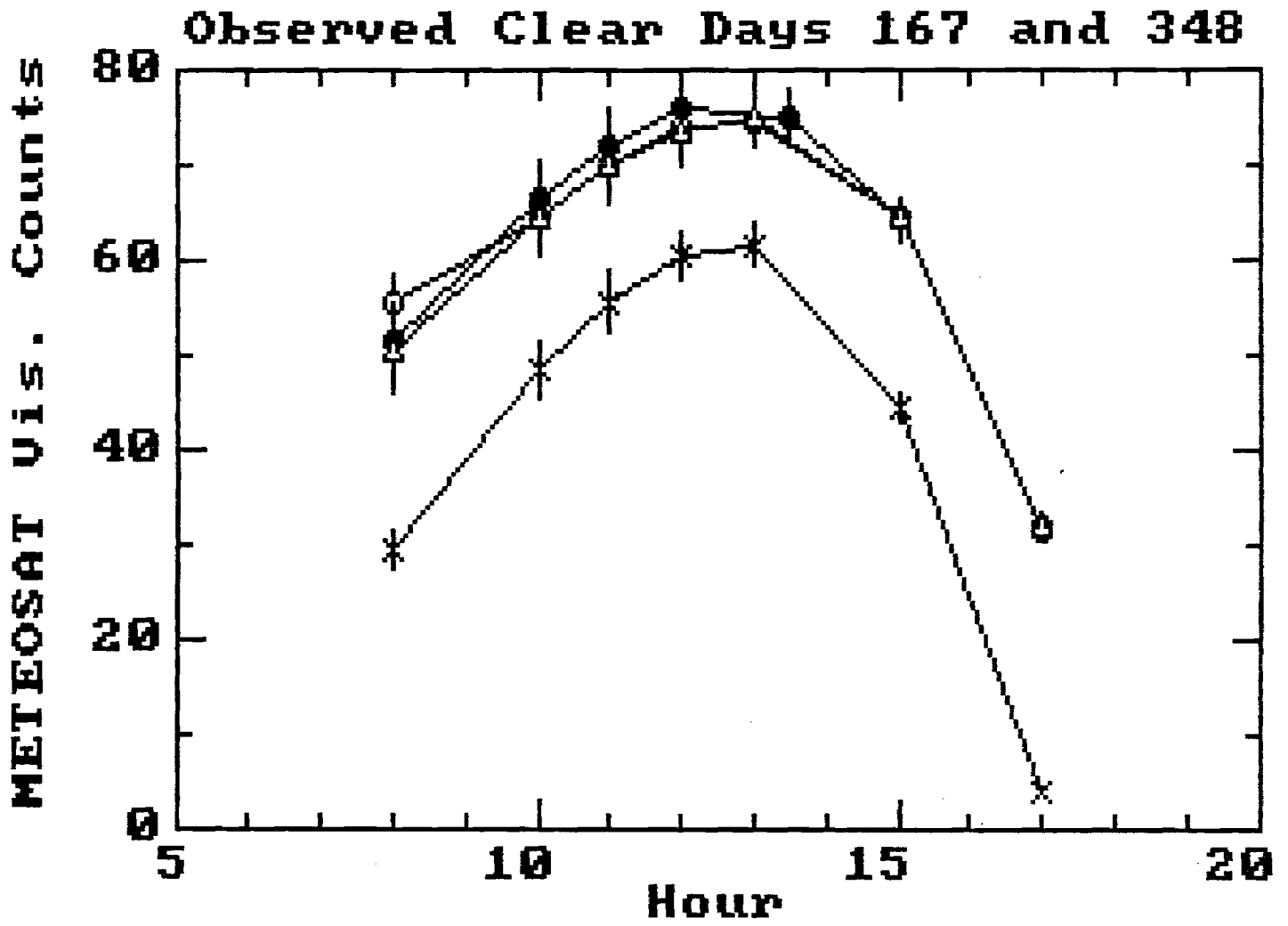


Fig. 8. Measured METEOSAT areal mean counts and standard deviations for the Riyadh monitoring site. Days 167 year 1982 (open circle), 1983 (solid circle), 1984 (triangle) and Day 348, 1982 (x's).

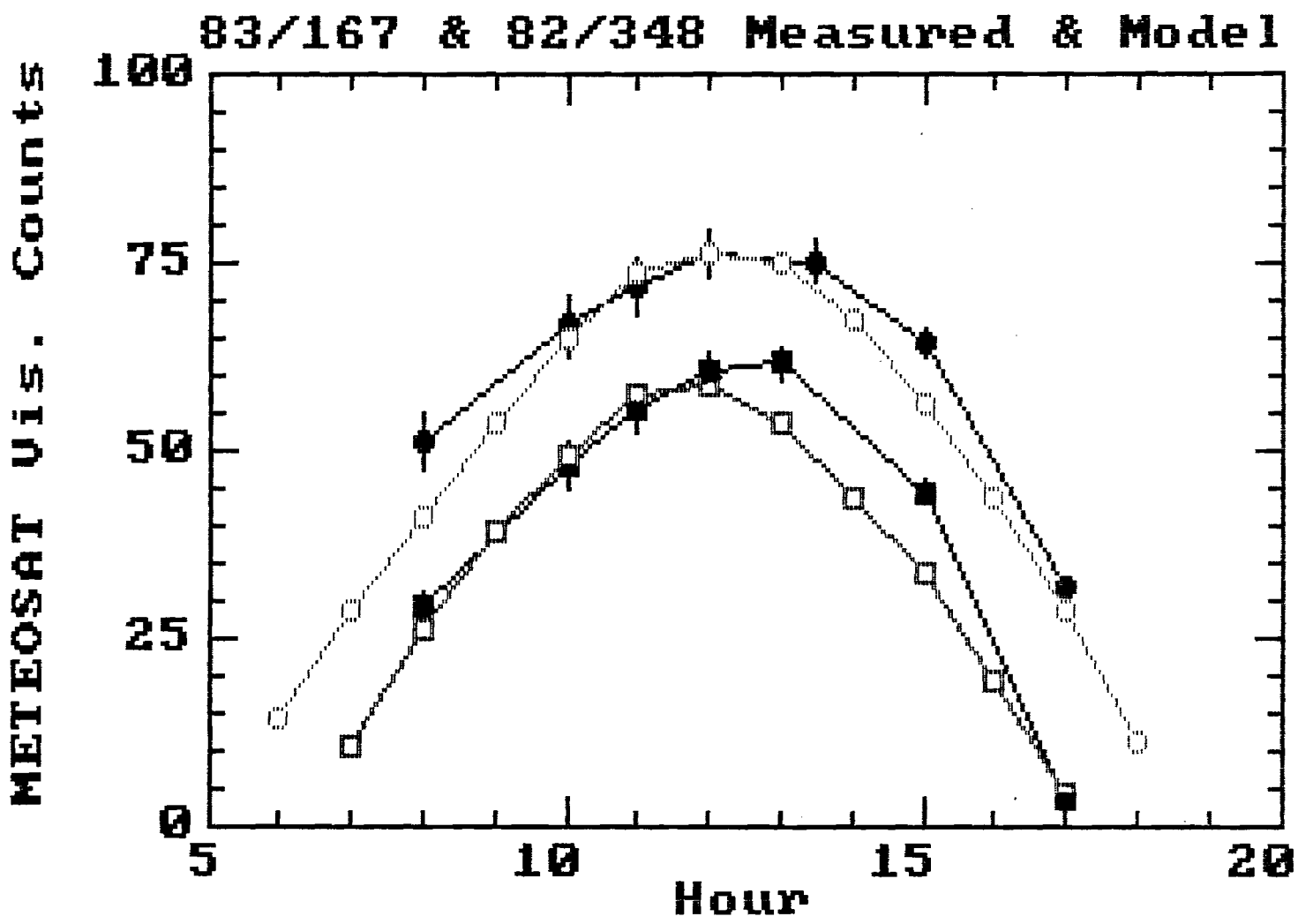


Fig. 9. Measured (solid symbols) and modeled (open symbols) METEOSAT visible sensor counts for Day 167 (1983) and Day 348 (1982).

Satellite Techniques of Solar
Resource Assessment for
Focusing and Non-Focusing
Solar Collector Systems

C. G. Justus

School of Geophysical Sciences
Georgia Institute of Technology
Atlanta, GA 30332

Technical Progress Report

January, 1987

Prepared by the
GEORGIA INSTITUTE OF TECHNOLOGY
for the
U. S. DEPARTMENT OF ENERGY
SOLERAS PROGRAM

Grant Number DE-FG02-84CH10200

Mr. Robert L. Martin, Midwest Research Institute, Technical
Monitor

Georgia Tech Project G-35-633

PROGRESS REPORT

METEOSAT and Surface Insolation Data Analysis

In the Previous year METEOSAT visible data from seven hours each on four clear days (June 16, 1982, June 16, 1983, June 15, 1984, and December 14, 1982) were analyzed. These days exhibit a range of aerosol and dust effects, allowing sensitivity to this effect to be studied. Images were processed on the ERDAS image processing system. Areal mean counts and standard deviation for an approximately 40 km x 40 km area around the Riyadh monitoring site were measured. The results of the previous analysis showed that the satellite-observed visible count values are fairly insensitive to the various aerosol and dust levels. This leads to a fairly inaccurate estimate of direct-beam insolation, although the global insolation estimates are accurate.

In the current year, seven infrared (IR) METEOSAT images from each of the June clear days, as well as seven visible images from two days with clouds (February 22, 1982 and December 14, 1982) were ordered and have been received. The purpose of the current study is to determine if the addition of IR information from the clear image scenes adds information on the amount of aerosol and dust loading which affects the cloud-free direct-beam values. Preliminary analysis (of an AVHRR image from the NOAA polar orbiting satellite for June 16, 1983) indicates that such bi-spectral analysis would provide significant improvement. The image processing of the newly-acquired METEOSAT data is now complete and the direct and global insolation estimates and comparisons with the Riyadh data are under way.

Image Processing Training Visit to Saudi Arabia

It was originally proposed that a one-week visit to Saudi Arabia be made for the purpose of image analysis training and transfer of sample data to an ERDAS system which it was anticipated would be acquired there. Based on the latest information, it appears that that system will not be available in Saudi Arabia and that this trip will not be necessary. If so, the travel budget (\$3000 for the Saudi Arabia trip plus one domestic conference trip) can be reduced. It is suggested that the reduced travel budget funds be used instead for one or the other of the following:

(1) Analysis of direct and global surface insolation from one or two Saudi Arabian sites other than Riyadh. This analysis could be done on the same six days for which METEOSAT data are currently on hand if hourly values of surface insolation are available for the additional site(s) on those days.

(2) Acquisition of two additional days of METEOSAT data for additional analysis of insolation from only the Riyadh station. Surface insolation data from several additional days are already on hand which could be used for this purpose.

U.S. DEPARTMENT OF ENERGY
NOTICE OF ENERGY RD&D PROJECT

FORM DOE 538
(1/78)

APPROVED FOR USE BY
SMITHSONIAN SCIENCE INFORMATION EXCHANGE

FORM APPROVED
OMB NO. 38 R-0190

1. DESCRIPTIVE TITLE OF WORK Satellite Techniques of Solar Resource Assessment for Focusing and Non-Focusing Solar Collector Systems				
2. PERFORMING ORGANIZATION CONTROL NUMBER G-35-633		3. CONTRACT, GRANT OR PURCHASE ORDER NUMBER DE-FG03-84CH10200		
4. CONTRACTOR'S PRINCIPAL INVESTIGATOR/PROJECT MANAGER AND ADDRESS WHERE WORK IS PERFORMED (404)				
a. NAME (Last, First, MI) <u>Justus, Carl G.</u>		PHONE <u>894-3890</u>		
b. BUSINESS ADDRESS: STREET <u>School of Geophysical Sciences, Georgia Tech</u>				
CITY <u>Atlanta</u>		STATE <u>GA</u>	ZIP <u>30332</u>	
5. a. NAME OF PERFORMING ORGANIZATION				
<u>Georgia Tech</u> (Organization)		<u>Geophysical Sciences</u> (Department)		
b. MAILING ADDRESS (If Different From 4B)				
c. TYPE OF ORGANIZATION PERFORMING THE WORK (Enter applicable code from instructions). <input checked="" type="checkbox"/> CU <input type="checkbox"/>				
6. SUPPORTING ORGANIZATION				
a. DOE PROGRAM DIVISION OR OFFICE (Full Name) <u>SERI Site Office</u>				
b. TECHNICAL MONITOR (Last, First, MI) <u>Williamson</u>				
c. ADDRESS (If Different from DOE Hqs) <u>SERI Site Office, 1617 Cole Blvd., Golden, CO 80401</u>				
d. ADMINISTRATIVE MONITOR (Last, First, MI) <u>Skinner, C.M.</u>				
7. PROJECT SCHEDULE				
(a) START DATE <u>June, 1984</u> (Month) (Year)		(b) EXPECTED COMPLETION DATE <u>June 1985</u> (Month) (Year)		
8. a. FUNDING OPERATING AND CAPITAL EQUIPMENT OBLIGATION (In Thousands of Dollars)				
FUNDING ORGANIZATION(S)	APPROXIMATE CUMULATIVE PRIOR FISCAL YEARS	CURRENT FY		
1. OOE	none	94		
2.				
3.				
b. DOE BUDGETING AND REPORTING CLASSIFICATION CODE _____				
9. DIRECT SCIENTIFIC AND TECHNICAL MANPOWER				
	PROFESSIONAL	GRAD. STUDENTS	OTHER	TOTAL
NUMBER	1	2		3
EQUIVALENT PERSONYEARS	0.2	1		1.4

10. SUMMARY OF WORK (Limit to 200 words or less - include a description, objective, approach and a final product expected.)

Development is proposed of several improvements in the NOAA satellite insolation estimation techniques, which will make them especially useful for solar energy resource assessment. In particular, techniques will be developed for estimating direct beam radiation for focusing collectors and solar radiation in spectral regions applicable to photovoltaic solar energy systems: A technique, employing combined GOES visible and IR data, will be developed to distinguish cloud-free snow-cover cases, and improve the insolation estimates in this situation. A study of the relative accuracy benefits of incorporating the precipitable water effect (as well as possible techniques to estimate atmospheric aerosol turbidity) will also be carried out as part of this project. For immediate application in solar energy resource assessment, a report will be produced containing maps of monthly mean insolation, and other statistics (e.g., standard deviation, spatial variability magnitude) for the continental U.S. and for Mexico and the parts of South America covered by the current insolation estimation algorithm. These maps will be prepared for the period since July 1982, a period when insolation data is no longer available in processed form from the DOE/NOAA surface insolation (SOLMET) monitoring network.

11. PROGRESS SINCE LAST REPORT (Limit to 100 words.)

No Previous Reports

12. List publications in the last year that are available to the public which have resulted from the product. (Please give a complete bibliographic citation. Use additional sheets if necessary.)

No Previous Contract

13. GENERAL TECHNOLOGY CATEGORIES (Enter applicable code or codes from instructions.)

D I

14. PHASE OF RD&D (Enter Project Percentages in Applicable Boxes)

- a. Basic Research
- b. Applied Research
- c. Technology Development
- d. Engineering Development
- e. Demonstration

15. KEYWORDS: (Minimum of 5)

Solar Resource
Remote Sensing
Insolation

16. A. RESPONDENT'S NAME & ADDRESS

C.G. Justus
School of Geophysical Sciences
Georgia Tech, Atlanta, GA 30332

B. PHONE NO.

4 0 4 - 8 9 4 - 3 8 9 0

C. DATE

11/14/84

ANNUAL REPORT
GEORGIA TECH PROJECT G-35-633

**SATELLITE TECHNIQUES OF SOLAR RESOURCE
ASSESSMENT FOR FOCUSING AND NON-FOCUSING
SOLAR COLLECTOR SYSTEMS**

C. G. Justus, Principal Investigator

Georgia Institute of Technology
Atlanta, Georgia 30332

Reporting Period 15 June, 1984 - 14 June, 1985

July 1985

Prepared for the
UNITED STATES DEPARTMENT OF ENERGY
SOLAR ENERGY RESEARCH INSTITUTE SITE OFFICE
SOLERAS PROGRAM

Grant Number DE-FG02-84CH10200

GEORGIA INSTITUTE OF TECHNOLOGY
A UNIT OF THE UNIVERSITY SYSTEM OF GEORGIA
SCHOOL OF GEOPHYSICAL SCIENCES
ATLANTA, GEORGIA 30332



Annual Report Georgia Tech Project G-35-633

**Satellite Techniques of Solar
Resource Assessment for
Focusing and Non-Focusing
Solar Collector Systems**

C. G. Justus, Principal Investigator

School of Geophysical Sciences
Georgia Institute of Technology
Atlanta, GA 30332

Reporting Period 15 June, 1984 - 14 June, 1985

July 1985

Prepared for the

UNITED STATES DEPARTMENT OF ENERGY
SOLAR ENERGY RESEARCH INSTITUTE SITE OFFICE
SOLERAS PROGRAM

Grant Number DE-FG02-84CH10200

Abstract

A 16-month set of surface-measured data has been used together with GOES satellite brightness information from NOAA, to produce a regression model for hourly total global horizontal irradiance, direct normal irradiance, and global irradiance on a tilted surface. Results for daily total irradiances show an rms difference between satellite estimates and observed data of 1.3 MJ/m² (8.4% of the mean value) for global horizontal, 3.1 MJ/m² (21.3% of the mean value) for direct normal, and 1.9 MJ/m² (11.1% of the mean value) for the global tilted. Data for the monthly average daily totals show an rms difference between satellite estimates and observed data of 0.4 MJ/m² (2.9% of the mean value) for the global horizontal, 1.0 MJ/m² (6.7% of the mean value) for the direct normal, and 0.8 MJ/m² (4.5% of the mean value) for the global tilted insolation. Considerable improvement in relative error is thus achieved for monthly average values as opposed to individual daily totals. Georgia Tech surface measurements with a Licor photocell sensor have also been used to develop a method for using the satellite data to estimate global horizontal or tilted irradiance as measured by these Licor photocell radiometers. The results of comparison of these estimates with the photocell radiometer measurements indicate comparable accuracies for the photocell irradiance measurements as for the Eppley instruments, giving rms differences for daily totals of 8.8% for the global horizontal and 11.0% for the global tilted values. Although the Licor radiometers are normally calibrated in terms of equivalent full solar spectrum irradiance, comparisons with spectral irradiance model results and photocell response curves, indicate that values of photocell collector system short circuit current in amps per square meter of collector can be estimated as 0.32 times the Licor photocell radiometer reading in W/m². Based on a reflectivity-brightness temperature relationship, a method is suggested for calculation of global horizontal insolation when snow cases are expected. The method allows certain cases to be treated as clear, ignoring the effects of measured reflectivity, while other cases are treated as cloud-covered, using the conventional cloud-modifier term. Data are presented which illustrate the sensitivity of clear global, clear direct normal, shortwave clear global, and shortwave clear direct normal transmittance both to precipitable water amount and to satellite brightness value (presumably an indication of aerosol turbidity in the atmosphere). An effect of the relationship between aerosols and precipitable water which appears in the observations, and which must be accounted for in models if they are to produce accurate results is that aerosol optical depth tends to increase with increasing precipitable water amount, because of hygroscopic aerosol formation processes. This effect is even more evident in the observations for global horizontal and direct normal irradiance at wavelengths below 630nm, a spectral region in which there is essentially no water vapor absorption. All effects of precipitable water level on the data below 630nm must therefore be from water-vapor-related aerosols, not from water vapor absorption effects.

TABLE OF CONTENTS

<u>Abstract</u>	i
<u>INTRODUCTION</u>	1
• Need for Satellite-Based Insolation Estimation Techniques	
• Development of Satellite Insolation Estimation Techniques	
• The NESDIS GOES Insolation Products	
• Review of Other Satellite Insolation Estimation Techniques	
• Need for Improved Satellite Insolation Methods	
<u>MONTHLY MEAN INSOLATION SUMMARY DATA</u>	5
• Monthly Mean and Variability Data	
• Comparison to Long-Term Monthly and Annual Mean	
<u>DEVELOPMENT OF A SATELLITE TECHNIQUE FOR DIRECT BEAM AND TILTED SURFACE INSOLATION ESTIMATES</u>	7
• Comparison with Other Regression and Physical Models	
<u>DEVELOPMENT OF A SATELLITE INSOLATION ESTIMATION TECHNIQUE FOR PHOTOVOLTAIC SYSTEMS</u>	13
<u>DEVELOPMENT OF A TECHNIQUE FOR SATELLITE INSOLATION ESTIMATION WITH SNOW COVER ON THE GROUND</u>	14
<u>INVESTIGATION OF ERROR REDUCTION IF PRECIPITABLE WATER IS INCLUDED</u>	16
<u>CONCLUSIONS</u>	17
<u>REFERENCES</u>	21
<u>APPENDIX</u>	60

INTRODUCTION

Need for Satellite-Based Insolation Estimation Techniques

For solar energy or other applications, continuous measurements of insolation are made with pyranometers located at a few weather stations and at scattered universities and agricultural experiment stations. However, operating and maintaining pyranometers and compiling and quality checking the data is an expensive and laborious task. Funding constraints have caused a sharp decline in the availability of routine insolation measurements, and pyranometer data are sparse to non-existent in some foreign countries. Since there are many more weather stations than pyranometer sites, efforts have been made to infer insolation from conventional meteorological observations such as cloud cover, cloud type, and precipitable water (e.g. Hanson, 1971; Atwater and Brown, 1974; Suckling and Hay, 1977; Atwater and Ball, 1978; Sherry and Justus, 1983, 1984). However, the weather station networks and techniques used are insufficient to produce accurate insolation estimates at all locations of interest, especially at remote locations (where solar energy is perhaps more economically viable). The only practical source of data with the required resolution and coverage is meteorological satellites.

Development of Satellite Insolation Estimation Techniques

In the summer of 1977, the NOAA (National Oceanic and Atmospheric Administration) National Environmental Satellite, Data and Information Service (NESDIS) and the Great Plains Agricultural Council undertook a joint experiment to determine if GOES (Geostationary Operational Environmental Satellite) data could be used to estimate surface insolation (Tarpley, et al., 1978). Techniques developed from this program (Tarpley, 1979; Brakke and Kanemasu, 1981) showed the GOES and other operationally available data could be used to derive insolation with errors of 10 to 15%. Both techniques developed from the Great Plains data set involved regression

against visible radiance from the GOES Visible and Infrared Spin Scan Radiometer (VISSR) instrument.

The NESDIS GOES Insolation Products

With the support of the AgRISTARS program a GOES insolation product was started by NESDIS in July 1980. Coverage included only the Eastern portion of the United States. Two years of research-mode operation revealed the need for more images per day to be used in the processing (initially five per day were used, if available; this was expanded to six or seven). Other problems identified during the research-mode operation were corrected when a new software system was completed in June 1982. At the same time, coverage was expanded to cover the entire 48 contiguous states (67-125°W, 25-49°N), and the agriculturally significant parts of Mexico (90-110°W, 16-30°N) and South America (40-67°W, 15-41°S). These areas are illustrated on the map in Figure 1.

The data are accessed from a 24-hour rotating data base maintained on the NOAA Central Computing Facility. The visible data are in the form of hourly images consisting of arrays of 6-bit count values measuring relative brightness. Each array extends to $\pm 50^\circ$ of latitude and longitude from the sub-satellite point. The resolution of the data, defined as the center-to-center distance between pixels, is about 8 km. Each hour's image remains on the computer disk system for 24 hours before being replaced by the subsequent day's data. The programs producing the insolation estimates are run in the late evening, after the last daylight observation for the day has been made. Hourly and daily total insolation values are then estimated and archived on magnetic tape.

As part of the present project, the NESDIS insolation estimates have been summarized into monthly means, standard deviations, and root-mean-square (rms) spatial differences. These data, as well as a more complete description of the NESDIS procedures, are presented by Justus and Tarpley (1984), and Justus, Paris and Tarpley (1985).

Review of Other Satellite Insolation Estimation Techniques

Other workers have developed physical models to estimate insolation from GOES data (Hay and Hanson, 1978; Gautier, et al., 1980; Diak and Gautier, 1983; Gautier, 1982,1983; Halpern, 1984; Gautier and Katsaros, 1984; Moser and Raschke, 1984). The relative applicability of these for operational application as well as the relative accuracy of these models has been reviewed by Raphael (1983), Riordan and Hulstrom (1982), Raphael and Hay (1984), and Riordan (1984). A summary of the statistics on estimated accuracy of some of these models is given in Table 1. The values indicated as "old regression" are from the NOAA/NESDIS algorithm in use prior to March, 1983. Values indicated as "new regression" are for the NOAA/NESDIS algorithm in use since March, 1983, either as it is used (without the effects of precipitable water) or with the effects of precipitable water included. The values identified as "physical model" are from a model described by Justus and Tarpley (1984) and Justus, Paris and Tarpley (1985). The values in Table 1 indicate that a lower limit in rms error of daily total insolation from satellite estimates is about $1.0-1.3 \text{ MJ/m}^2$ (25-30 Ly).

The most accurate method currently available is that of Gautier. However, it has the disadvantage of requiring time-consuming manual "navigation" of the satellite imagery, and the need for calibrated sensor radiances if the accuracy levels noted in Table 1 are to be achieved. The NOAA/NESDIS regression results and study of the physical model approach noted in Table 1 utilized automated data analysis, and relied only on the regularly provided nominal image navigation values. All satellite estimation techniques of the present study also use only automated, nominal image navigation.

Because of the significant variation in mean insolation for the data sets compared in Table 1, error comparisons are probably more meaningful on an absolute basis rather than as a percentage of the mean. Whereas the mean value of 24.6 MJ/m^2 (586 Ly) is typical of

the Great Plains in the summer, the mean value of 14.6 MJ/m^2 (349 Ly) is typical for an annual average over the eastern and central United States (Hulstrom et al., 1981).

One satellite estimation technique for which data are not included in Table 1 is that of Halpern (1984). He examined only three days at two closely-spaced sites (for which he averaged the surface measurements). Although he gives values for the "total integrated flux" over the observation period for each day, no values for daily total insolation are reported. Errors as low as 2-3% were claimed for the "total integrated flux" of 133-150 (units not specified by Halpern and seemingly unrelated to his Ly/min units for the hourly insolation estimates). However, over the three days studied there was only one hour for which the observed insolation fell as low as 60% of the clear-sky values. For this hour, Halpern's method overestimated the observed hourly total insolation value by 880 kJ/m^2 (21 Ly) or 49% of the observed value of 1810 kJ/m^2 (43.2 Ly). Overcast clouds should produce insolation values on the order of 30% of clear sky values. Therefore it is considered that Halpern's method has not yet received adequate study under a complete range of cloud-cover conditions.

Need for Improved Satellite Insolation Methods

All of the currently available methods for insolation estimation from satellites, produce estimates for global horizontal insolation only. For solar energy applications, it would be much more useful to have techniques which can estimate global insolation on tilted surfaces (e.g. collector tilt angle), direct beam insolation, and insolation within the spectral range of spectrally selective collector systems, such as photovoltaics.

Other areas for improvement would be in methods for insolation estimates when there is snow cover - currently snow cannot be distinguished from clouds in the automatic processing systems such as that used by NOAA/NESDIS. Adjustments for insolation estimation

over very dark surface areas (e.g. water) or very bright areas (e.g. desert sand) need to be better understood also. To address these needs this DOE/SOLERAS project was undertaken, with the following task areas to be addressed:

1. A Report on Monthly Mean Solar Energy Resource from Current Satellite Insolation Data
2. Development of a Satellite Technique for Direct Beam Insolation Estimates
3. Development of a Satellite Insolation Estimation Technique for Photovoltaic Systems
4. Development of a Technique for Satellite Insolation Estimation with Snow Cover on the Ground
5. Investigation of Error Reduction if Precipitable Water is Included

The following sections of the report give results and conclusions concerning each of these areas.

MONTHLY MEAN INSOLATION SUMMARY DATA

Monthly Mean and Variability Data

The insolation estimates produced by the Satellite Applications Laboratory of the National Oceanic and Atmospheric Administration (NOAA), under the AgRISTARS program, are based on GOES satellite data. Daily estimates of global horizontal insolation are produced for the entire continental United States, Mexico, and parts of South America. These are available on computer tape from NOAA at a spatial resolution of 1° x 1° in latitude-longitude. The daily data

have been summarized into monthly mean values, standard deviations about the monthly mean, and root-mean-square (rms) differences across 1° of latitude or longitude. A report outlining the NOAA insolation methodology and giving in atlas form the monthly statistical results has been prepared. An abstract of this report, "Atlas of Satellite-Measured Insolation in the United States, Mexico, and South America", is in the Appendix. Figure 2 shows a comparison of the monthly mean daily total values derived from the NOAA satellite estimates with monthly means of surface-measured insolation at the Georgia Tech insolation monitoring site. The rms difference between the satellite-estimated and ground-observed monthly mean daily total values shown in Figure 2 is 0.77 MJ/m², or 5.2% of the mean value of 14.8 MJ/m². Figures 3-14 give samples of the maps of monthly mean data which are shown in the atlas report. These figures show the annual mean daily total global horizontal insolation, the annual mean standard deviation, and the annual mean rms difference over one degree of latitude or one degree of longitude for the continental United States, Mexico, and parts of South America for the year 1983.

Comparison to Long-Term Monthly and Annual Mean

Compared to long-term, surface-measured insolation in the United States (Hulstrom, et al., 1981), the satellite-derived means for the reported period were found to be somewhat low, especially in the central and southwestern United States. Lowest standard deviation areas tend to be associated with areas of high mean insolation, such as deserts, where high values tend to persist from day to day. Some of the areas with high mean insolation also exhibit low spatial variability, with nearby areas of higher-than-average spatial variability where the insolation regime changes to one of lower mean value. An exceptionally large spatial variability is found in the mountainous regions of Bolivia and Argentina. The southern and central Rocky Mountain regions of the United States also show somewhat higher than average spatial variability. The rms spatial variability, which has not been reported before for such an extensive geo-

graphical region, is important in assessing the reliability of interpolations or extrapolations to other locations from sites with measured insolation. The full report of these results (Justus and Tarpley, 1984; Justus, Paris and Tarpley, 1985) also describes the atlas of satellite-measured insolation and variability which shows the entire study region on a month-by-month basis, as well as the annual averages.

DEVELOPMENT OF A SATELLITE TECHNIQUE FOR
DIRECT BEAM AND TILTED SURFACE INSOLATION ESTIMATES

The current insolation estimates being done by NOAA/NESDIS are only for global horizontal irradiance. Although this is adequate to meet the needs of the agriculturally oriented AgRISTARS program, solar energy researchers and systems designers would find estimates for direct normal (for focusing collectors) and global irradiance on tilted surfaces (non-focusing collectors) of considerable additional benefit. A 16-month set of surface-measured data has been used together with GOES satellite brightness information from NOAA, to produce a regression model for hourly total global horizontal irradiance, and for hourly total direct normal irradiance. These two estimates can be combined, using a relation by Klucher (1979), to produce an estimate of global irradiance on a tilted surface (estimates have been compared here to measurements taken on a latitude tilt).

The form of the model equations to calculate hourly total direct normal and global horizontal insolation is given by

$$\text{Dir} = \text{Dir}(\text{Clr}) - \Delta\text{Dir} , \tag{1}$$

and

$$\text{Glo} = \text{Glo}(\text{Clr}) - \Delta\text{Glo} , \tag{2}$$

where Dir(Clr) and Glo(Clr) are the clear-sky components of direct normal and global horizontal, respectively, and Δ Dir and Δ Glo are the cloud-modifier components of direct normal and global horizontal, respectively. Dir(Clr) is computed by the relation

$$\begin{aligned} \text{Dir(Clr)} = & \text{ETR} \{ a_0 + a_1 \text{PW} + a_2 \Delta C_0 + a_3 \text{PW} \Delta C_0 + \\ & \cos(\text{ZA}) [a_4 + a_5 \text{PW} + a_6 \Delta C_0] + \\ & \cos^2(\text{ZA}) [a_7 + a_8 \text{PW} + a_9 \Delta C_0] \} , \end{aligned} \quad (3)$$

where ETR is the hourly total extraterrestrial insolation on a horizontal surface, PW is the column precipitable water, in mm, ΔC_0 is the difference between observed GOES VISSR counts (6-bit scale) and clear counts (maximum value $\Delta C_0 = 5$ for clear conditions, otherwise use an average value $\Delta C_0 = 0.75$), and ZA is the solar zenith angle. The coefficient values found to give these best fit to the observations were $a_0 = 2.493$, $a_1 = -0.01588$, $a_2 = -0.07174$, $a_3 = -3.845 \times 10^{-4}$, $a_4 = -3.505$, $a_5 = 0.02983$, $a_6 = -0.1244$, $a_7 = 1.769$, $a_8 = -0.01897$, and $a_9 = 0.1845$. ETR, in kJ/m^2 , is given by $4921 \cos(\text{ZA})$.

Δ Dir is computed by

$$\begin{aligned} \Delta \text{Dir} = & \Delta C [b_0 + b_1 \cos(\text{ZA})] + \Delta C^2 [b_2 + b_3 \cos(\text{ZA})] + \\ & \sigma_C [b_4 + b_5 \cos(\text{ZA})] + \Delta C \sigma_C [b_6 + b_7 \cos(\text{ZA})] , \end{aligned} \quad (4)$$

where ΔC is the difference between VISSR counts and clear-sky counts, ΔC^2 is the difference in the square of the counts from the square of the clear-sky counts, and σ_C is the standard deviation in the counts (from the target array of 5×5 , 8-km resolution pixels). The coefficient values are found to be $b_0 = -67.85$, $b_1 = -314.4$,

$b_2 = -0.6681$, $b_3 = 4.825$, $b_4 = -502.4$, $b_5 = 639.3$, $b_6 = 31.65$, and $b_7 = -36.87$ (for ΔDir in kJ/m^2).

Glo(Clr) is computed by the relation

$$\begin{aligned} \text{Glo(Clr)} = & \text{ETR} \{ c_0 + c_1 \text{PW} + c_2 \Delta C_0 + c_3 \text{PW} \Delta C_0 + \\ & \cos(\text{ZA}) [c_4 + c_5 \text{PW} + c_6 \Delta C_0] + \\ & \cos^2(\text{ZA}) [c_7 + c_8 \text{PW} + c_9 \Delta C_0] \} \quad . \end{aligned} \quad (5)$$

The coefficient values found to give these best fit to the observations were $c_0 = 0.3521$, $c_1 = 0.002624$, $c_2 = 0.03645$, $c_3 = -0.0002131$, $c_4 = 1.022$, $c_5 = -0.01446$, $c_6 = -0.1594$, $c_7 = -0.5885$, $c_8 = 0.01088$, and $c_9 = 0.1284$.

ΔGlo is computed by

$$\begin{aligned} \Delta \text{Glo} = & \Delta C [d_0 + d_1 \cos(\text{ZA})] + \Delta C^2 [d_2 + d_3 \cos(\text{ZA})] + \\ & \sigma_C [d_4 + d_5 \cos(\text{ZA})] + \Delta C \sigma_C [d_6 + d_7 \cos(\text{ZA})] \quad , \end{aligned} \quad (6)$$

The coefficient values are found to be $d_0 = 5.845$, $d_1 = -89.95$, $d_2 = -0.9903$, $d_3 = 1.015$, $d_4 = -99.39$, $d_5 = 114.3$, $d_6 = 9.166$, and $d_7 = -9.847$ (for ΔGlo in kJ/m^2).

With the direct and global components evaluated from equations (1) and (2) [with the application of equations (3)-(6)], the insolation on a latitude-tilted surface is calculated by the Klucher (1979) relation by

$$\text{Tilt} = \text{Dir} \cos(\phi) + [\text{Glo} - \text{Dir} \cos(\text{ZA})] f h \quad , \quad (7)$$

where ϕ is the solar zenith angle with respect to the normal to the tilted plane, f is $[1 + \cos(\text{Lat})]/2$, and h is

$$h = (1 + S g)[1 + g \cos^2(\phi) \sin^3(\text{ZA})] \quad , \quad (8)$$

where S is $\{[1 - \cos(\text{lat})]/2\}^{3/2}$, and g is $[1 - \text{Dir} \cos(\text{ZA})/\text{Glo}]^2$.

Results for observed versus satellite-estimated daily total global horizontal irradiance are shown in Figure 15, for 1982-1983 Georgia-Tech data. The rms difference between satellite estimates and observed data in this figure is 1.3 MJ/m², or 8.2% of the mean value of 15.8 MJ/m². This accuracy is somewhat better than from a similar comparison against the operational NOAA estimates, interpolated to the Atlanta, Georgia Tech site, which yielded an rms difference of 1.9 MJ/m², or 12.8% of the mean value of 14.9 MJ/m². Similar comparisons between surface observations and the new satellite methods for estimating daily totals of direct normal and global latitude-tilted irradiances are shown in Figures 16 and 17. The direct normal values cannot be estimated as accurately as the global horizontal, giving an rms difference of 3.1 MJ/m², or 21.3% of the mean value of 14.4 MJ/m². Because it relies in part on the direct normal estimate, the estimated global tilted values are also slightly less accurate than the global horizontal values, with the data in Figure 17 having an rms difference of 1.9 MJ/m², or 11.1% of the mean value of 17.2 MJ/m². This error estimate for the daily total global tilted irradiance is, however, comparable to the estimated accuracy in the current NOAA operational estimates of daily total global horizontal irradiance.

Data for the monthly average daily totals for global horizontal, direct normal, and global latitude-tilted insolation are shown in Figures 18-20. The rms difference between satellite estimates and observed data is 0.4 MJ/m², or 2.9% of the mean value of 15.1

MJ/m² for the global horizontal. For the direct normal, the rms error is 1.0 MJ/m², or 6.7% of the mean value of 15.0 MJ/m²; while for the latitude-tilted insolation, the rms error is 0.8 MJ/m², or 4.5% of the mean value of 17.5 MJ/m². Considerable improvement in relative error is thus achieved for monthly average values as opposed to individual daily totals.

Comparison with Other Regression and Physical Models

The NOAA/NESDIS model for global horizontal insolation uses a simplified form of equations (5) and (6). In the NOAA/NESDIS method, Glo(Clr) is computed by the relation

$$\text{Glo(Clr)} = \text{ETR} \{c_0 + c_4 \cos(\text{ZA}) + c_7 \cos^2(\text{ZA})\} \quad (9)$$

while ΔGlo is computed by

$$\Delta\text{Glo} = d_2 \Delta C^2 \quad (10)$$

The simplified form of equation (10) is based on the assumption that the difference between the satellite-measured radiance and the clear radiance value is proportional to the difference between downwelling surface irradiance and clear-sky irradiance. The use of the simplified cloud-modifier term of equation (10) does produce fairly accurate results when compared with the 1982-83 Georgia Tech surface measurements: the resulting rms error in daily totals being 1.45 MJ/m² (compared to 1.30 MJ/m² for the complete form of cloud modifier in equation (6)).

The reason the simple cloud modifier term can do so well in estimating the global horizontal insolation is illustrated by some results of physical modeling, shown in Figure 21. In this figure, the spectral model of Justus and Paris (1985) is used to calculate

the clear-sky global transmissivity to the surface and the GOES VISSR-band reflectance at the top of the atmosphere. Clear-sky values are the points with highest transmissivity on each curve in Figure 21. Also plotted in this figure are the global transmissivities and VISSR-band reflectances for cloud layers of optical depths 2, 4, 8, 16, 32, and 64 (calculated using a form of the Justus and Paris spectral model which treats a cloud layer with the delta-Eddington radiative transfer procedure). Partly cloudy cases (i.e. cases with a mixture of clear conditions and conditions represented by clouds of a given optical depth) would presumably fall somewhere on a line connecting the clear-sky point and the cloud layer point in Figure 21. The results of Figure 21 show that, for global surface irradiance, partly cloudy cases would correspond closely to overcast cloud layer cases which would result from clouds of somewhat lower optical depth than those actually present in partial cloud cover amount. The linearity of the curves for the various cloud layer cases in Figure 21 is a confirmation of the assumption used as the basis for the simple cloud modifier, equation (10), i.e. that the difference between the satellite-measured radiance and the clear radiance value is proportional to the difference between downwelling surface irradiance and clear-sky irradiance.

For the direct normal irradiance, the same result does not hold, however, as seen by the physical model simulation results in Figure 22. In this case, the direct normal irradiance rapidly drops to zero as the cloud layer optical depth increases. Partly cloudy cases could fall essentially anywhere in the large triangular area of Figure 22 which is delineated by the dashed lines. This result explains the significantly larger errors which result in the satellite estimates of direct normal irradiance, and also explains why the more complete cloud-modifier term of equation (4) does significantly better for direct normal insolation than does one of the simple form analogous to equation (10). The inclusion of terms in σ_C are particularly helpful in characterizing the effects of partly cloudy situations for the direct normal insolation estimates, in a way that is not necessary for the global horizontal case.

DEVELOPMENT OF A SATELLITE INSOLATION
ESTIMATION TECHNIQUE FOR PHOTOVOLTAIC SYSTEMS

In addition to the highly accurate Eppley radiometers used as surface observation data to develop the methods for satellite estimation of the global horizontal, direct normal, and global tilted, the Georgia Tech solar radiation monitoring site also includes Licor photocell radiometers, operated both on the horizontal and on a latitude tilt angle. Figure 23 shows a comparison of the spectral response curve of the Licor photocell radiometer to that for typical crystalline silicon photocell material (Bird and Hulstrom, 1982). Georgia Tech surface measurements during 1982 and 1983 have also been used to develop a method for using the satellite data to estimate global horizontal or tilted irradiance as measured by these Licor photocell radiometers.

The same form of the equations (1)-(8) can be used to estimate the global, direct and latitude-tilted insolation for the Licor photocell range of the spectrum. Different values of the coefficients are required, however. For example the coefficients for use in equations (5) and (6) for the Licor photocell would be $c_0 = 0.4788$, $c_1 = -0.0006354$, $c_2 = 0.003435$, $c_3 = -0.0007331$, $c_4 = 0.6819$, $c_5 = -0.004569$, $c_6 = -0.01052$, $c_7 = -0.3761$, $c_8 = 0.004149$, and $c_9 = 0.02500$. The coefficients of the terms which depend on precipitable water are generally smaller than for the broad-band model, because the limited wavelength range of the Licor photocell is less sensitive to water vapor absorption effects. The coefficients for the cloud modifier term, equation (6), would be $d_0 = 14.71$, $d_1 = -89.77$, $d_2 = -1.344$, $d_3 = 1.283$, $d_4 = -89.63$, $d_5 = 85.54$, $d_6 = 9.526$, and $d_7 = -9.391$.

The results of comparison of these estimates with the photocell radiometer measurements are shown in Figures 24 and 25. These comparisons indicate comparable accuracies for the photocell irradiance

measurements as for the Eppley instruments, giving rms differences of 8.8% for the global horizontal and 11.0% for the global tilted values for the daily totals. Although the Licor radiometers are normally calibrated in terms of equivalent full solar spectrum irradiance, comparisons with spectral irradiance model results and between the curves in Figure 23, indicate that values of photocell collector system short circuit current in amps per square meter of collector can be estimated as 0.32 times the Licor photocell radiometer reading in W/m^2 .

DEVELOPMENT OF A TECHNIQUE FOR SATELLITE INSOLATION ESTIMATION WITH SNOW COVER ON THE GROUND

The current NOAA operational method for satellite estimation of insolation does not automatically distinguish between high brightness values produced by clouds and by snow cover on the ground. Consequently, clear conditions with snow on the ground will be interpreted as cloudy conditions and the insolation will be significantly underestimated. A set of SOLMET station data for the last part of 1980 was merged with the NOAA GOES satellite brightness data for use in developing a technique to handle the snow cases. These data also include the GOES infrared brightnesses, which can be used to distinguish between cold, bright clouds and (relatively) warm, snow covered ground surfaces. A total of 685 hourly observations with snow cover were identified in the data set from 8 SOLMET sites. Of these, 98 occurred in clear conditions, 365 occurred in overcast conditions, and the remainder were under various degrees of partial cloud cover.

In order to assess the effects of snow and clouds on the transmissivity and reflectivity, the data were paired with clear-sky data by month and hour of the day. Figure 26 shows the results of plotting the observed transmissivity decrease below the corresponding clear-sky transmissivity versus the reflectivity increase above the

corresponding clear-sky reflectivity. Overcast clouds (solid dots in Figure 26) produce large transmissivity decreases to accompany the large reflectivity increases. Clear-sky snow cases (solid triangles) show no transmissivity decrease (and usually a small transmissivity increase) at all reflectivity values. Partly cloudy cases, with and without snow, show intermediate effects, with cases including snow showing the larger increases in reflectivity.

Conceptually, the satellite-measured brightness temperature can be used to distinguish between snow and clouds. Clouds would have temperatures corresponding to the atmospheric temperature at the altitude of their tops, and would generally indicate significantly reduced brightness temperatures in association with their higher reflectance values. Snow, on the other hand, would be relatively less cold compared to normal surface temperatures and should exhibit less temperature decrease in association with the higher reflectances caused by the snow. As the data show in Figure 27, the separation of snow from non-snow cases is not so clear-cut if partial cloud cover is also present. Some effects which obscure the expected signals of temperature and reflectivity are: (1) the snow-covered surface may be somewhat colder than the non-snow covered surface on clear days at the same time (i.e. clear-sky insolation will be more effective in warming non-snow covered ground than snow-covered ground), (2) snow is frequently accompanied by low stratus clouds which are not much colder than surface temperatures because they are not very high.

Based on the data in Figure 27, the method suggested for calculation of global horizontal insolation when snow cases are expected is to: (1) treat the case as clear, ignoring the effects of measured reflectivity, if the reflectivity-temperature point for the case falls to the left of the line drawn in Figure 27, (2) treat the case as cloud-covered, using the conventional cloud-modifier term, if the temperature-reflectivity point falls to the right of the line drawn in Figure 27.

INVESTIGATION OF ERROR REDUCTION IF
PRECIPITABLE WATER IS INCLUDED

Figure 28 shows a scatter plot of observed global transmittance (ratio of global to extraterrestrial horizontal) versus cosine of solar zenith angle for clear skies and low precipitable water (<1.7 cm), with x's showing observations which have less than average observed satellite brightness values, and +'s having higher than average brightness. Figure 29 shows comparable results for the clear cases with high precipitable water (>1.7 cm). These figures illustrate the sensitivity of clear global transmittance both to precipitable water amount and to satellite brightness value (presumably an indication of aerosol turbidity in the atmosphere). Figures 30 and 31 show comparable results for direct normal data.

For comparison, model calculated direct and global transmissivities are also indicated on these figures, as computed by the spectral model of Justus and Paris (1985). For the low-precipitable water cases, PW = 1.0 cm was used, while 2.5 cm was taken for the high precipitable water cases. The aerosol optical depth was taken to be 0.1 for the low brightness cases, and 0.4 for the high brightness case model comparisons. These figures show that the aerosol and precipitable water effects observed are accounted for in the model calculations. However, there is an effect of the relationship between aerosols and precipitable water which appears in the observations, and which must be accounted for in models if they are to produce accurate results: namely that aerosol optical depth tends to increase with increasing precipitable water amount, because of hygroscopic aerosol formation processes.

This effect is even more evident in the observations shown in Figures 32-35, which are for global horizontal and direct normal irradiance at wavelengths below 630nm, a spectral region in which there is essentially no water vapor absorption. All effects of precipitable water level on the data below 630nm must therefore be from water-vapor-related aerosols, not from water vapor absorption

effects.

CONCLUSIONS

Following is a statement of the accomplishments, significant results, and conclusions obtained on the project during the reporting period:

1. A Solar Energy Resource Report from Current Satellite Insolation Data

The insolation estimates made by the Satellite Applications Laboratory of the National Oceanic and Atmospheric Administration (NOAA), under the AgRISTARS program, available on computer tape from NOAA at a spatial resolution of $1^\circ \times 1^\circ$ in latitude-longitude, have been summarized into monthly mean values, standard deviations about the monthly mean, and root-mean-square (rms) deviations across 1° of latitude or longitude. A report outlining the NOAA insolation methodology and giving in atlas form the monthly statistical results has been prepared. An abstract of this report, "Atlas of Satellite-Measured Insolation in the United States, Mexico, and South America", appears in the Appendix. The rms difference between the satellite-estimated and ground-observed monthly mean daily total values is 0.77 MJ/m^2 , or 5.2% of the mean value of 14.8 MJ/m^2 .

2. Development of a Satellite Technique for Direct Beam Insolation Estimates

A 16-month set of surface-measured data has been used together with GOES satellite brightness information from NOAA, to produce a regression model for hourly total global horizontal irradiance, and for hourly total direct normal irradiance. These two estimates can

be combined, using a relation by Klutcher (Solar Energy, 23, 111-114, 1979), to produce an estimate of global irradiance on a tilted surface (estimates have been compared here to measurements taken on a latitude tilt). Results show an rms difference between satellite estimates and observed data of 1.3 MJ/m², or 8.4% of the mean value of 15.8 MJ/m². This accuracy is somewhat better than from a similar comparison against the operational NOAA estimates, interpolated to the Atlanta, Georgia Tech site, which, for the same observation period, showed an rms difference between satellite estimates and observed data of 1.9 MJ/m², or 12.8% of the mean value of 14.9 MJ/m². The direct normal values cannot be estimated as accurately as the global horizontal, giving an rms difference of 3.1 MJ/m², or 21.3% of the mean value of 14.4 MJ/m². Because it relies in part on the direct normal estimate, the estimated global tilted values are also slightly less accurate than the global horizontal values, with an rms difference of 1.9 MJ/m², or 11.1% of the mean value of 17.2 MJ/m². This error estimate for the daily total global tilted irradiance is, however, comparable to the estimated accuracy in the current NOAA operational estimates of daily total global horizontal irradiance.

Data for the monthly average daily totals for global horizontal, direct normal, and global latitude-tilted insolation show an rms difference between satellite estimates and observed data of 0.4 MJ/m², or 2.9% of the mean value of 15.1 MJ/m² for the global horizontal. For the direct normal, the rms error is 1.0 MJ/m², or 6.7% of the mean value of 15.0 MJ/m²; while for the latitude-tilted insolation, the rms error is 0.8 MJ/m², or 4.5% of the mean value of 17.5 MJ/m². Considerable improvement in relative error is thus achieved for monthly average values as opposed to individual daily totals.

3. Development of a Satellite Insolation Estimation Technique for Photovoltaic Systems

Georgia Tech surface measurements with a Licor photocell sensor during 1982 and 1983 have also been used to develop a method for using the satellite data to estimate global horizontal or tilted irradiance as measured by these Licor photocell radiometers. The results of comparison of these estimates with the photocell radiometer measurements indicate comparable accuracies for the photocell irradiance measurements as for the Eppley instruments, giving rms differences of 8.8% for the global horizontal and 11.0% for the global tilted values. Although the Licor radiometers are normally calibrated in terms of equivalent full solar spectrum irradiance, comparisons with spectral irradiance model results and between the curves in Figure 6, indicate that values of photocell collector system short circuit current in amps per square meter of collector can be estimated as 0.32 times the Licor photocell radiometer reading in W/m^2 .

4. Development of a Technique for Satellite Insolation Estimation with Snow Cover on the Ground

Based on the reflectivity-brightness temperature data in Figure 27, the method suggested for calculation of global horizontal insolation when snow cases are expected is to: (1) treat the case as clear, ignoring the effects of measured reflectivity, if the reflectivity-temperature point for the case falls to the left of the line drawn in Figure 27, (2) treat the case as cloud-covered, using the conventional cloud-modifier term, if the temperature-reflectivity point falls to the right of the line drawn in Figure 27.

5. Investigation of Error Reduction if Precipitable Water is Included

Data presented in Figures 28-35 illustrate the sensitivity of clear global, clear direct normal, shortwave clear global, and shortwave clear direct normal transmittance both to precipitable water amount and to satellite brightness value (presumably an indication of aerosol turbidity in the atmosphere). An effect of the relationship between aerosols and precipitable water which appears in the observations, and which must be accounted for in models if they are to produce accurate results is that aerosol optical depth tends to increase with increasing precipitable water amount, because of hygroscopic aerosol formation processes. This effect is even more evident in the observations shown in Figures 32-35, which are for global horizontal and direct normal irradiance at wavelengths below 630nm, a spectral region in which there is essentially no water vapor absorption. All effects of precipitable water level on the data below 630nm must therefore be from water-vapor-related aerosols, not from water vapor absorption effects.

REFERENCES

- Atwater, M. A. and J. T. Ball (1978): "A Numerical Solar Radiation Model Based on Standard Meteorological Observations", Solar Energy, 21, 163-170.
- Atwater, M. A. and P. S. Brown, jr. (1974): "Numerical Computations of the Latitudinal Variation of Solar Radiation for an Atmosphere of Varying Opacity", J. Appl. Meteorol., 13, 289-297.
- Bird, R. E., and R. L. Hulstrom (1982): "Extensive Modeled Terrestrial Solar Spectral Data Sets with Solar Cell Analysis", SERI/TR-215-1598, December.
- Brakke, T. W. and E. T. Kanemasu (1981): "Insolation Estimation from Satellite Measurements of Reflected Radiation", Proceedings of the First Workshop on Terrestrial Solar Resource Forecasting and on the Use of Satellites for Terrestrial Solar Resource Assessment, Washington, DC, 2-5 February, American Solar Energy Society, Newark, DE
- Diak, G. R., and C. Gautier (1983): "Improvements to a Simple Physical Model for Estimating Insolation from GOES Data", J. Clim. Appl. Meteorol., 22, 505-508.
- Gautier, C. (1982): "Mesoscale Insolation Variability Derived from Satellite Data", J. Appl. Meteorol., 21, 51-58.
- Gautier, C. (1983): "Insolation Estimates from Satellites", final report for NOAA contract NA81AA-H-00024, mod.2, May.
- Gautier, C. and K. B. Katsaros (1984): "Insolation During STREX 1. Comparisons Between Surface Measurements and Satellite Estimates", J. Geophys. Res., 89(D7), 11,779 - 11,788.
- Gautier, C. et al. (1980): "A Simple Physical Model to Estimate Incident Solar Radiation at the Surface from GOES Satellite Data", J. Appl. Meteorol., 19, 1005-1012.
- Halpern, P. (1984): "Ground Level Solar Energy Estimates Using Geostationary Operational Environmental Satellite Measurements and Realistic Model Atmospheres", Remote Sensing of Environment, 15, 47-61.
- Hanson, K. J. (1971): "Studies of Cloud and Satellite Parameterization of Sol. Dept. Commerce, 133-148.
- Hay, J. E. and K. J. Hanson (1978); "A Satellite-Based Methodology for Determining Solar Irradiance at the Ocean Surface During GATE", Bull. Amer. Meteor. Soc., 59, 1549.
- Hulstrom, R. L., et al. (1981): "Solar radiation energy resource atlas of the United States", SERI/SP-642-1037, October.

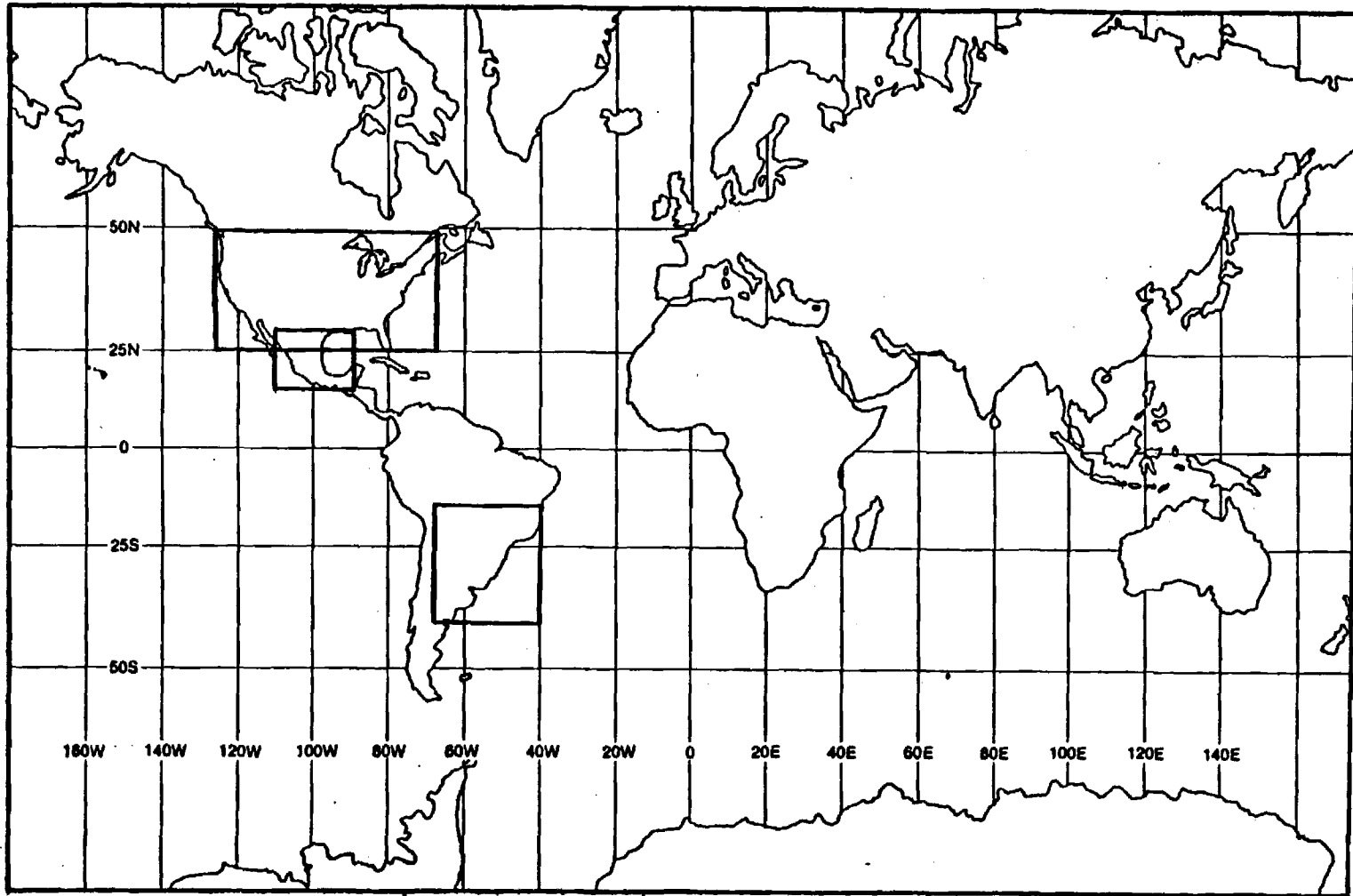
- Justus, C. G. (1984): "Atmospheric and Surface Short-Wave Energy Balance from Combined Satellite and Ground-Based Data", Conf. on Satellite Meteorology, Remote Sensing and Applications, Clearwater Beach, FL, June 25-29.
- Justus, C. G. and M. V. Paris (1985): "A Model for the Solar Spectral Irradiance and Radiance at the Bottom and Top of a Cloudless Atmosphere", J. Clim. Appl. Meteor., 24, 193-205.
- Justus, C. G., M. V. Paris, and J. D. Tarpley (1985): "Satellite-Measured Insolation in the United States, Mexico and South America", submitted to Remote Sensing of Env.
- Justus, C. G. and J. D. Tarpley (1983): "Accuracy and Availability of Solar Radiation Data from Satellites and from Forecast Estimates", Proc. 5th AMS Conf. on Atmospheric Radiation, Oct.31-Nov.4, 1983, Baltimore, MD.
- Justus, C. G. and J. D. Tarpley (1984): "Atlas of Satellite-Measured Insolation in the United States, Mexico and South America", Technical Report on DOE/SOLERAS Grant DE-FG02-84CH10200, Georgia Tech Project G-35-633.
- Klucher, T. M. (1979): "Evaluation of Models to Predict Insolation on Tilted Surfaces", Solar Energy, 23, 111-114.
- Moser, W. and E. Raschke (1984): "Incident Solar Radiation over Europe Estimated from METEOSAT Data", J. Clim. Appl. Meteorol., 23, 166-170.
- Raphael, C. (1983): "Models for Estimating Solar Irradiance at the Earth's Surface from Satellite Data: An Initial Assessment", Canadian Climate Centre Report No. 83-1.
- Raphael, C., and J. E. Hay (1984): "An Assessment of Models Which Use Satellite Data to Estimate Solar Irradiance at the Earth's Surface", J. Clim. Appl. Meteorol., 23, 832-844.
- Riordan, C. J. (1984): "A Preliminary Comparison of Insolation Measurements, Forecasts, and Estimates from Satellite Imagery, SERI/TR-215-2046.
- Riordan, C. J. and R. L. Hulstrom (1982): "A Review of Potential Satellite Techniques for Mesoscale Mapping of Insolation", SERI/TR-215-1824.
- Sherry, J. E. and C. G. Justus (1983): "A Simple Hourly Clear-Sky Solar Radiation Model Based on Meteorological Parameters", Solar Energy, 30, 425-431.
- Sherry, J. E. and C. G. Justus (1984): "A Simple Hourly All-Sky Solar Radiation Model Based on Meteorological Parameters", Solar Energy, 32, 195-204.

- Suckling, P. W. (1983): "Extrapolation of Solar Radiation Measurements: Mesoscale Analyses from Arizona and Tennessee Valley Authority Regions", J. Clim. Appl. Meteor., 22, 488-494.
- Suckling, P. W. and J. E. Hay (1977): "A Cloud Layer-Sunshine Model for Estimating Direct, Diffuse and Total Solar Radiation", Atmosphere, 15, 194-207.
- Tarpley, J. D. (1979): "Estimating Incident Solar Radiation at the Surface from Geostationary Satellite Data", J. Appl. Meteorol., 18, 1172-1181.
- Tarpley, J. D. (1980): "Estimating Insolation from Geostationary Satellites", Proc. Annual ASES Meeting.
- Tarpley, J. D., S. R. Schneider, J. E. Bragg and M. P. Waters, III (1978): "Satellite Data Set for Solar Incoming Radiation Studies", NOAA Tech. Memo., 96, 36pp.

Table 1. Comparison of Error Estimates for Daily Total Insolation from Various Satellite Techniques

<u>Data Set</u>	<u>Mean Daily Total MJ/m² (Ly)</u>	<u>rms Error MJ/m² (Ly)</u>	<u>rms Error % of Mean</u>
Great Plains (1) 896 site-days	24.6 (586)	2.11 (50.4)	8.6
East & Central U.S. 1021 site-days			
Old Regression	14.6 (349)	1.76 (42.1)	12.1
New Regression	14.6 (349)	1.59 (37.9)	10.8
New Regression w/PW	14.6 (349)	1.40 (33.3)	9.5
Physical Model	14.6 (349)	1.25 (29.8)	8.5
Canada (2) 184 site-days	19.4 (462)	1.55 (37)	8
Canada (3) 21 site-days	20.8 (496)	1.25 (30)	6.1(4)
	20.8 (496)	1.05 (25)	5.1(4)
Canada (5) 108 site-days			
Gautier (1980)	12.3 (294)	1.06 (25)	8.6
Hay & Hanson (1978)	12.3 (294)	1.2 (29)	9.8
Old Regression	12.3 (294)	1.5 (36)	12.2

-
- (1) Tarpley (1979), Table 3.
(2) Gautier (1982), Figure 4.
(3) Gautier (1983), Table 5.
(4) Diak and Gautier (1983).
(5) Raphael (1983), Table 7.1.



GOES INSOLATION COVERAGE

Figure 1. Map of AgRISTARS GOES Insolation Estimation Areas.

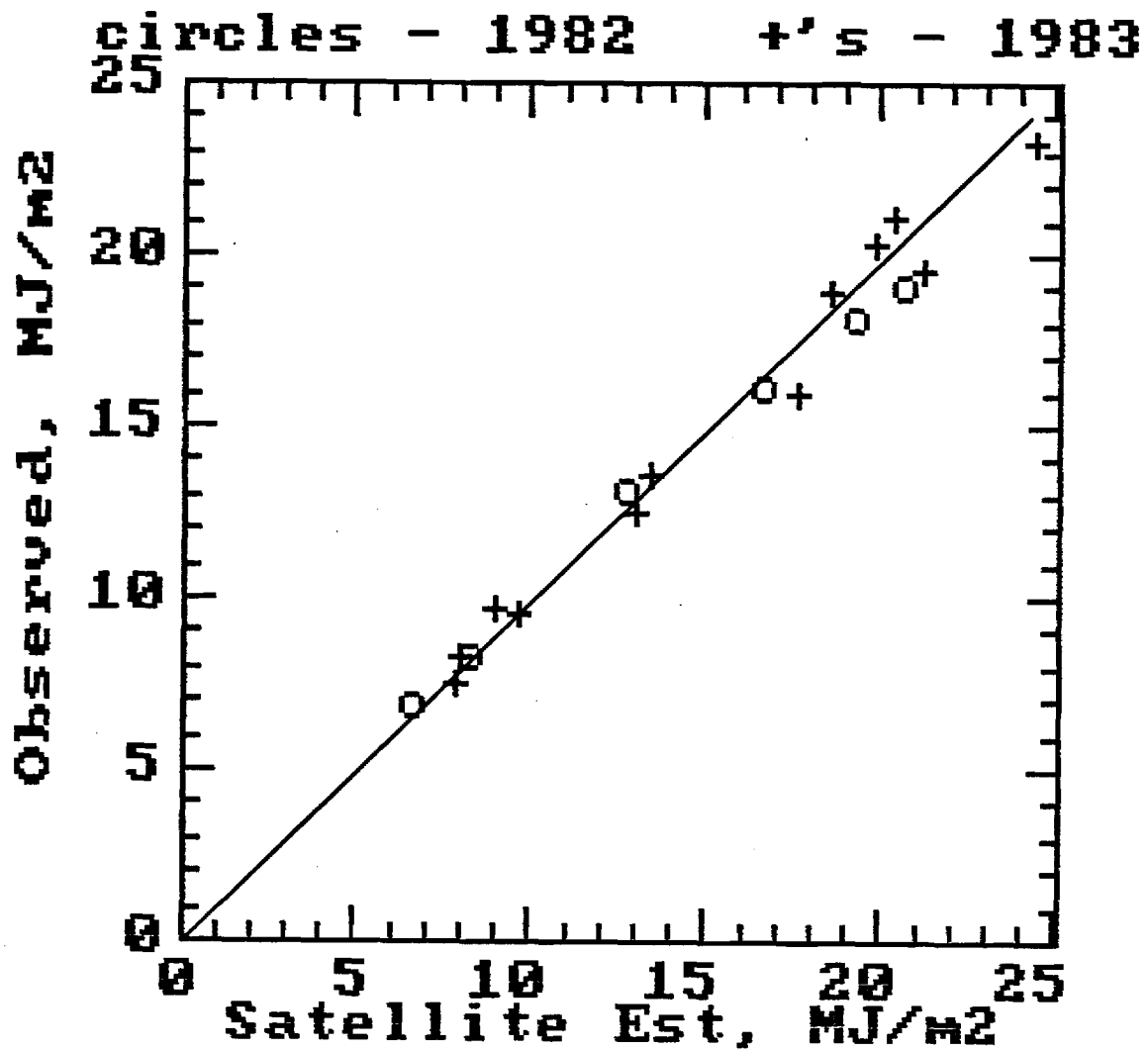


Figure 2. Observed Monthly Mean Insolation at Georgia Tech versus GOES Satellite Estimates for 1982 and 1983. The rms difference between satellite and surface values is 0.77 MJ/m^2 , or 5.2% of the mean value of 14.8 MJ/m^2 .

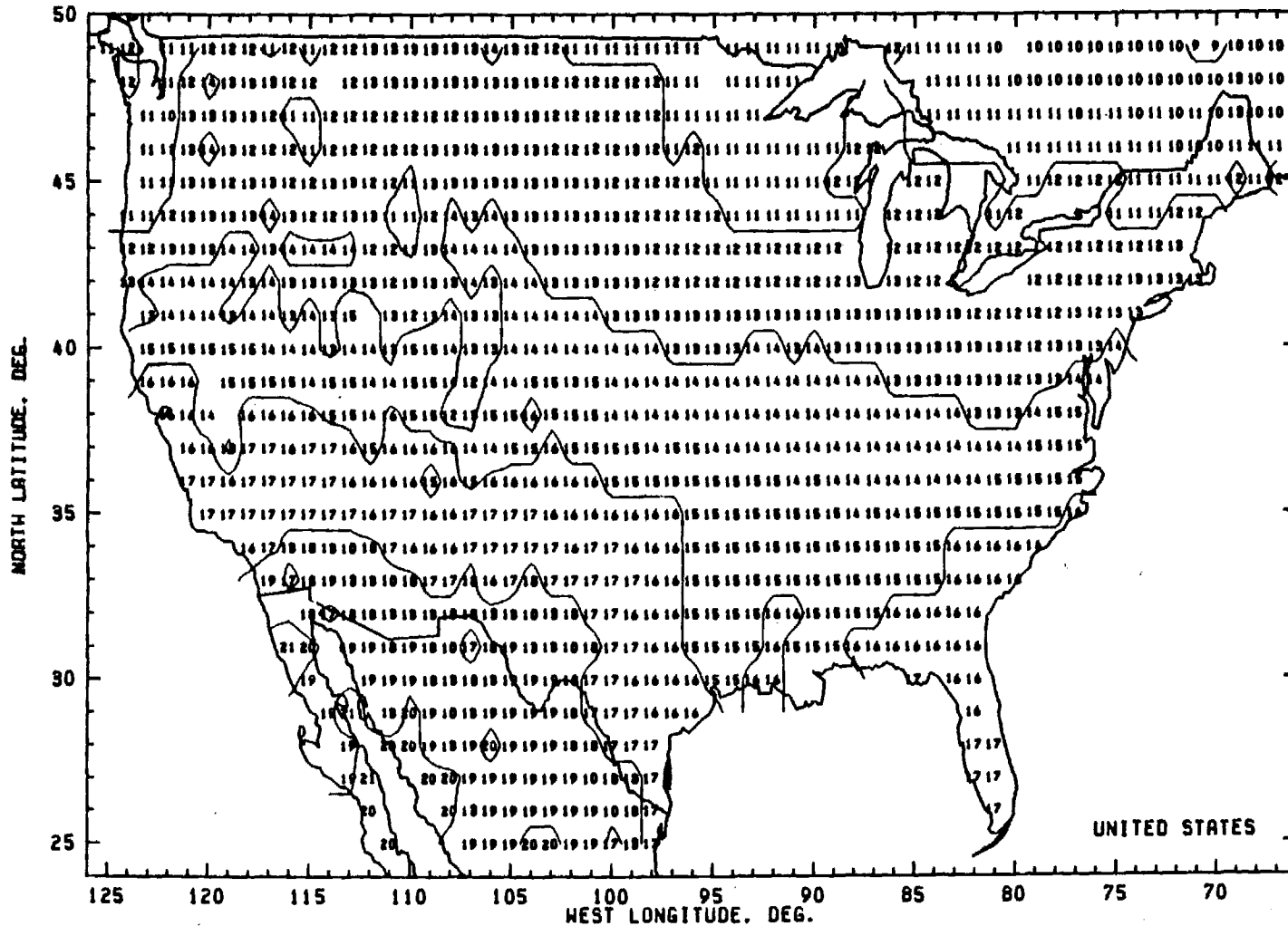


Fig. 3: 1983 Annual Average Daily Total Insolation, MJ/m^2 , Estimated by NOAA/NESIDS Satellite Technique for Continental United States.

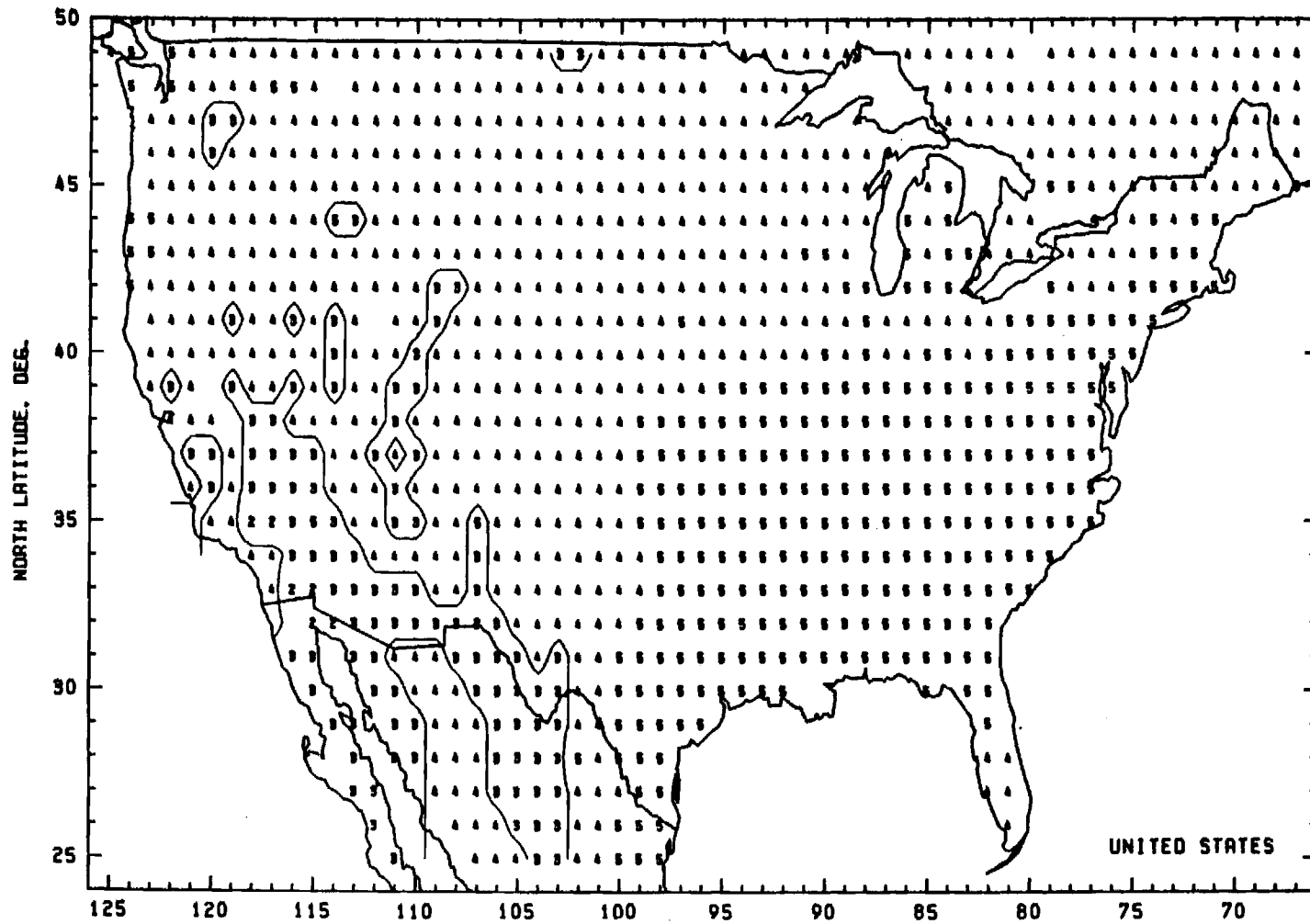


Fig. 4: As in Figure 3 for Standard Deviation of Daily Totals About Monthly Average Daily Total, MJ/m².

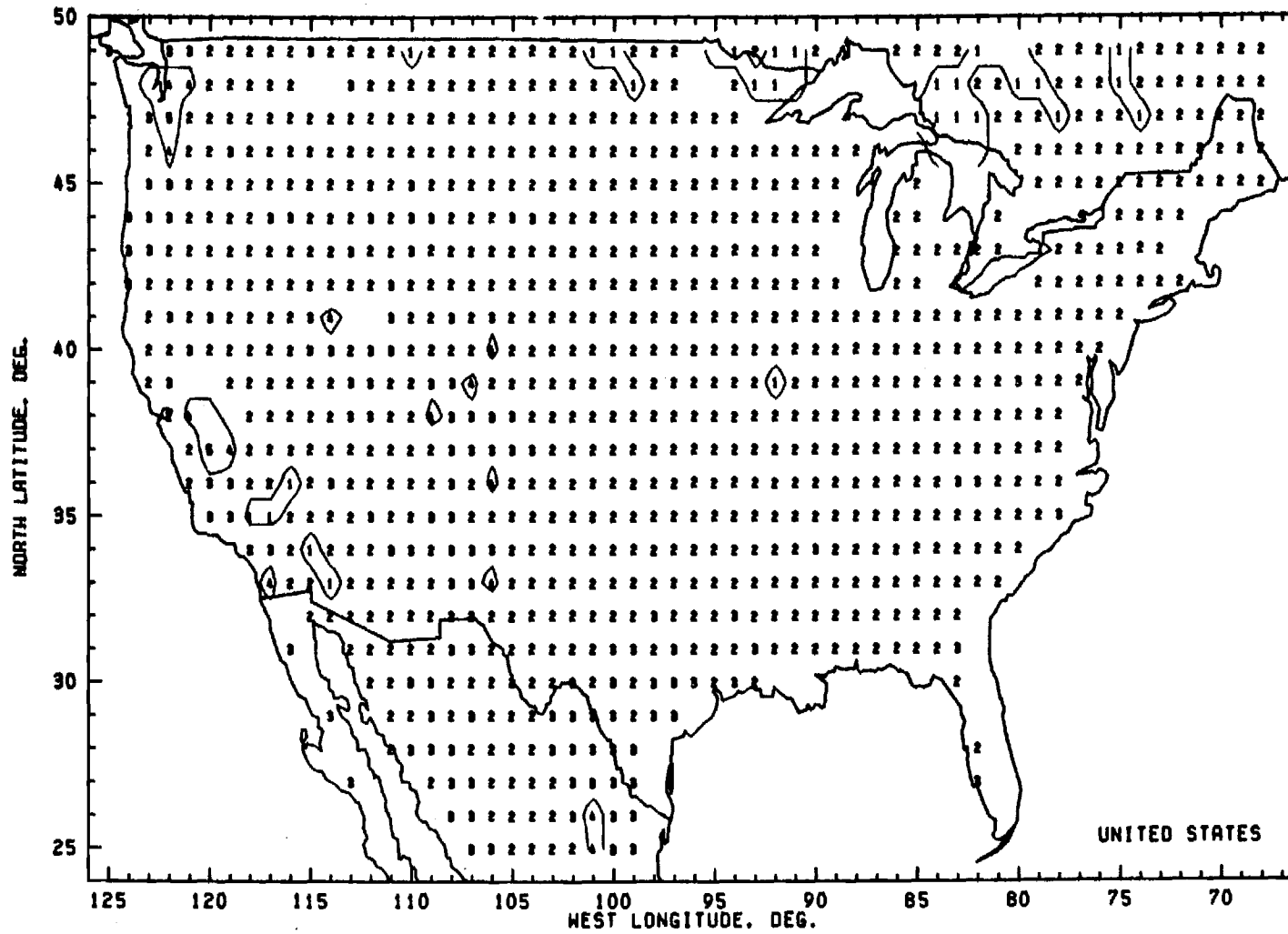


Fig. 5: As in Figure 3 for Root-Mean-Square Difference Across One Degree of Longitude Spacing, MJ/m^2 .

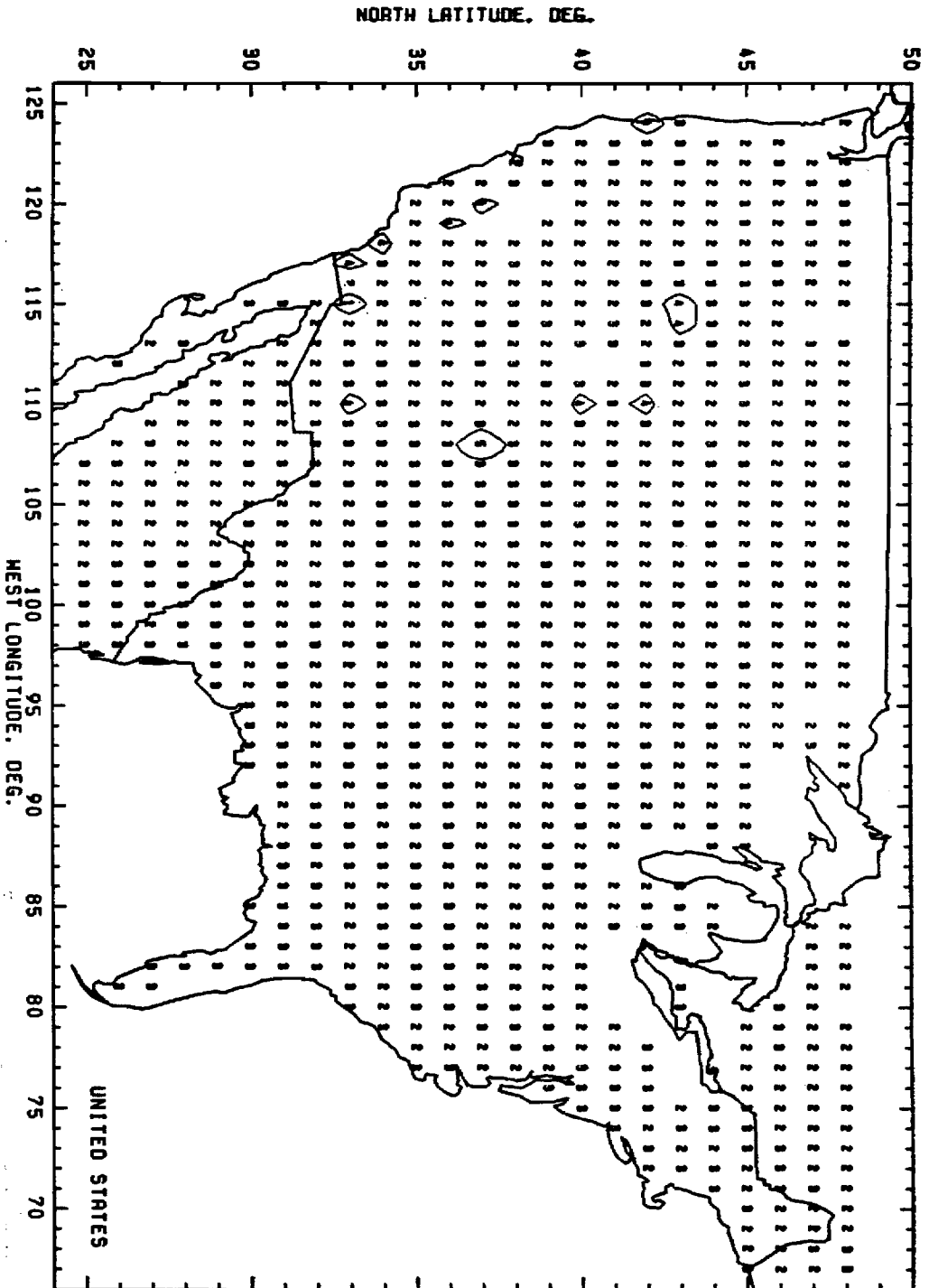


Fig. 6: As in Figure 3 for Root-Mean-Square Difference Across One Degree of Latitude Spacing, MJ/m².

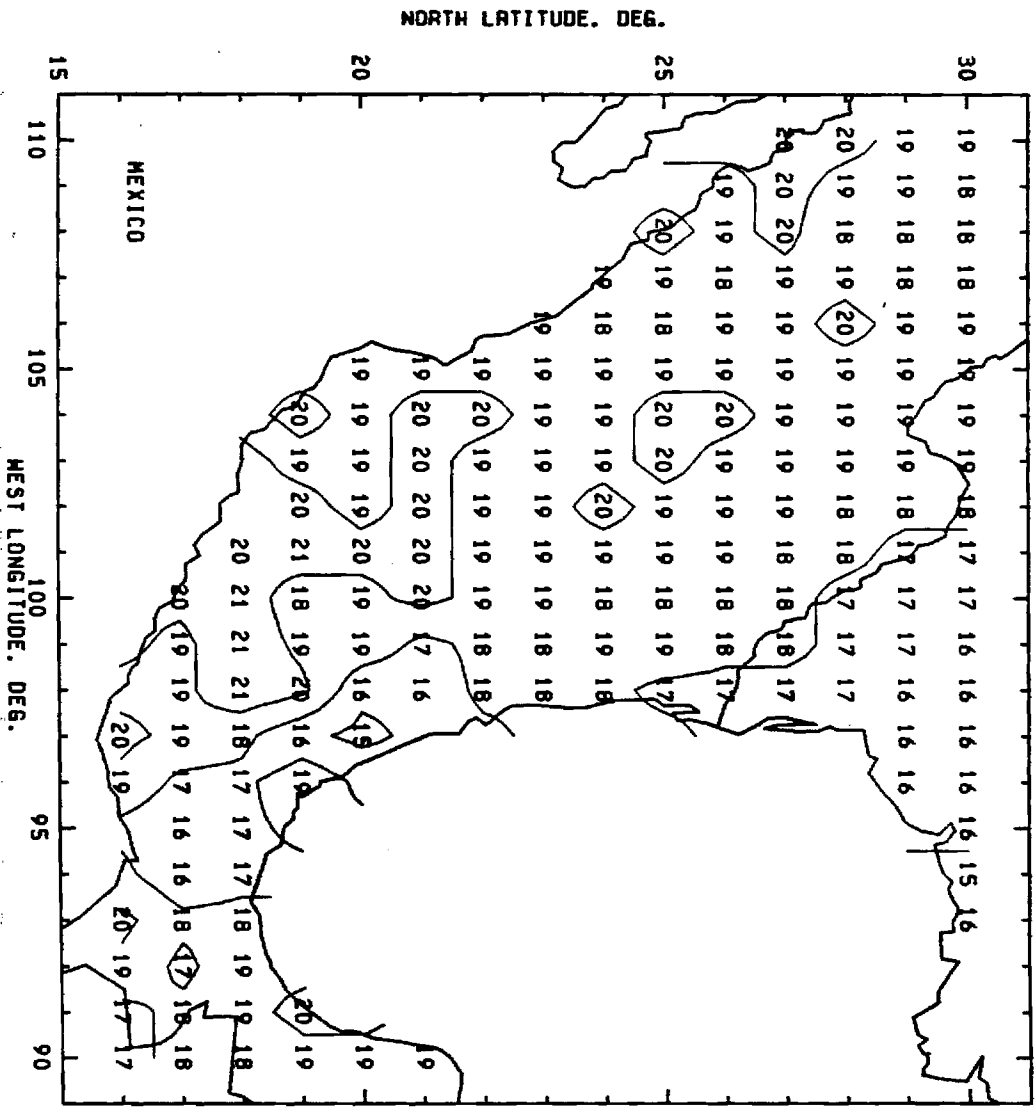


Fig 7: 1983 Annual Average Daily Total Insolation, MJ/m², Estimated by NOAA/NESDIS Technique for Mexico.

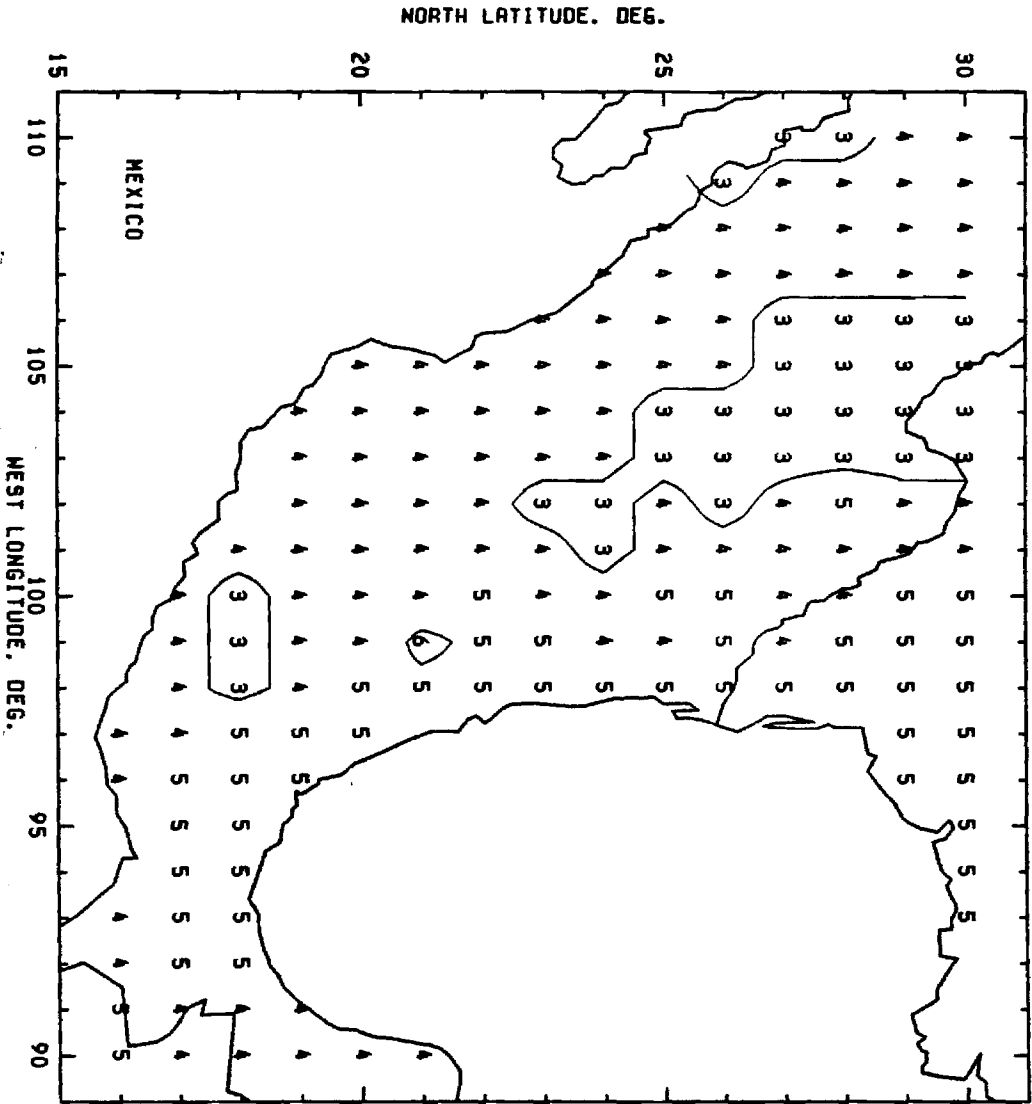


Fig. 8: As in Figure 7 for Standard Difference of Daily Totals About Monthly Average Daily Total, MJ/m².

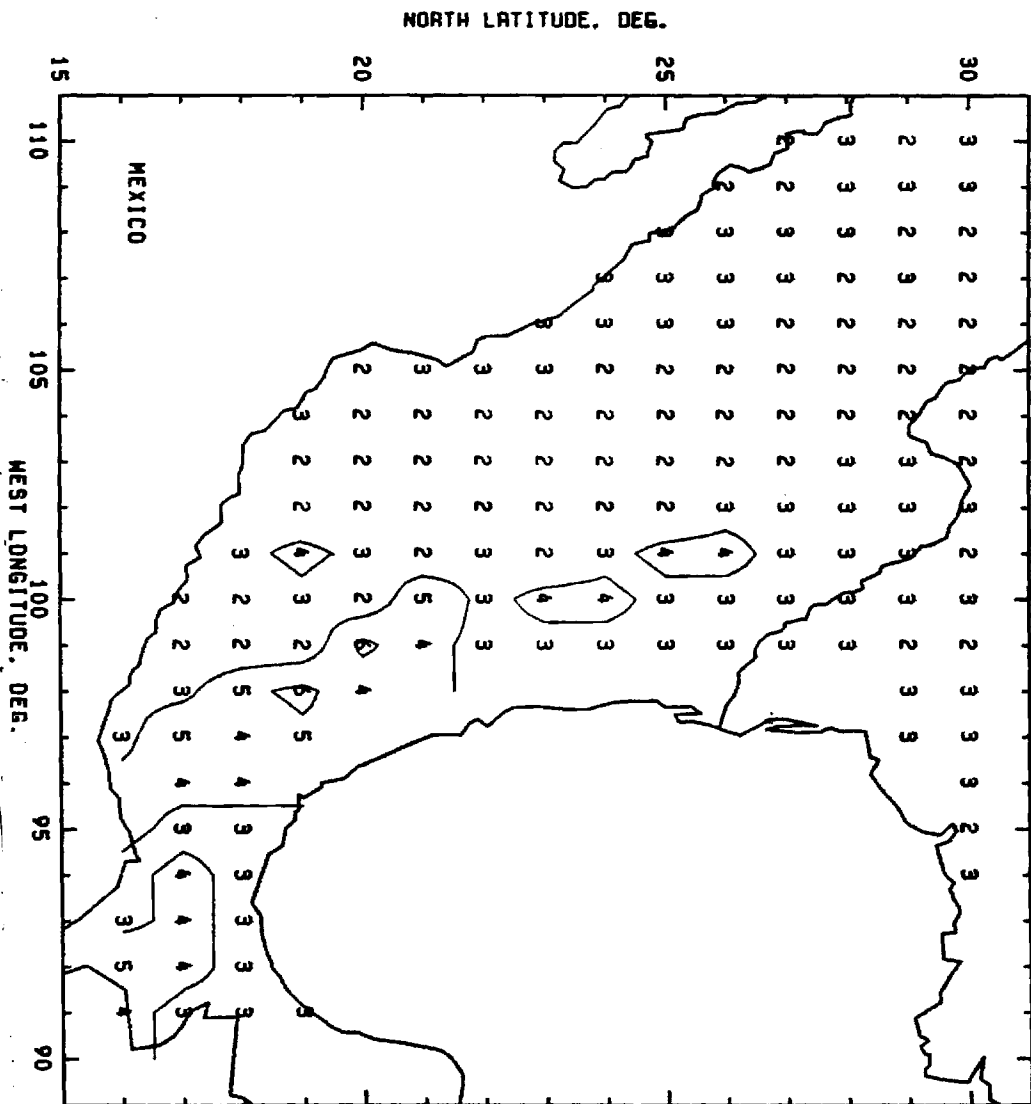


Fig. 9: As in Figure 7 for Root-Mean-Square Difference Across One Degree of Longitude Spacing, MJ/m².

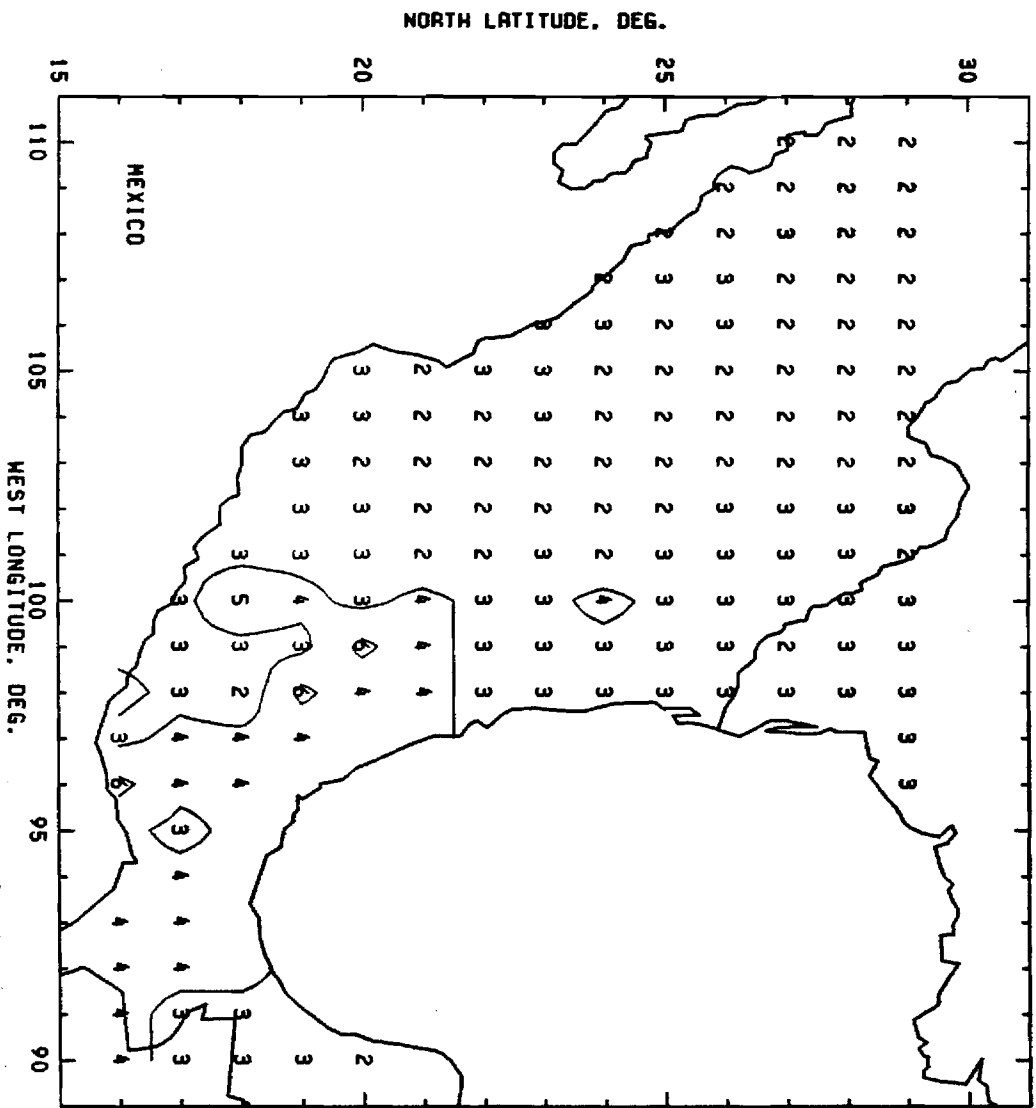


Fig. 10: As in Figure 7 for Root-Mean-Square Difference Across One Degree of Latitude Spacing, MJ/m².

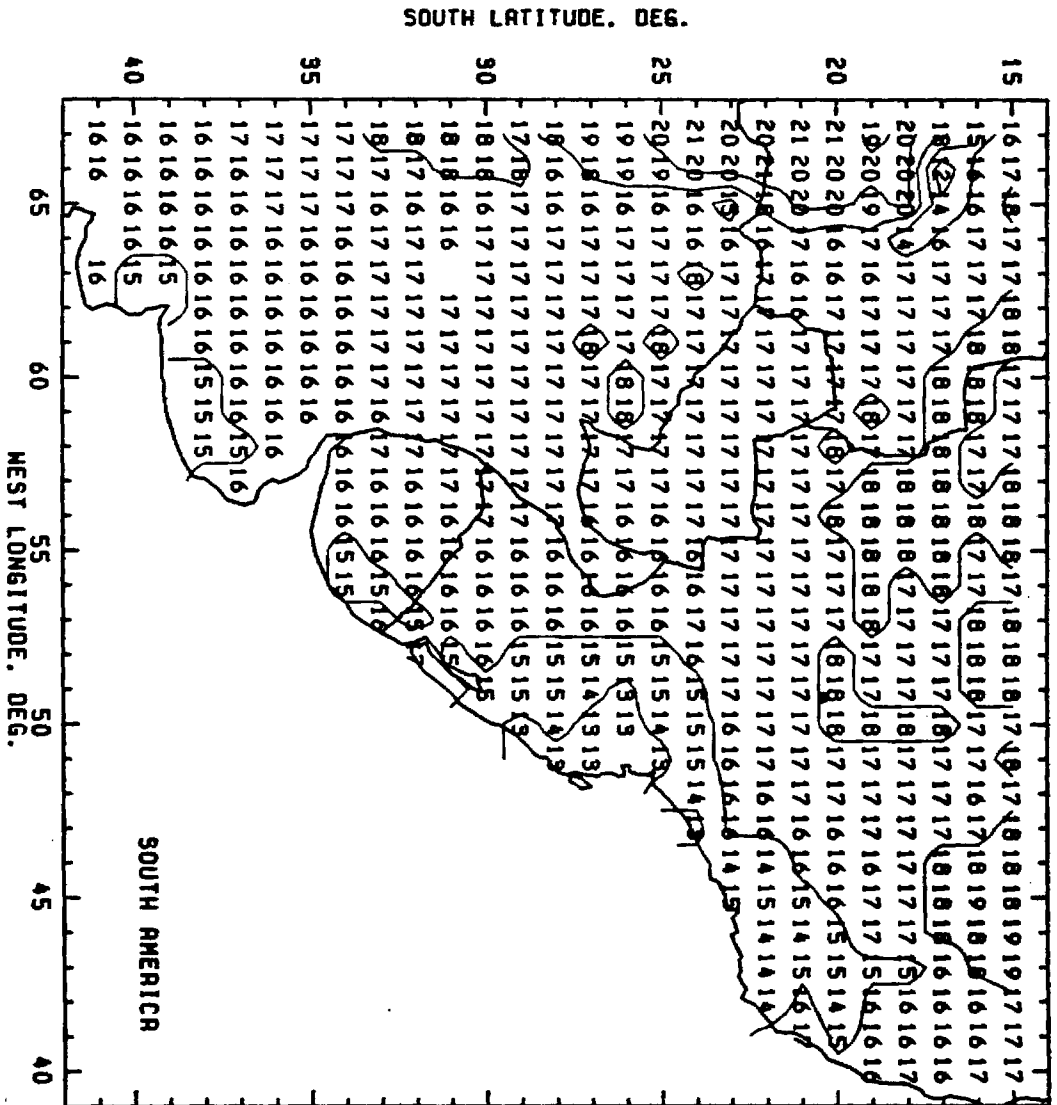


Fig. 11: 1983 Annual Average Daily Total Insolation, MJ/m², Estimated by NOAA/NESDIS Satellite Technique, for Part of South America.

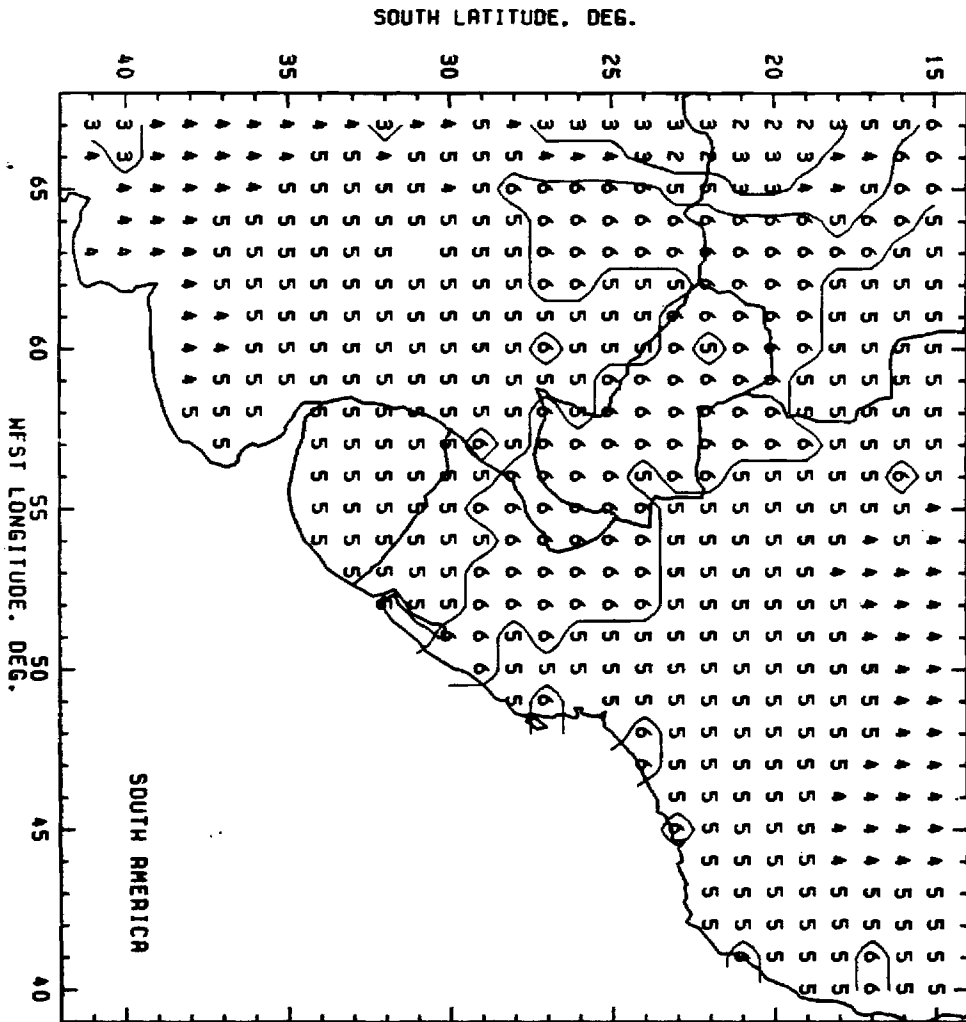


Fig. 12: As in Figure 11 for Standard Deviation of Daily Totals About Monthly Average Daily Total, MJ/m².

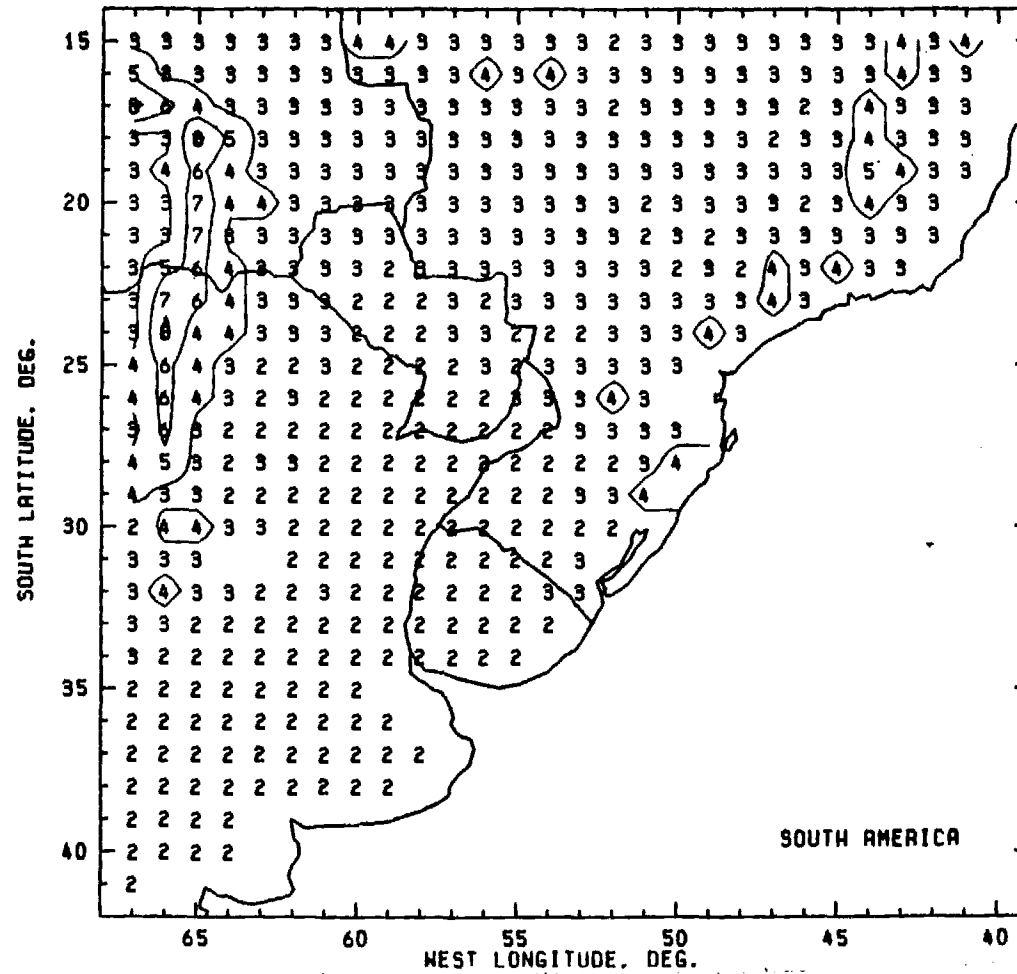


Fig. 13: As in Figure 11 for Root-Mean-Square Difference Across One Degree of Longitude Spacing, MJ/m².

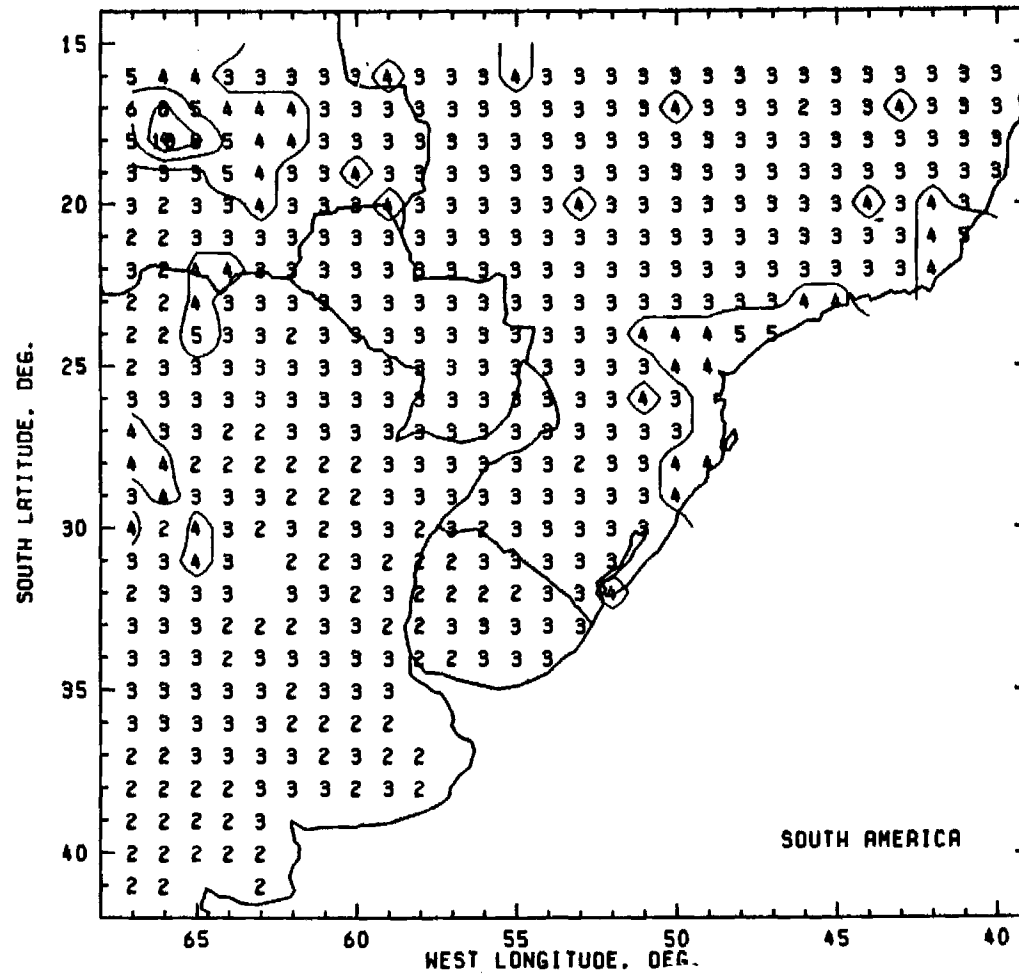


Fig. 14: As in Figure 11 for Root-Mean-Square Difference Across One Degree Latitude Spacing, MJ/m².

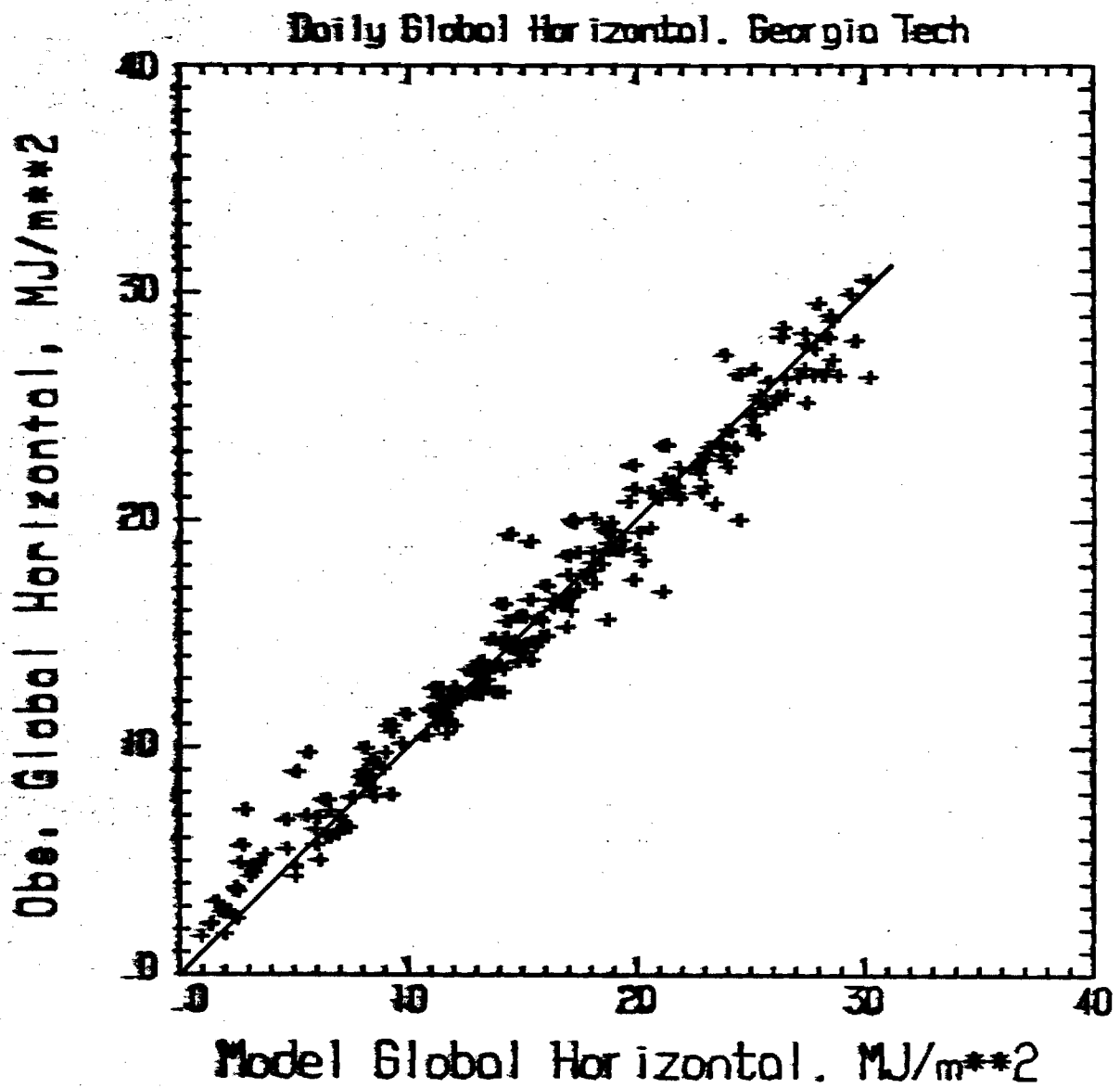


Fig. 15: Observed Daily Total Global Horizontal Irradiance Versus Satellite Estimated, Georgia Tech Site, 1982-1983.

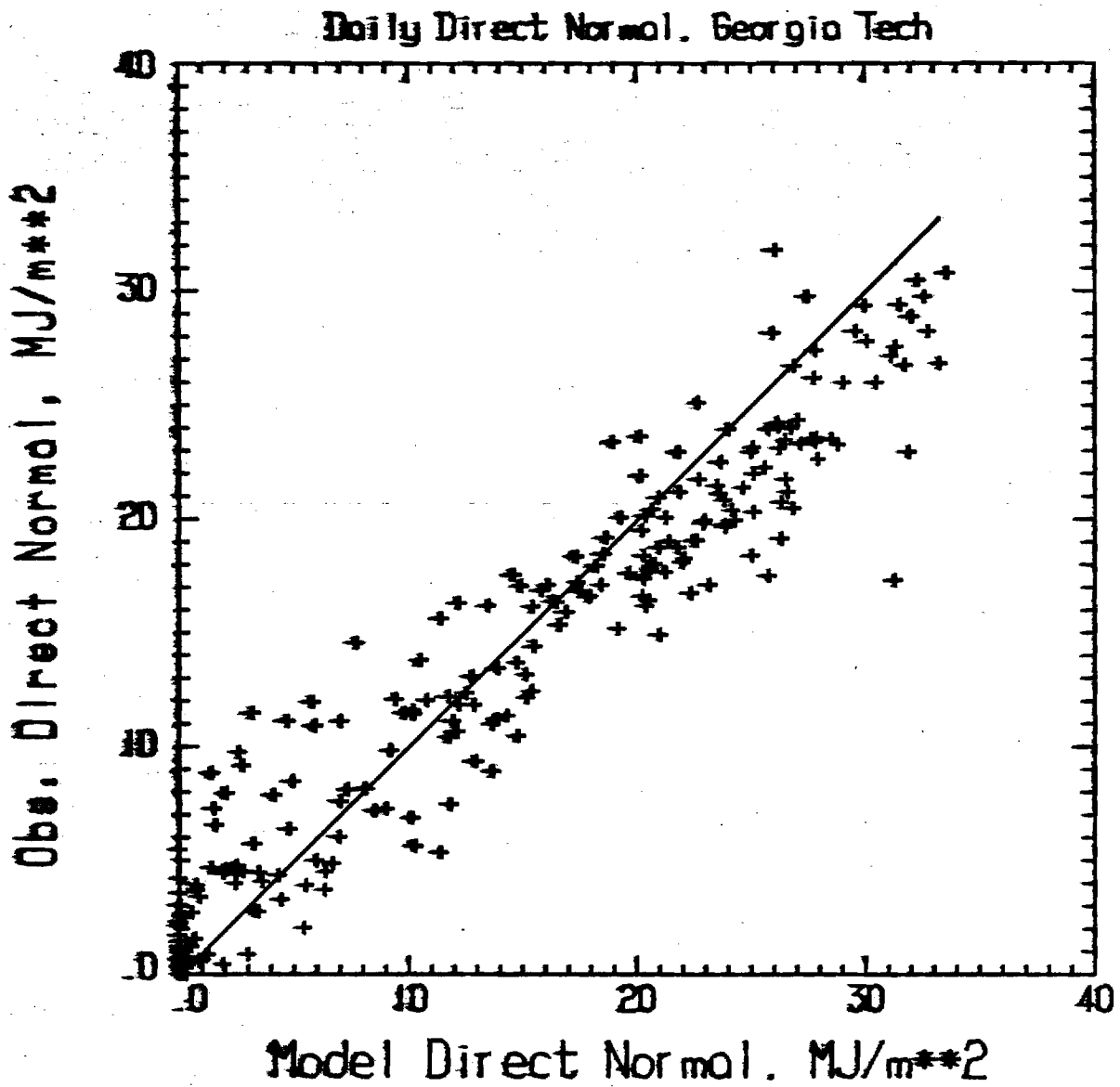


Fig. 16: As in Figure 15 for Direct Normal.

Daily Global Tilted. Georgia Tech

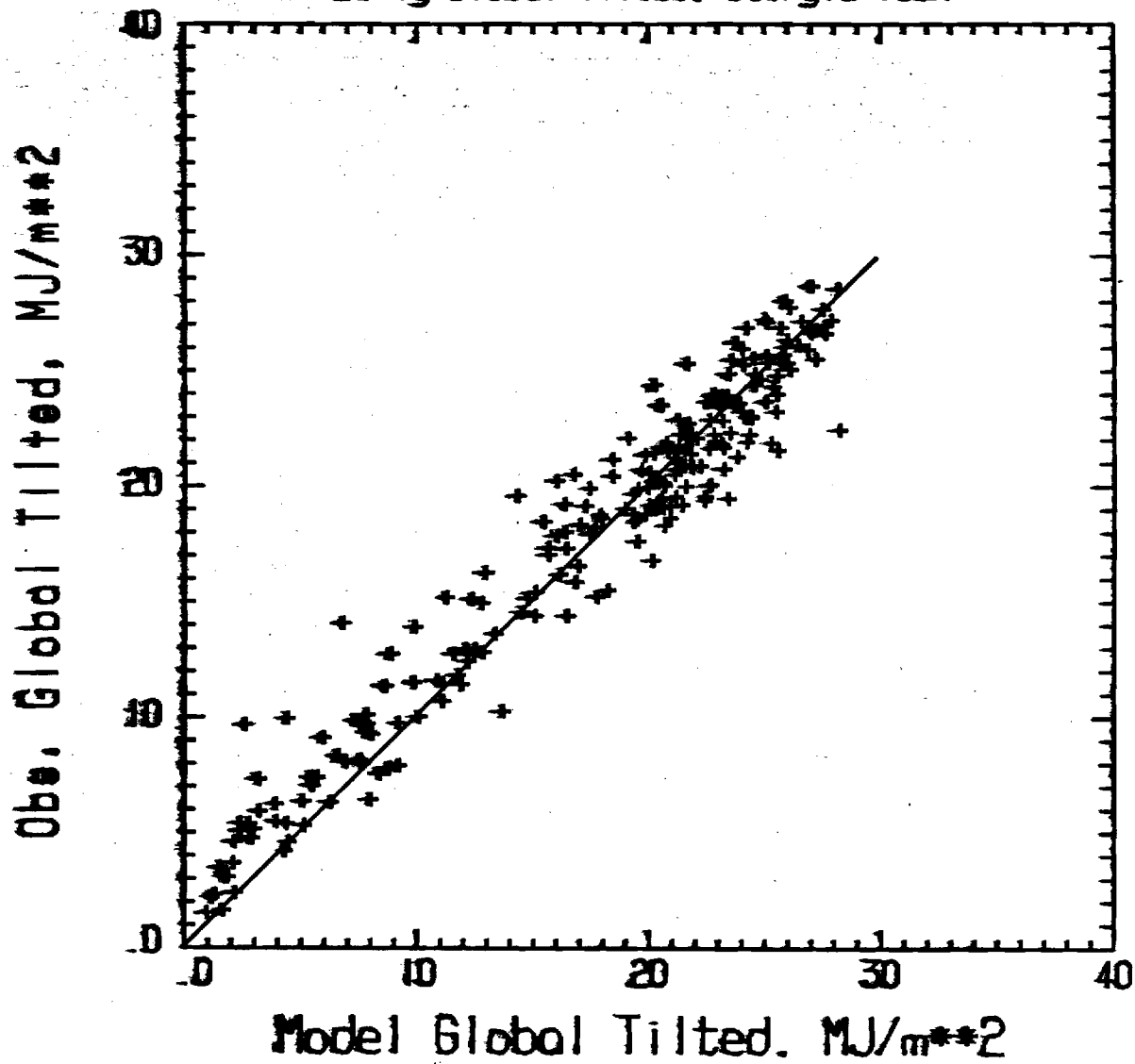


Fig. 17: As in Figure 15 for Global Irradiance on a Latitude Tilted Surface.

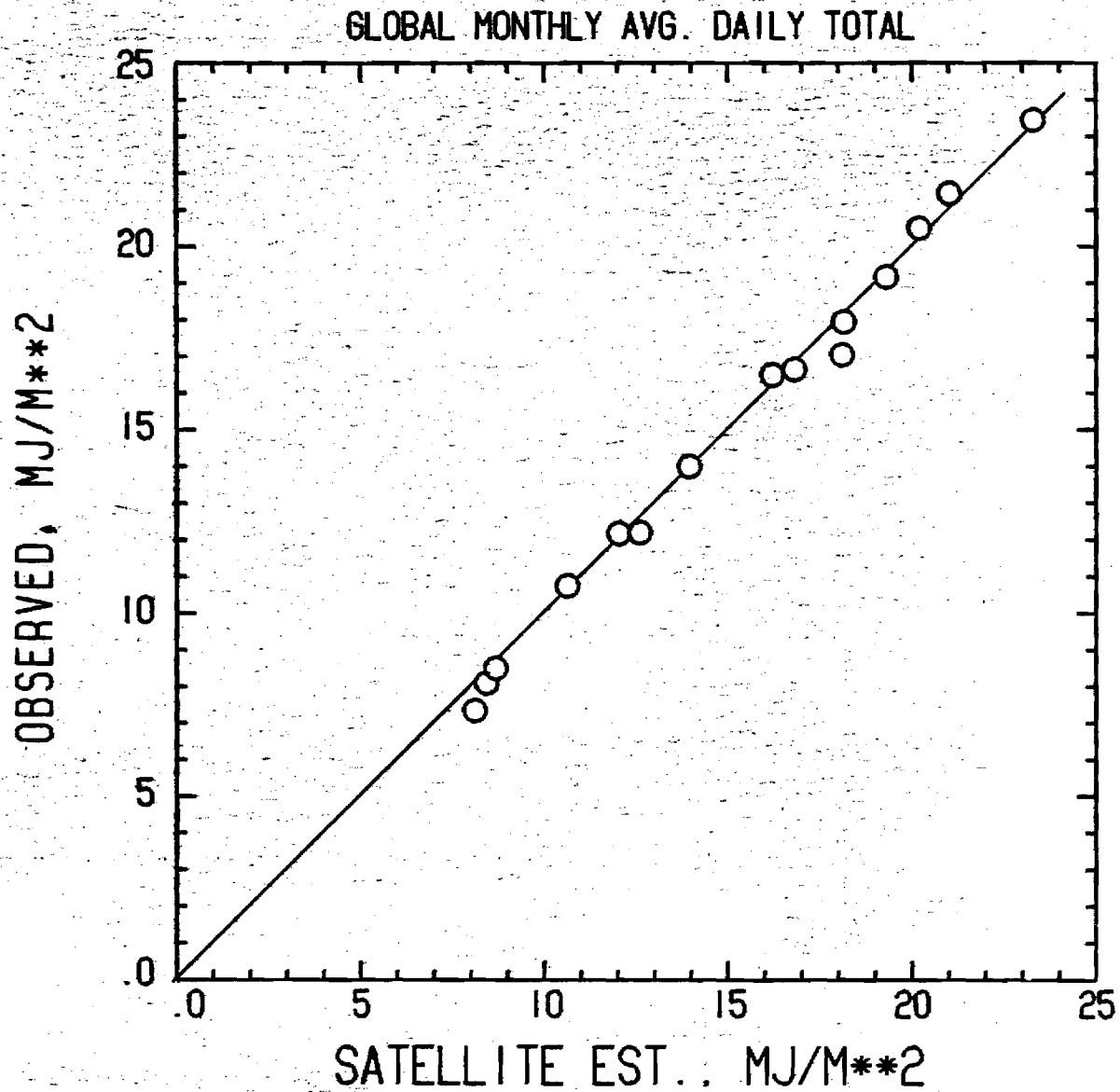


Fig. 18: Comparison of Satellite-Estimated Monthly Mean Insolation on a Horizontal Surface with Ground-Based Measurements Made at Georgia Tech, 1982-1983. RMS difference is 0.4 MJ/m² or 2.9% of Mean Value of 15.1 MJ/m².

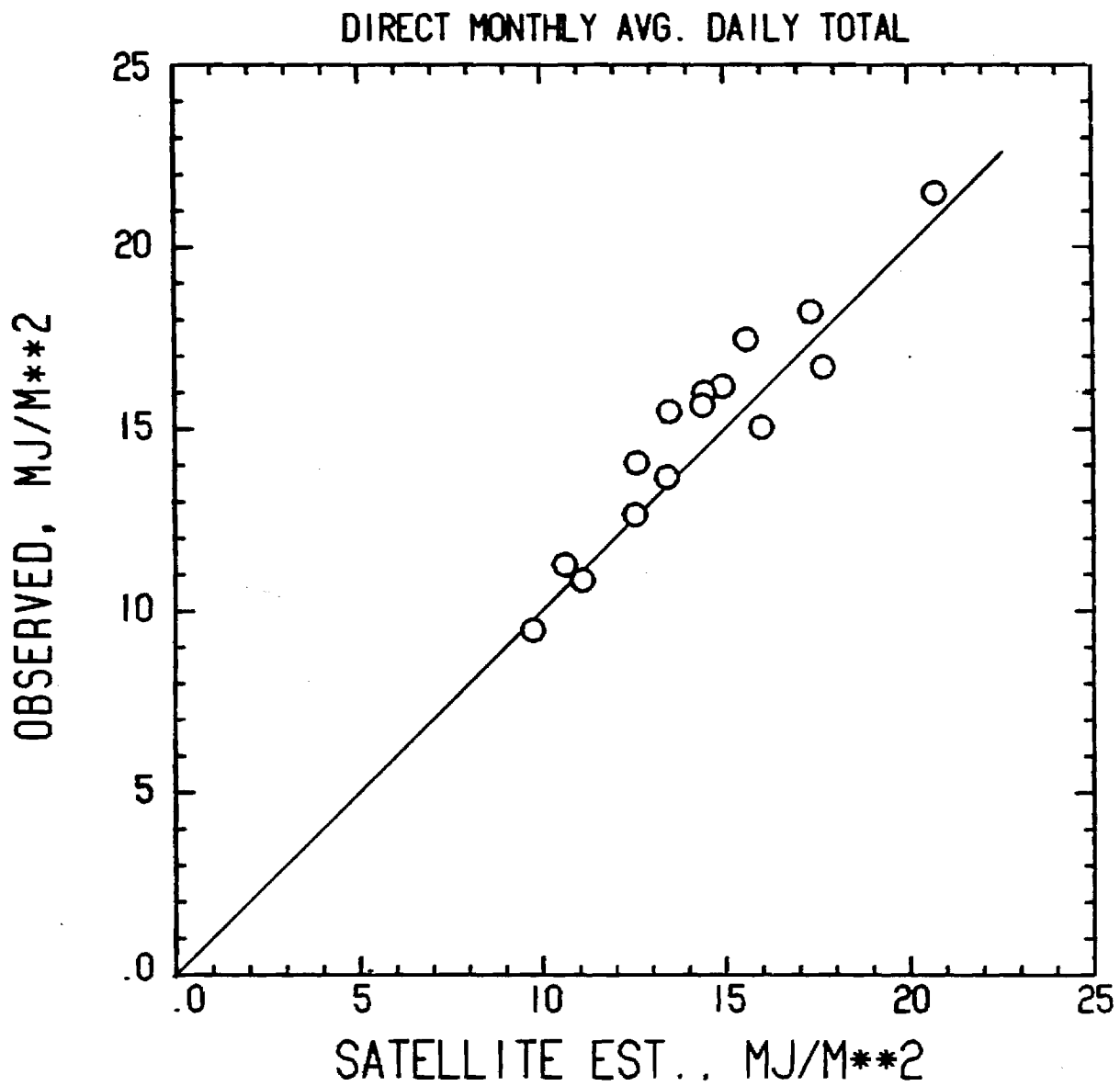


Fig. 19: As in Figure 18 for Direct Normal Insolation. RMS difference is 1.0 MJ/m², or 6.7% of mean value of 15.0 MJ/m².

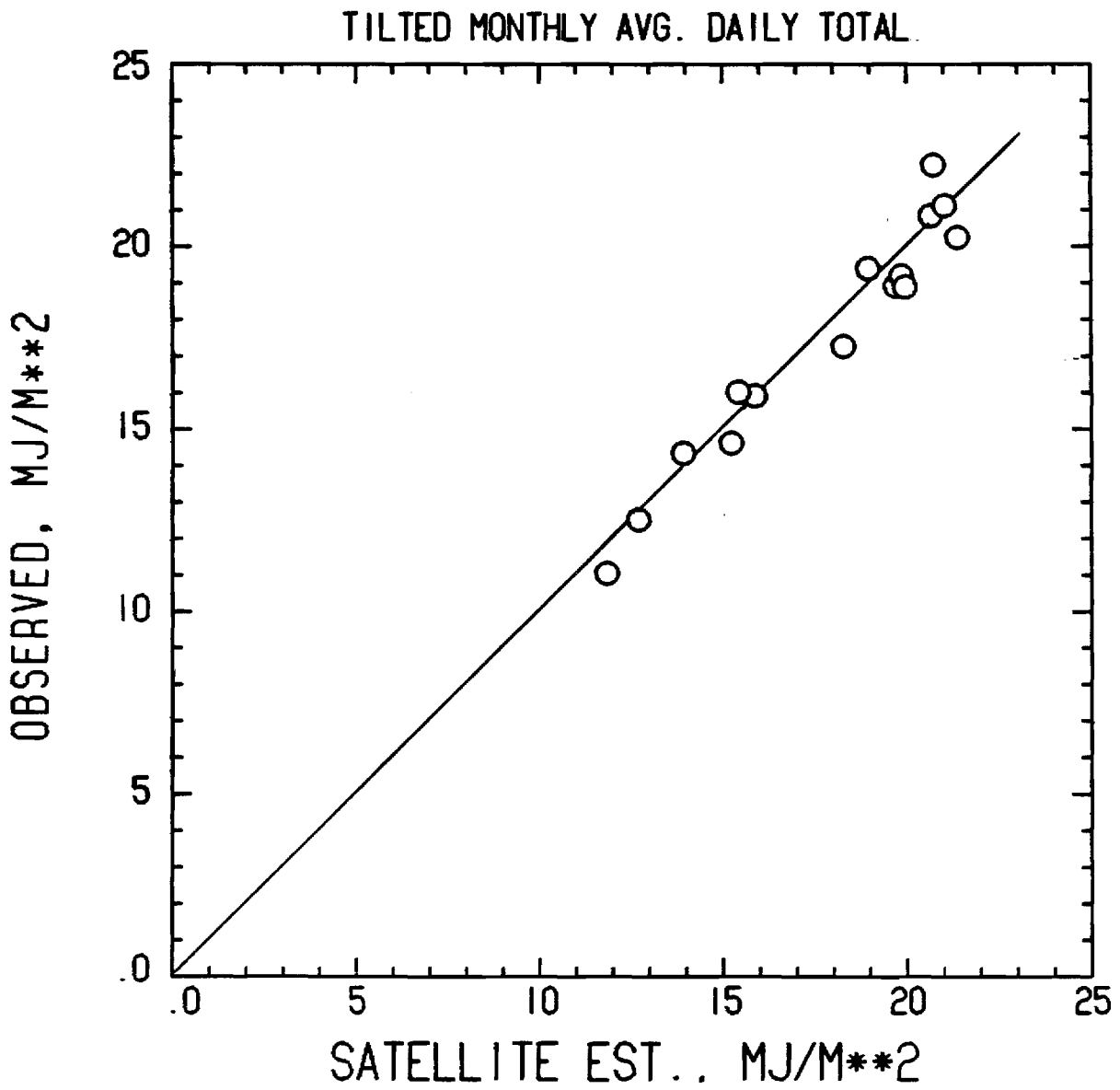


Fig. 20: As in Figure 18 for Latitude-Tilted Insolation. RMS difference is 0.8 MJ/m², or 4.5% of mean value of 17.5 MJ/m².

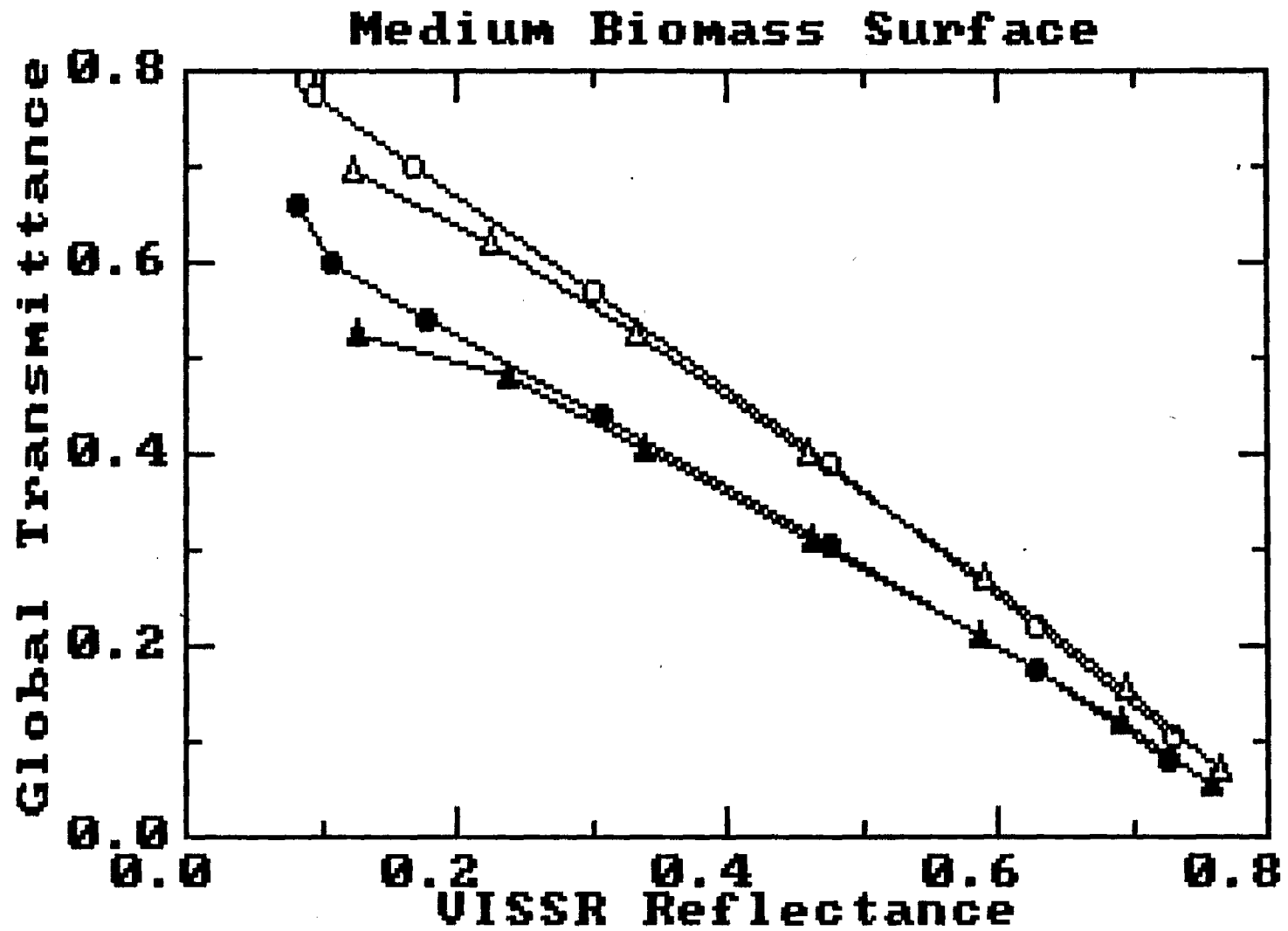


Fig. 21: Global Transmittance versus VISSR Reflectance for Clear-Skies, and Clouds of Optical Depth 2, 4, 8, 16, 32 and 64. Solar zenith angles are 0° (circles) and 60° (triangles) with precipitable water 1 cm (open symbols) or 4 cm (solid symbols).

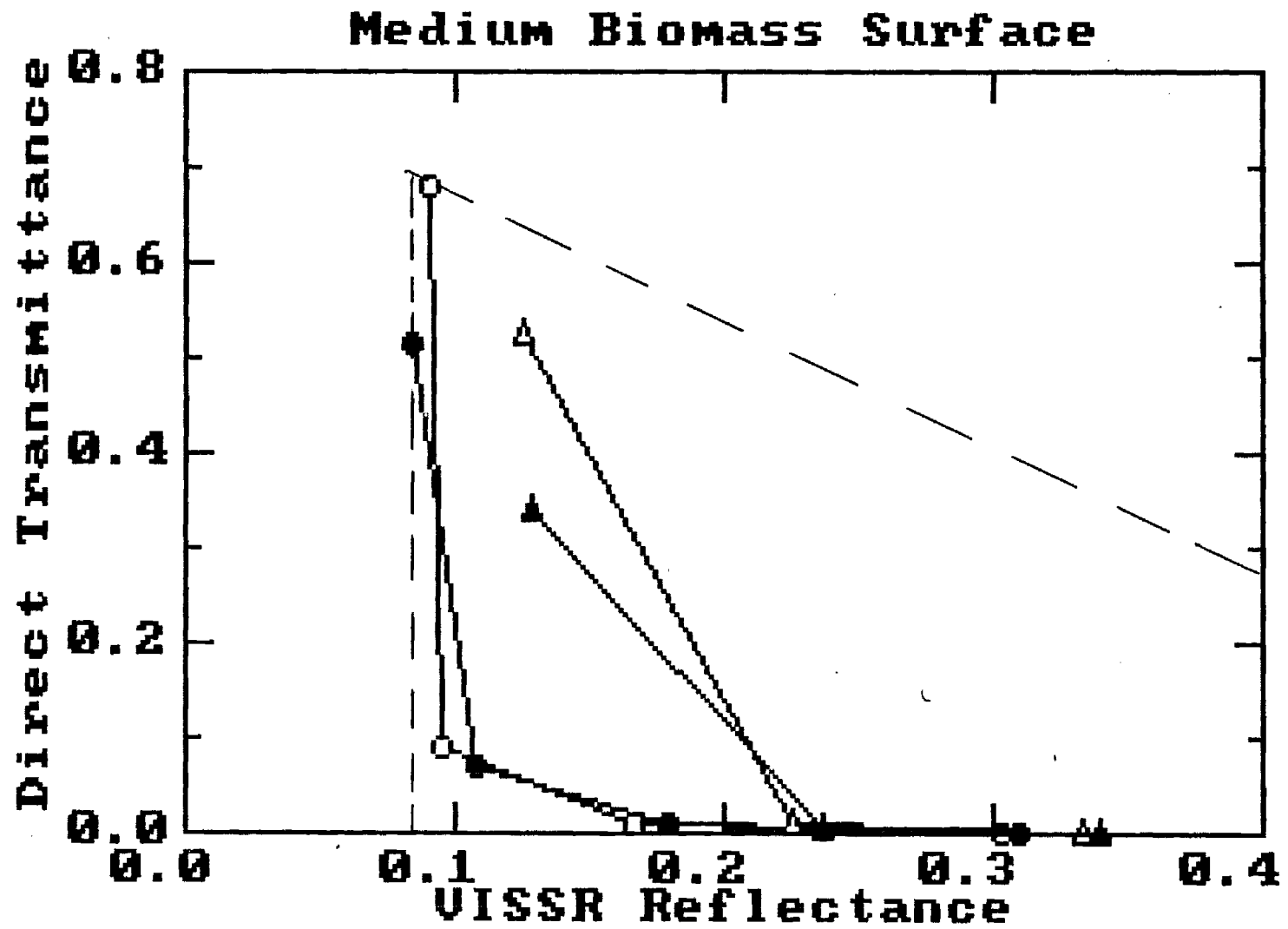


Fig. 22: As in Figure 21 for Direct Normal Transmissivity.

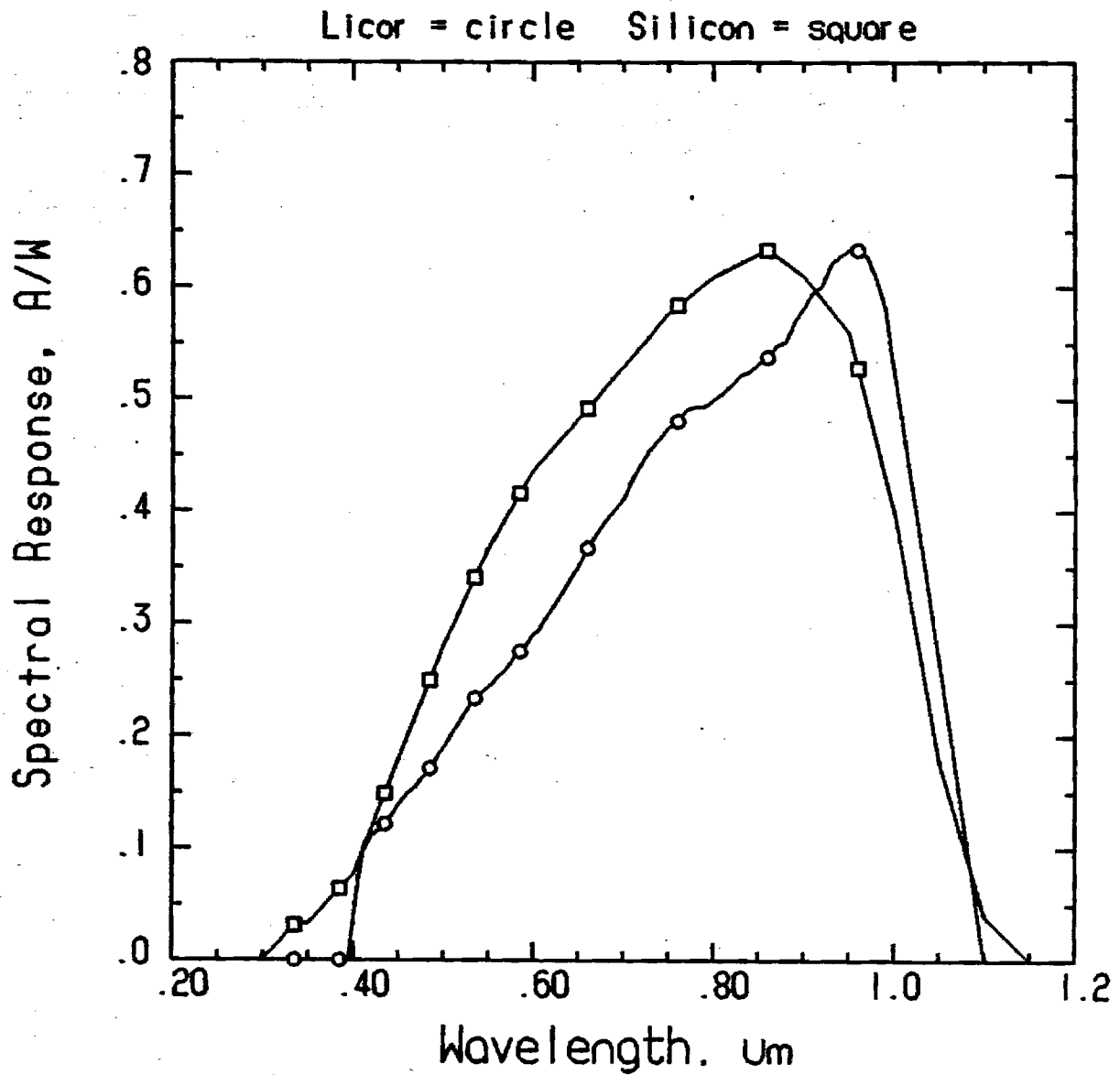


Fig. 23: Comparison of Filter Curve of Licor Photocell Radiometer (Normalized to 0.63 peak) with Spectral Response Curve (in amps/watt) for Crystalline Silicon Photocell Material (Bird and Hulstrom, SERI/TR-215-1598, 1982).

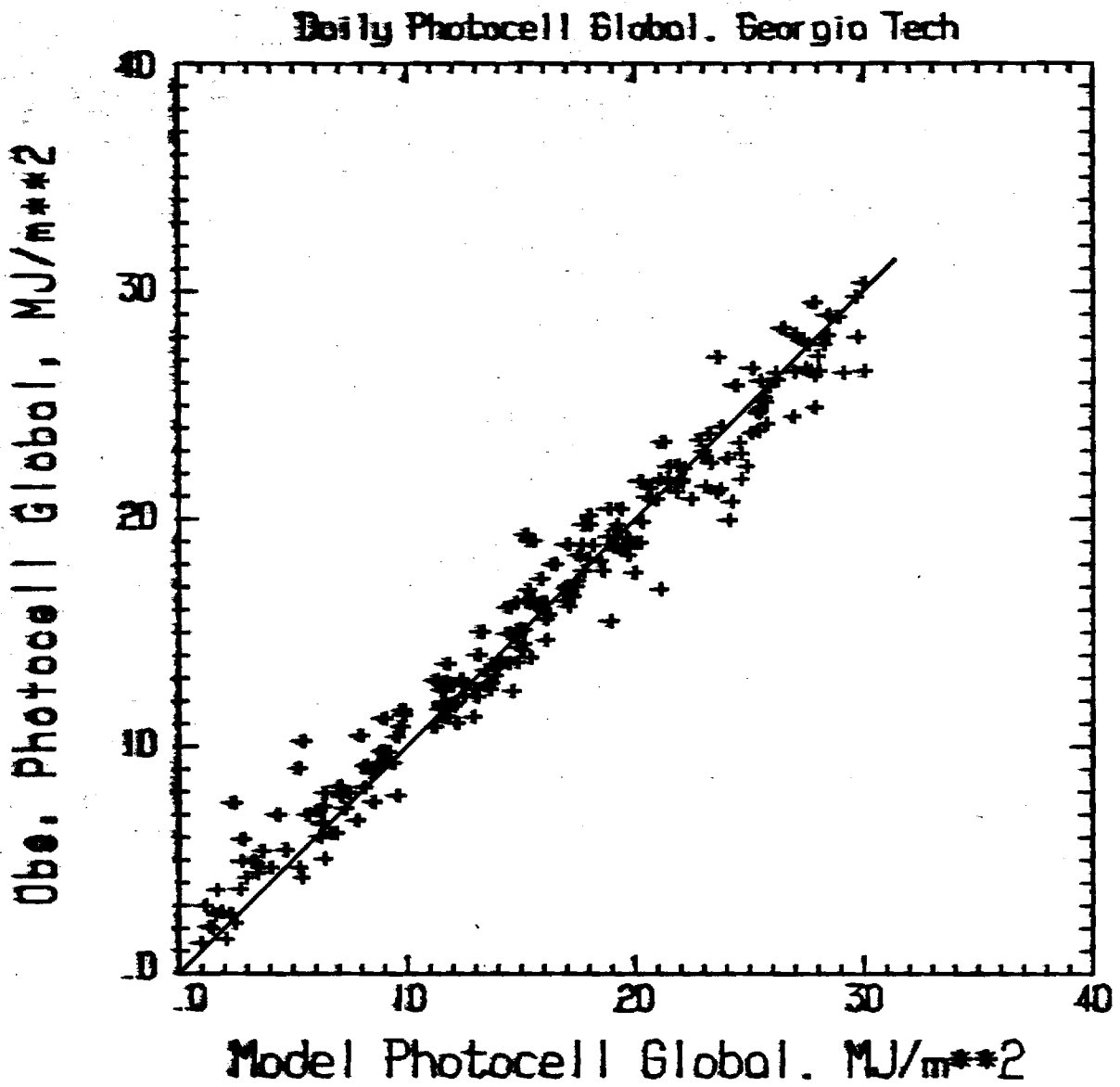


Fig. 24: Photocell Radiometer Observed Daily Total Global Horizontal Irradiance versus Satellite Estimated, Georgia Tech Site, 1982-83.

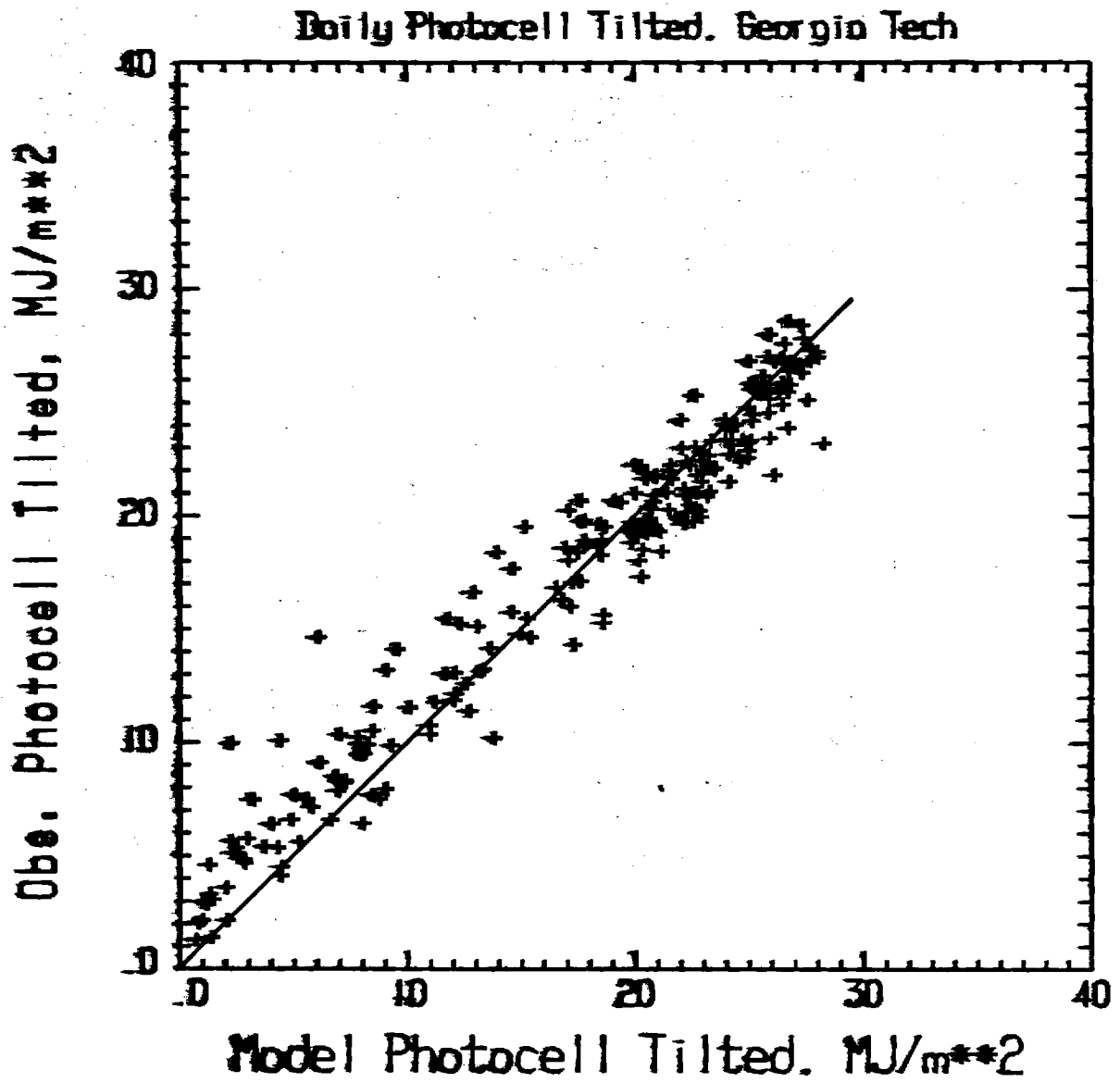


Fig. 25: As in Figure 24 for Photocell Radiometer on Latitude-Tilted Surface.

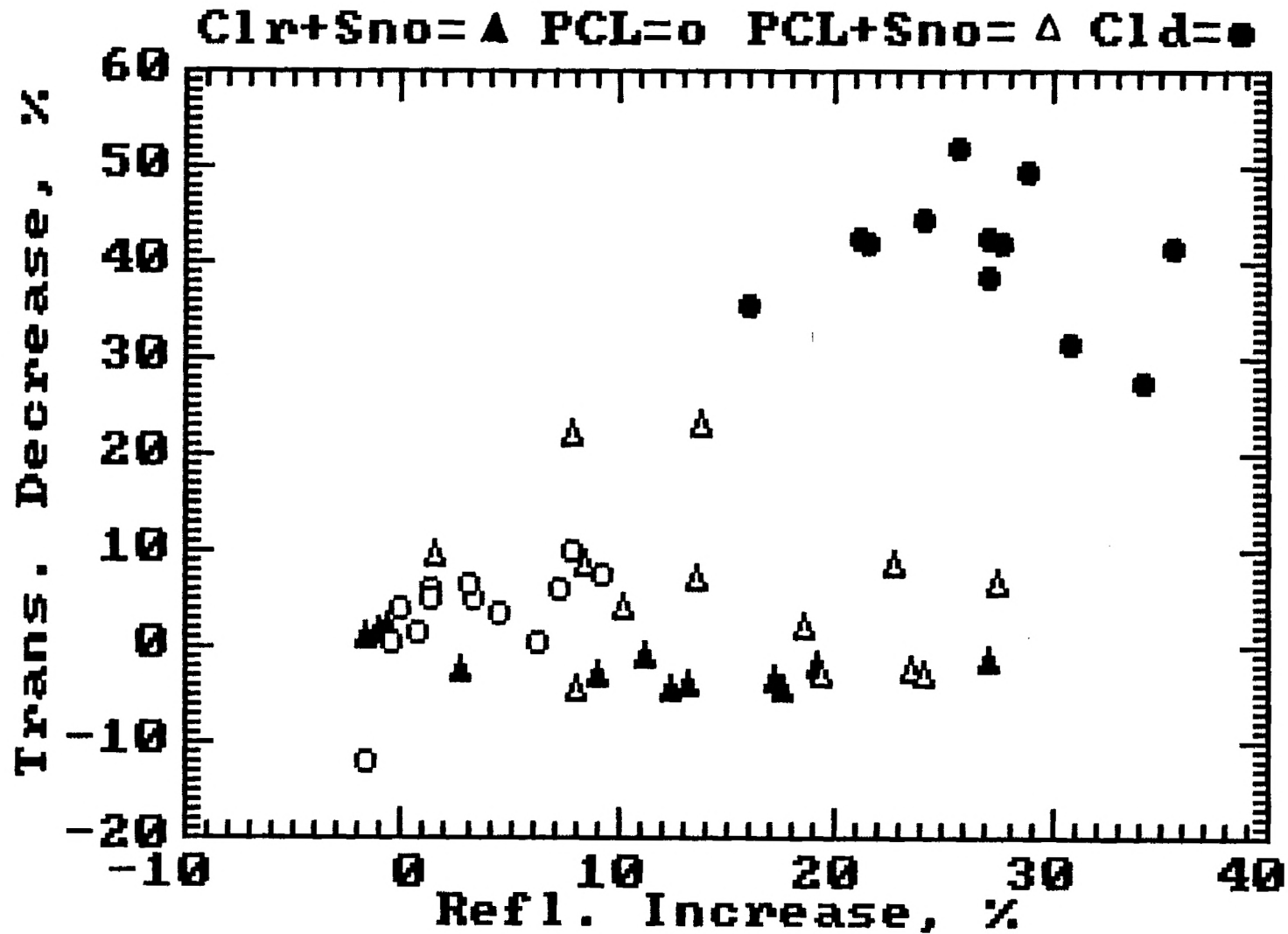


Fig. 26: Observed Decrease from Clear Transmissivity vs. Increase from Clear Reflectivity for Clear-with-snow, partly-cloudy-with-snow, partly-cloudy-without-snow, and cloudy conditions.

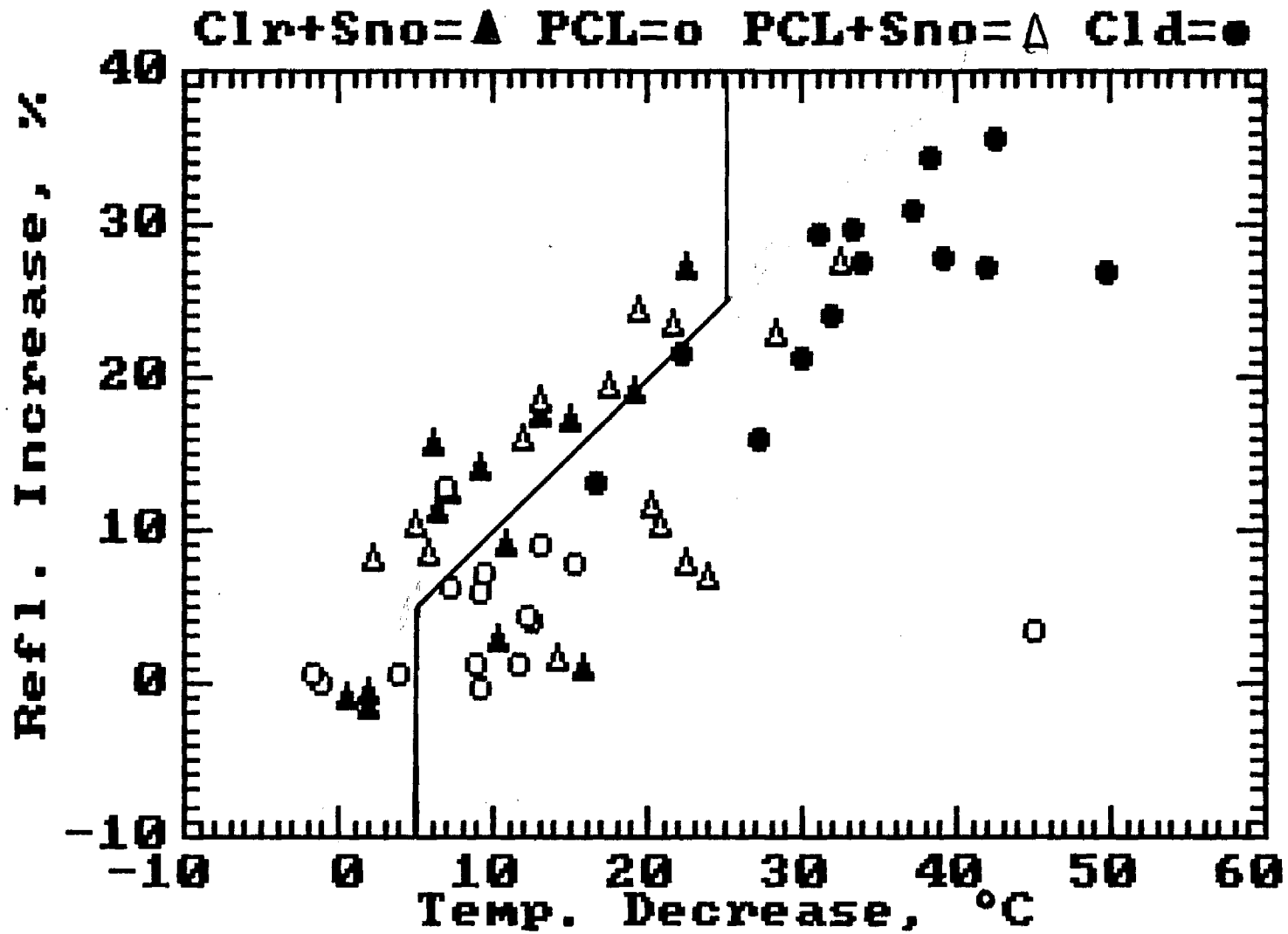


Fig. 27: As in Figure 26 for Increase from Clear Reflectivity versus Decrease from Clear Brightness Temperature.

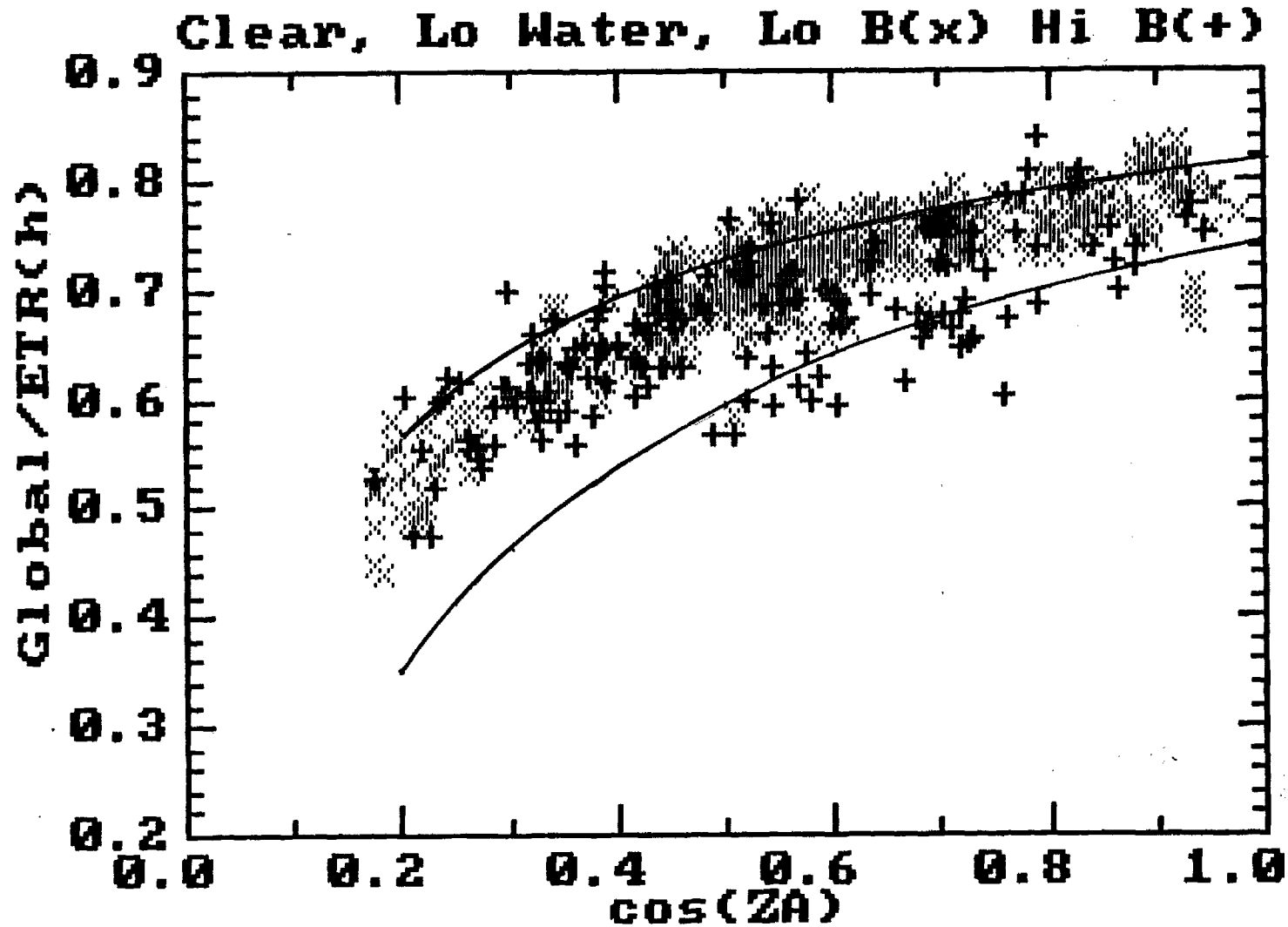


Fig. 28: Observed Ratio of Global to Extraterrestrial Horizontal Under Clear Conditions and Low Precipitable water, versus cosine of solar zenith angle for low and high satellite brightness ranges. Model curves are for PW = 1 cm, aerosol optical depth 0.1 (top) or 0.4 (bottom)

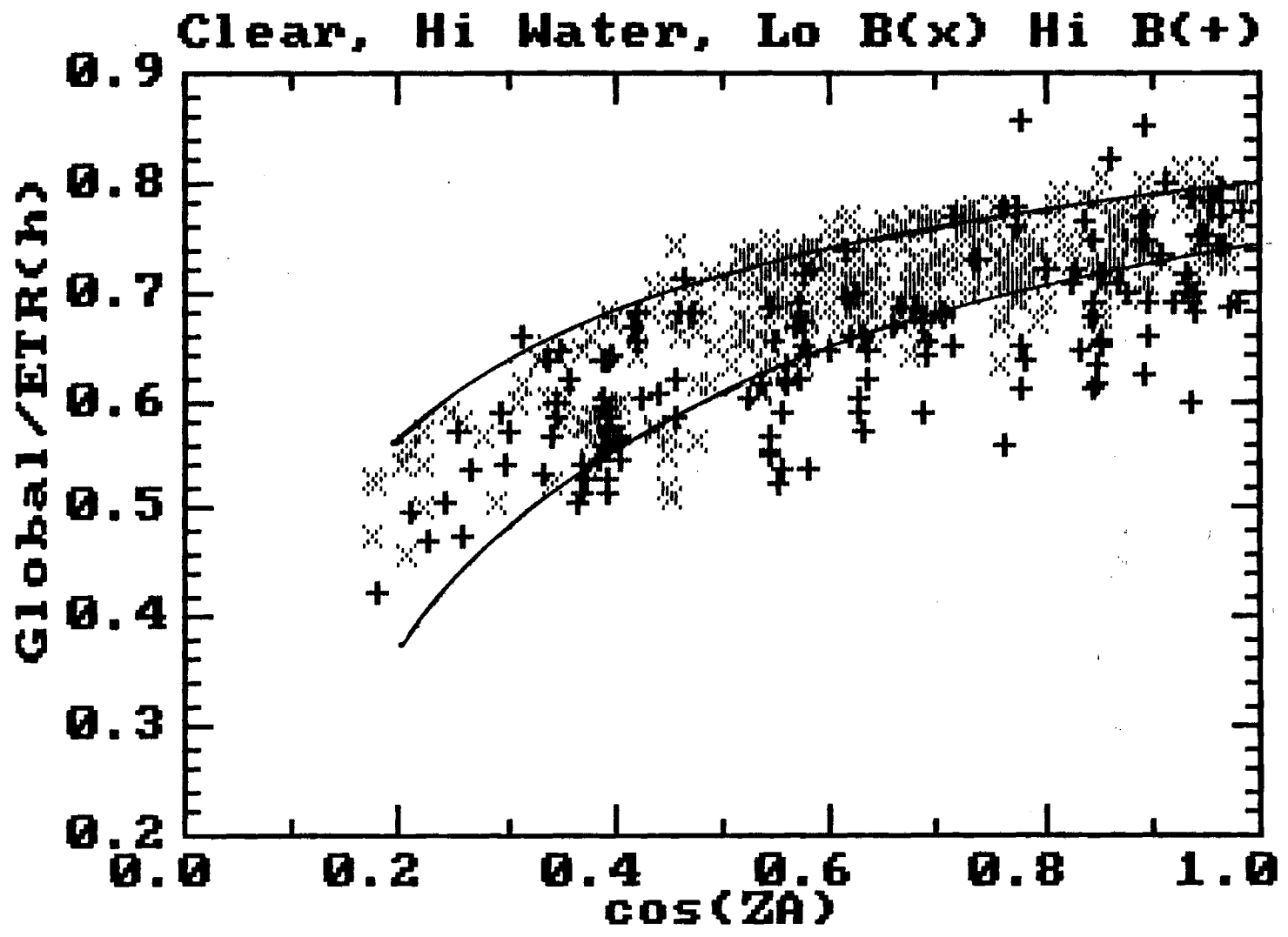


Fig. 29: As in Figure 28 for high precipitable water range. Model curves are for $pw = 2.5$ cm, aerosol optical depth 0.1 (top) or 0.4 (bottom).

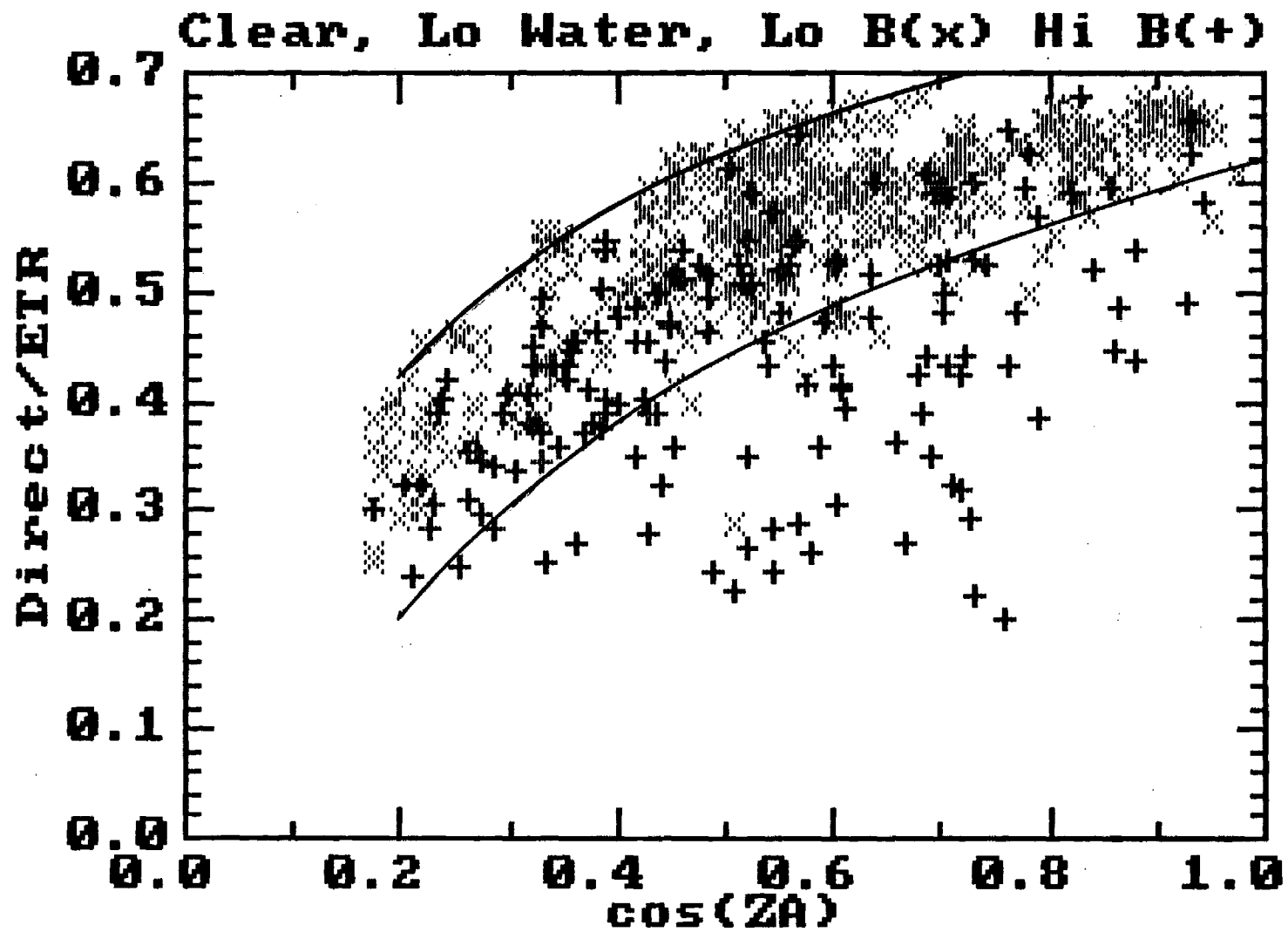


Fig. 30: As in Figure 28 for Direct Normal, Low PW Range.

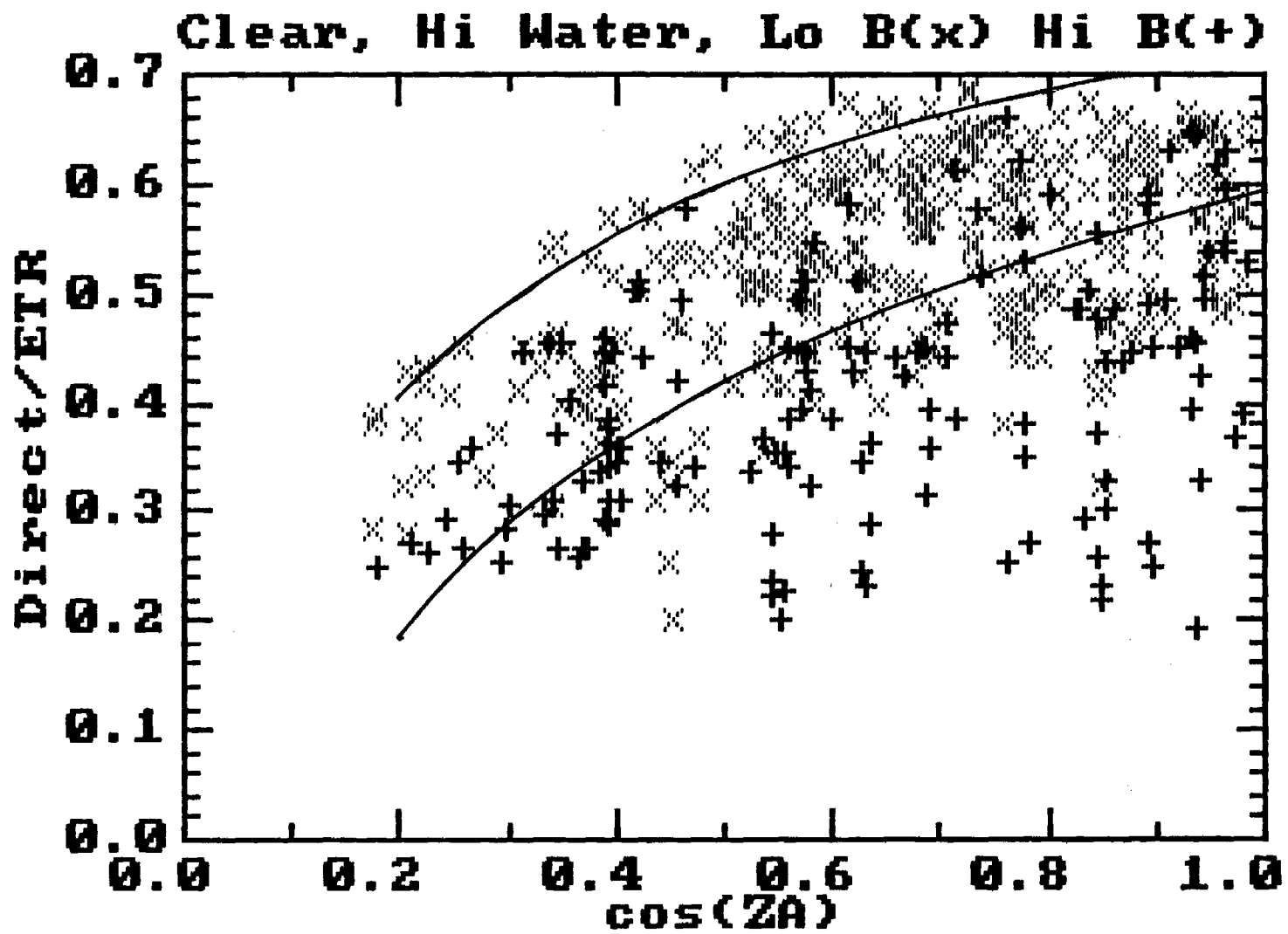


Fig. 31: As in Figure 29 for Direct Normal, High PW Range.

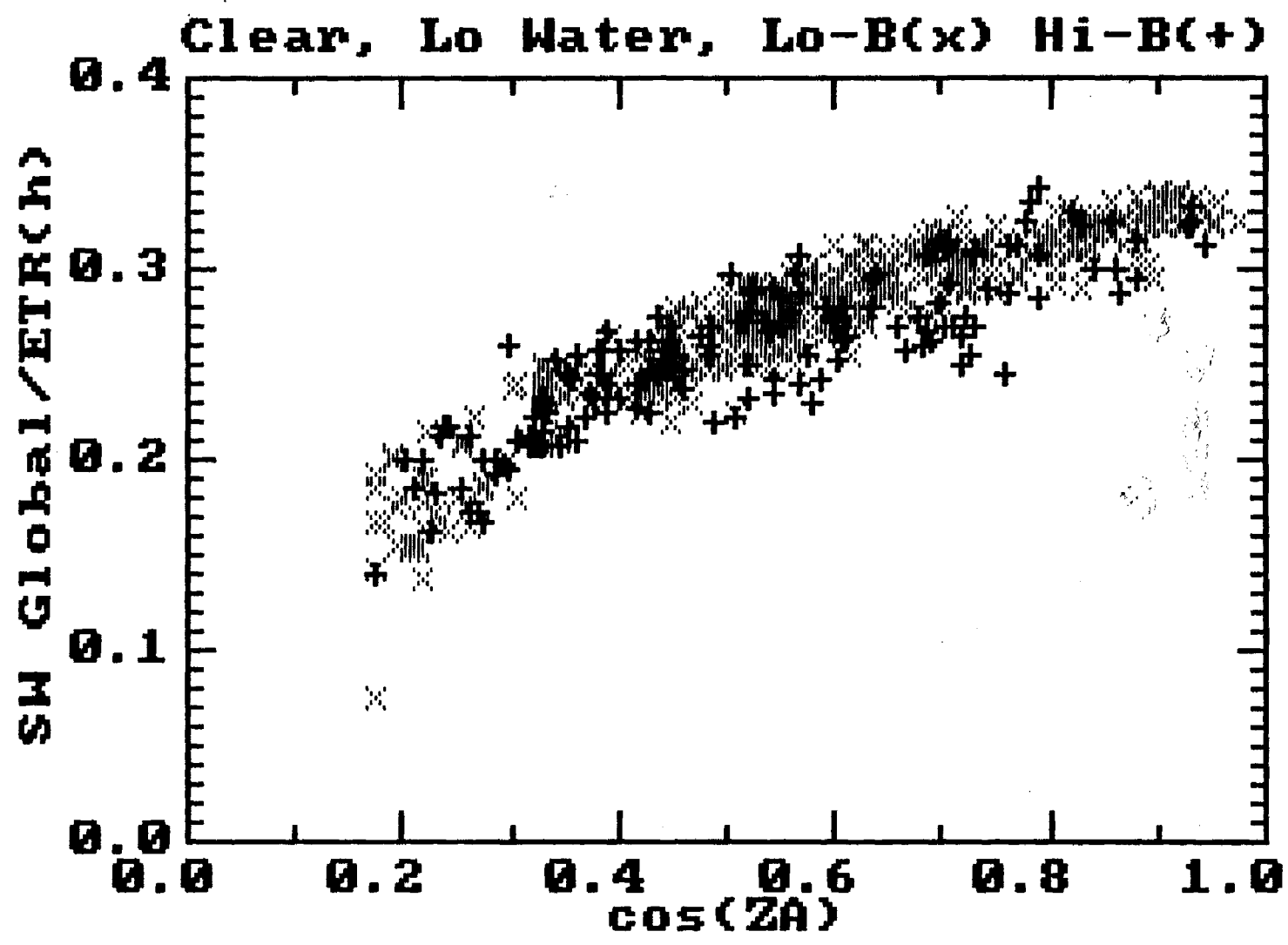


Fig. 32: As in Figure 28 for Global < 630 nm, Low PW Range.

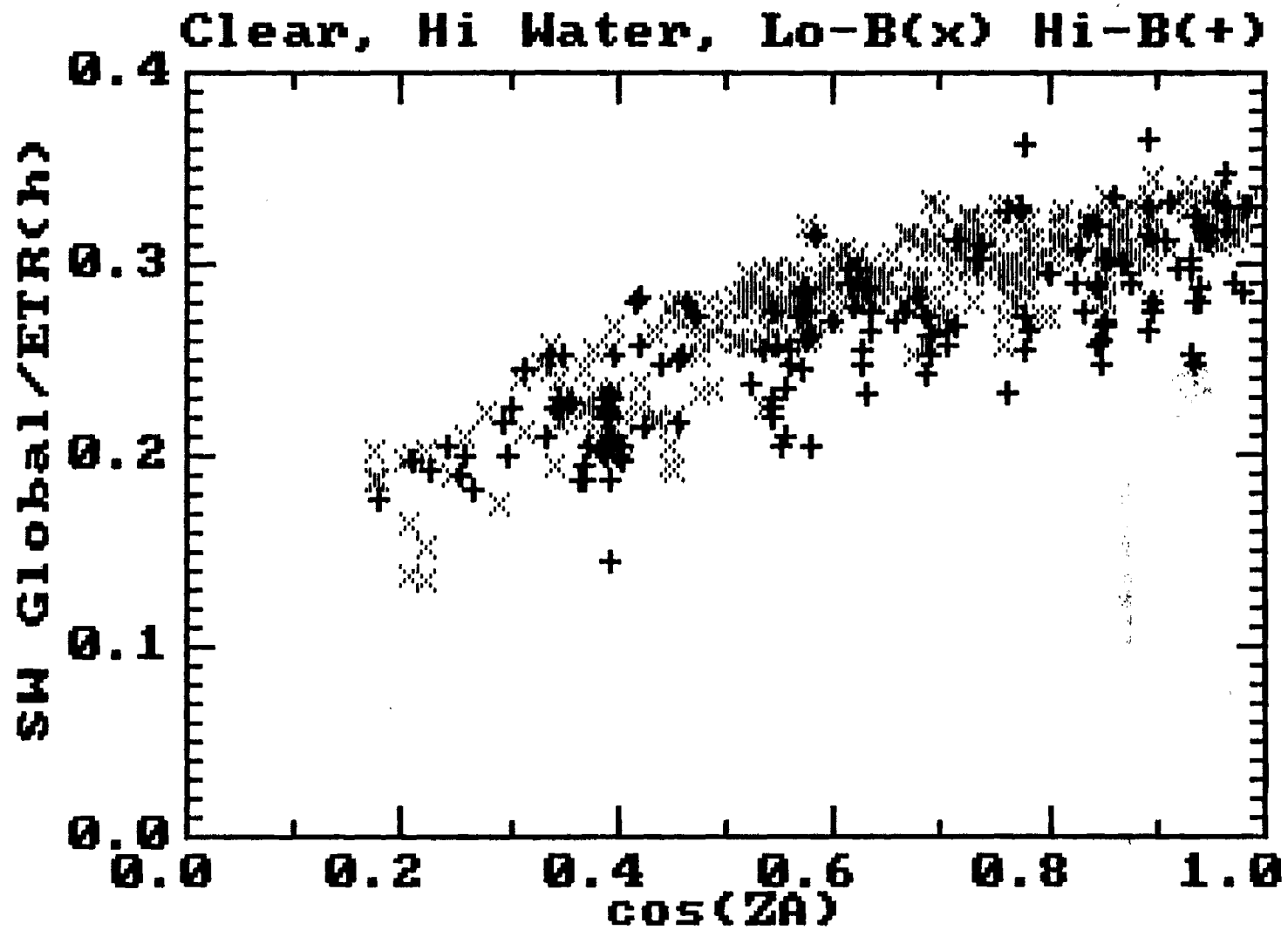


Fig. 33: As in Figure 29 for Global > 630 nm, High PW Range.

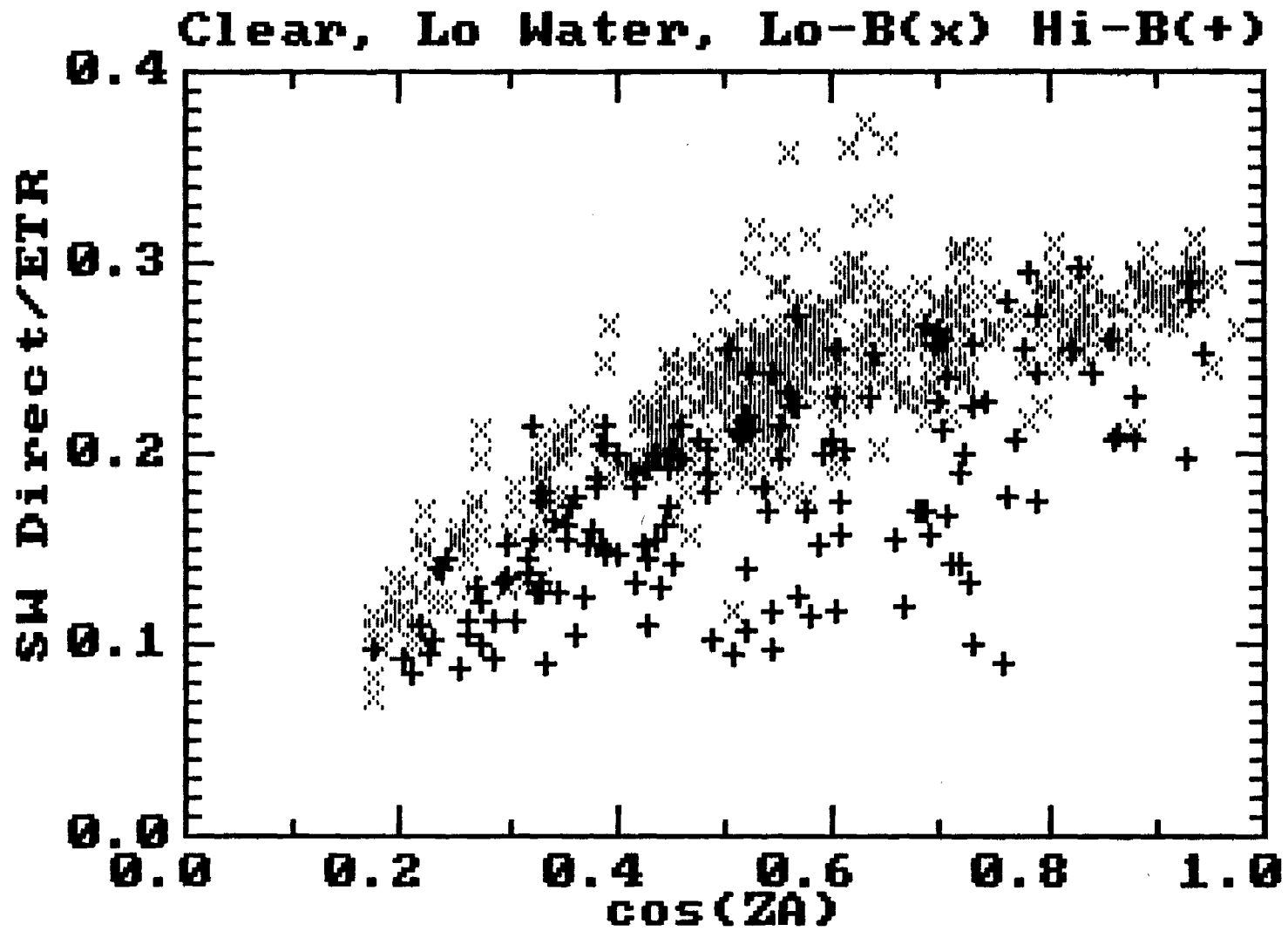


Fig. 34: As in Fig. 28 for Direct Normal < 630 nm, Low PW Range.

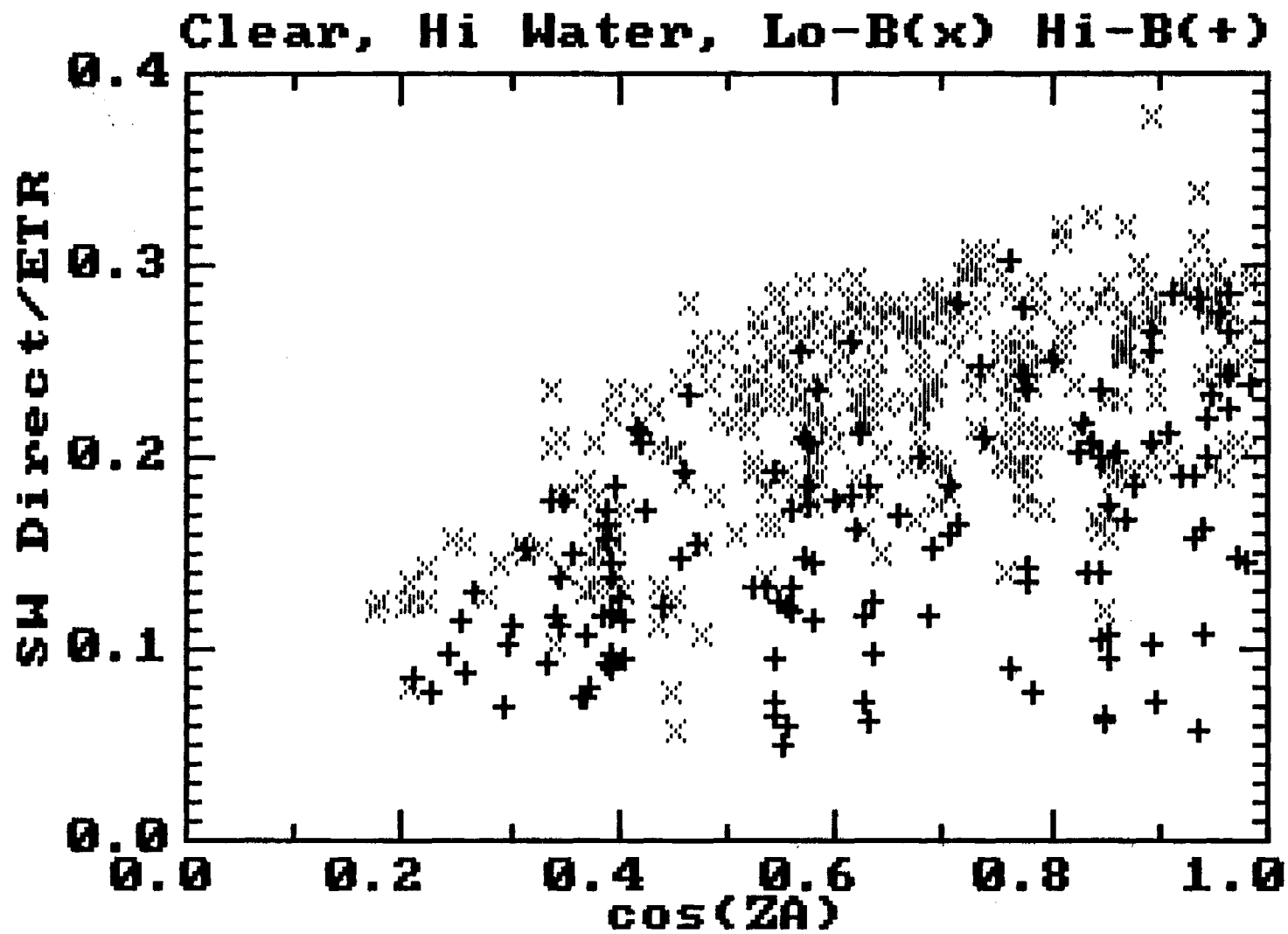


Fig. 35: As in Figure 29 for Direct Normal < 630 nm, High PW Range.

APPENDIX

Abstract of Technical Progress Report

ATLAS OF SATELLITE-MEASURED INSOLATION IN THE UNITED STATES,
MEXICO AND SOUTH AMERICA

ATLAS OF SATELLITE-MEASURED INSOLATION IN THE
UNITED STATES, MEXICO, AND SOUTH AMERICA

Abstract

A summary is given of the development, testing and applications of the satellite insolation estimation project of the National Oceanic and Atmospheric Administration (NOAA) Agriculture and Resources Inventory Surveys through Aerospace Remote Sensing (AgRISTARS) program. The NOAA/AgRISTARS procedure uses data from the Geostationary Operational Environmental Satellite (GOES) to estimate daily total insolation (on a horizontal surface) at an array of $1^\circ \times 1^\circ$ latitude-longitude locations throughout the continental United States, Mexico, and parts of South America. This methodology is compared with some other satellite techniques in terms of accuracy and applicability. Summary maps of monthly average daily total insolation for the period July, 1982 through December, 1983, as well as annual total maps for 1983, are presented for all three geographic coverage areas. As measures of temporal and spatial variability, monthly and annual data are also presented for the standard deviation of the daily insolation values about the monthly mean, and for root-mean-square values of both north-south and east-west differences over 1° latitude or longitude spacing. From the estimated error analysis the monthly mean values appear to be accurate to about 5% of the mean value, except for the western part of the United States when GOES-1 was put back into temporary service as the western GOES satellite. Compared to long-term surface-measured insolation in the United States, the satellite-derived means for the reported period are somewhat low, especially in the central and southwestern United States. Lowest standard deviation areas tend to be associated with areas where then mean insolation is high, e.g. desert regions where high values tend to persist from day to day. Some of the areas with high mean insolation also exhibit low spatial variability, with nearby areas of higher-than-average spatial variability where the insolation regime changes to one of lower mean value. An area of exceptionally large spatial variability is found in the mountainous areas of Bolivia and Argentina. Areas of somewhat higher-than-average spatial variability are also found throughout the southern and central Rocky Mountains of the United States. The rms spatial vari-

ability, which has not been reported before for such extensive geographic regions, is important is assessing the reliability of interpolations or extrapolations from sites with measured insolation to other locations where insolation values are desired.

Final Report
Georgia Tech Project G-35-633

DOE/CH/10200-3

**Satellite Techniques of Solar Resource
Assessment for Focusing and Non-Focusing
Solar Collector Systems**

By:
C. G. Justus, Principal Investigator
School of Geophysical Sciences
Georgia Institute of Technology

Submitted to the:
UNITED STATES DEPARTMENT OF ENERGY
SOLAR ENERGY RESEARCH INSTITUTE AREA OFFICE
SOLERAS PROGRAM

Under:
Grant Number DE-FG02-84CH10200

September 1987

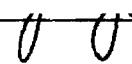
GEORGIA INSTITUTE OF TECHNOLOGY
A UNIT OF THE UNIVERSITY SYSTEM OF GEORGIA
SCHOOL OF GEOPHYSICAL SCIENCES
ATLANTA, GEORGIA 30332



U. S. DEPARTMENT OF ENERGY

UNIVERSITY CONTRACTOR, GRANTEE, AND COOPERATIVE AGREEMENT
RECOMMENDATIONS FOR ANNOUNCEMENT AND DISTRIBUTION OF DOCUMENTS

See Instructions on Reverse Side

1. DOE Report No. DOE/CH/10200-3	3. Title Satellite Techniques of Solar Resource Assessment for Focusing and Non-Focusing Solar Collector Systems	
2. DOE Contract No. DE-FG02-84CH10200		
4. Type of Document ("x" one) <input type="checkbox"/> a. Scientific and technical report <input type="checkbox"/> b. Conference paper: Title of conference _____ Date of conference _____ Exact location of conference _____ Sponsoring organization _____ <input checked="" type="checkbox"/> c. Other (Specify) <u>Final Report</u>		
5. Recommended Announcement and Distribution ("x" one) <input checked="" type="checkbox"/> a. Unrestricted unlimited distribution. <input type="checkbox"/> b. Make available only within DOE and to DDE contractors and other U. S. Government agencies and their contractors. <input type="checkbox"/> c. Other (Specify) _____		
6. Reason for Recommended Restrictions _____		
7. Patent and Copyright Information: Does this information product disclose any new equipment, process, or material? <input checked="" type="checkbox"/> No <input type="checkbox"/> Yes If so, identify page nos. _____ Has an invention disclosure been submitted to DOE covering any aspect of this information product? <input checked="" type="checkbox"/> No <input type="checkbox"/> Yes If so, identify the DOE (or other) disclosure number and to whom the disclosure was submitted. Are there any patent-related objections to the release of this information product? <input checked="" type="checkbox"/> No <input type="checkbox"/> Yes If so, state these objections. Does this information product contain copyrighted material? <input checked="" type="checkbox"/> No <input type="checkbox"/> Yes If so, identify the page numbers _____ and attach the license or other authority for the government to reproduce.		
8. Submitted by C. G. Justus, Professor	Name and Position (Please print or type) _____	
Organization School of Geophysical Sciences, Georgia Tech		
Signature 	Phone 404-894-3890	Date September 21, 1987

FOR DOE OR OTHER AUTHORIZED
USE ONLY

9. Patent Clearance ("x" one)
 a. DOE patent clearance has been granted by responsible DOE patent group.
 b. Report has been sent to responsible DOE patent group for clearance.

**Satellite Techniques of Solar Resource
Assessment for Focusing and Non-Focusing
Solar Collector Systems**

C. G. Justus, Principal Investigator

School of Geophysical Sciences
Georgia Institute of Technology
Atlanta, GA 30332

Final Report

Georgia Tech Project G-35-633

Submitted to the

UNITED STATES DEPARTMENT OF ENERGY
SOLAR ENERGY RESEARCH INSTITUTE AREA OFFICE
SOLERAS PROGRAM

Grant Number DE-FG02-84CH10200

INTRODUCTION

In the previous project periods, techniques were developed for GOES satellite estimates of daily total global horizontal, direct normal, and global tilted-surface insolation (Justus, 1985). Daily and monthly mean insolation values estimated from the satellite data were compared with those observed at the Georgia Tech insolation monitoring site. These results indicated the basic accuracy (based on rms deviation from observed) to be about 4.9% for monthly mean global horizontal insolation or 6.7% for the monthly mean direct normal (see Figures 1 and 2).

With the ultimate goal of developing an atlas of the solar energy resources for the country of Saudi Arabia, by the use of satellite estimation techniques, the previous and current (final) year's activity involved study of techniques for the use of METEOSAT data to estimate global horizontal and direct normal insolation. Since one or more years of METEOSAT data would be very expensive to acquire, the scope of the project was to examine a small number of days of insolation from the Riyadh monitoring site with the corresponding METEOSAT data. The primary purpose was to determine if the bright sandy surface (which limits the contrasting signal between clear and cloud conditions) or the large satellite zenith angle for Saudi Arabian sites would cause any problems. A second purpose was to determine if the METEOSAT data could be used to determine the expected large variations in clear-sky direct and global insolation due to optically thick aerosol and dust clouds which are frequently present.

Study of both summer and winter clear days (Justus, 1986) indicated that the brightness of the sandy surface and the satellite viewing angle will present no problems. Results from clear days indicated, however, that because of large variations due to optically thick aerosol and dust layers the METEOSAT visible sensor data alone was not able to provide accurate hourly direct normal insolation estimates. The major focus of this study is to determine whether information from the thermal IR channel of METEOSAT can be used to improve the satellite estimates of direct normal insolation on cloud-free days, and to develop and test algorithms for estimating both direct normal and global horizontal insolation under both cloudy and cloud-free conditions.

DEVELOPMENT OF THE INSOLATION ALGORITHMS

The general form of the model equations used to calculate hourly total direct normal and global horizontal insolation is given by (Justus, 1985)

$$\text{Dir} = \text{Dir}(\text{Clr}) - \Delta\text{Dir}, \quad (1)$$

and

$$\text{Glo} = \text{Glo}(\text{Clr}) - \Delta\text{Glo}. \quad (2)$$

$\text{Dir}(\text{Clr})$ and $\text{Glo}(\text{Clr})$ are model-calculated values of direct normal and global horizontal surface broad-band irradiance under cloud-free conditions (Justus and Paris, 1985). The terms ΔDir and ΔGlo are the departures from cloud-free irradiance which are due to cloud cover. These may be computed either by a model for broad-band irradiance through clouds (see Figures 21 and 22 of Justus, 1985 or Figure 1 of Justus, 1986), or by empirical relations derived from comparison between measured surface irradiance and satellite-measured brightness (count) values (see equations 4 and 6 of Justus, 1985).

Hourly values of direct normal and global horizontal irradiance measured at the Riyadh site have been compared with simultaneously observed shortwave radiances measured by the visible channel of the METEOSAT satellite. These data are shown in Figures 3 and 4 in the form of the reduction in irradiance below that calculated from nominal atmospheric conditions with the clear-sky model plotted versus the increase in satellite-measured radiance counts from those expected under the same clear-sky atmospheric conditions. Nominal atmospheric conditions assumed are an aerosol optical depth of 0.3 (at 500 nm). The desert surface albedo is assumed to be 0.45 within the spectral range of the METEOSAT visible sensor, and the METEOSAT calibration of Koepke (1982) is assumed for purposes of calculating the expected clear-sky sensor counts.

The solid line in Figure 3 provides an estimate of insolation from satellite-observed counts via

$$\text{Glo} = \text{Glo}(\text{Clr}) - 13.85(\text{Counts} - \text{Clear Counts}) \quad , \quad (3)$$

while the solid line in Figure 4 can be expressed as

$$\text{Dir} = \text{Dir}(\text{Clr}) [1. - 0.02835(\text{Counts} - \text{Clear Counts})] \quad . \quad (4)$$

For some cases, these relations will provide adequate estimates of direct normal and global horizontal irradiance. However, both Figures 3 and 4 show a substantial number of data points, measured under apparently cloud-free conditions, for which slight reductions in surface insolation are accompanied by substantial reductions in satellite-measured visible radiance counts below that expected for clear-sky conditions (negative values of Counts - Clear Counts). These cases are due to overcast aerosol or dust layers which reduce the insolation (with the direct normal affected more than the global horizontal), while not increasing (or perhaps even decreasing) the amount of reflected radiation seen by the satellite. In Figure 4, there are also a substantial number of cases in which there is a considerable reduction in surface direct normal irradiance (values of relative direct irradiance from about 0.5 to 1) without a corresponding increase in the satellite-measured visible radiance counts. Some of these may be due to thin, patchy clouds which substantially reduce the direct normal hourly average (without much effect on the global irradiance), but are not reflective enough to significantly increase the reflected radiation seen by the satellite.

For these problem areas, the ability of satellite-measured infrared radiance counts (IR) to improve the insolation estimates over that found by using the satellite-measured visible radiance counts (VIS) only has been examined by evaluating a multiple regression relation between surface irradiance and both of these satellite measurements. The results are expressed as

$$\text{Glo} = \text{Glo}(\text{Clr}) + 0.1685[\text{VIS} - \text{VIS}(\text{Clr})] - 3.918[\text{IR} - \text{IR}(\text{Clr})] \quad , \quad (5)$$

and

$$\text{Dir} = \text{Dir}(\text{Clr})(1 - 0.01338[\text{VIS} - \text{VIS}(\text{Clr})] - 0.01948[\text{IR} - \text{IR}(\text{Clr})]) \quad (6)$$

The ability of the VIS-only relations (equations 3 and 4) or the VIS+IR relations (equations 5 and 6) to reproduce the observed surface direct normal and global horizontal irradiance are examined in the following section.

EVALUATION AND TESTING OF THE INSOLATION ALGORITHMS

For cloud-free days without substantial overcast aerosol or dust layers, such as shown in Figures 5 and 6 for Day 348, 1982, and for cases with substantial cloud influence, such as shown in Figures 7-10 for Days 53, 1982 and 105, 1984, the VIS-only technique adequately reproduces the observed direct normal and global horizontal irradiance. For some specific hours problems arise, such as with the direct normal values at hour 17 on the two cloudy days, and with both the direct normal and global horizontal irradiance at hour 11 on day 105, when a small observed satellite-measured visible radiance counts would indicate substantially larger surface irradiance values than are observed at the Riyadh site.

Some of these problems are due to the inherent mismatch between satellite-measured values and the corresponding surface irradiance data. The surface irradiance is averaged over an hourly period at one location (the Riyadh site), while the satellite-measured radiance is essentially a "snapshot" value of reflected radiation made near the beginning of the hour. The mismatch can be partially (but not completely) compensated by using satellite radiance averaged over an approximately 40 x 40 km target area as a surrogate for the hourly averaging process at the individual surface site. The type of errors caused by this mismatch problem tend to be somewhat random and tend to partially cancel when daily and monthly averaged data are considered (e.g. hourly rms errors of the order of 15%, daily rms errors of the order of 10%, and monthly rms error of the order of 5%).

For cloud-free days with substantial overcast of aerosol or dust layers, as illustrated by day 167 for 1982, 1983 and 1984, shown in Figures 11-16, the VIS-

only technique of equations 3 and 4 significantly overestimates the observed global horizontal and direct normal irradiance, while the VIS+IR technique of equations 5 and 6 offers substantial improvement in the irradiance estimates.

CONCLUSIONS

For cloudy days or days with partial cloud cover, and for cloud-free days without substantial overcast of aerosol or dust layers, the VIS-only technique of equations 3 and 4 provides adequate accuracy for estimating global horizontal and direct normal insolation from the satellite-measured visible radiance counts. For days with substantial overcast of aerosol or dust layers, the VIS+IR technique of equations 5 and 6 provides the additional information necessary for estimating surface direct normal and global horizontal irradiance.

Combined with the results from the earlier studies, that the bright desert background and the large satellite viewing angles present no substantial problems, these results mean that monthly average direct normal and global horizontal irradiance estimates of comparable accuracy to those estimated for the Georgia Tech site from GOES data (Figures 1 and 2), should be achievable from METEOSAT observations over Saudi Arabia.

REFERENCES

- Justus, C.G. (1985): Satellite Techniques of Solar Resource Assessment for Focusing and Non-Focusing Solar Collector Systems, Annual Report, DOE/SOLERAS Grant DE-FG02-84CH10200.
- Justus, C.G. (1986): Satellite Techniques of Solar Resource Assessment for Focusing and Non-Focusing Solar Collector Systems, Annual Report, DOE/SOLERAS Grant DE-FG02-84CH10200.
- Justus, C.G. and M.V. Paris (1985): A Model for the Solar Spectral irradiance and Radiance at the Bottom and Top of a Cloudless Atmosphere, J. Clim. Appl. Meteorol., 24, 193-205.
- Koepke, P. (1982): Viacrious Satellite CALibration in the Solar Spectral Range by Means of Calculated Radiances and its Application to METEOSAT, Appl. Optics, 21, 2845-2854.

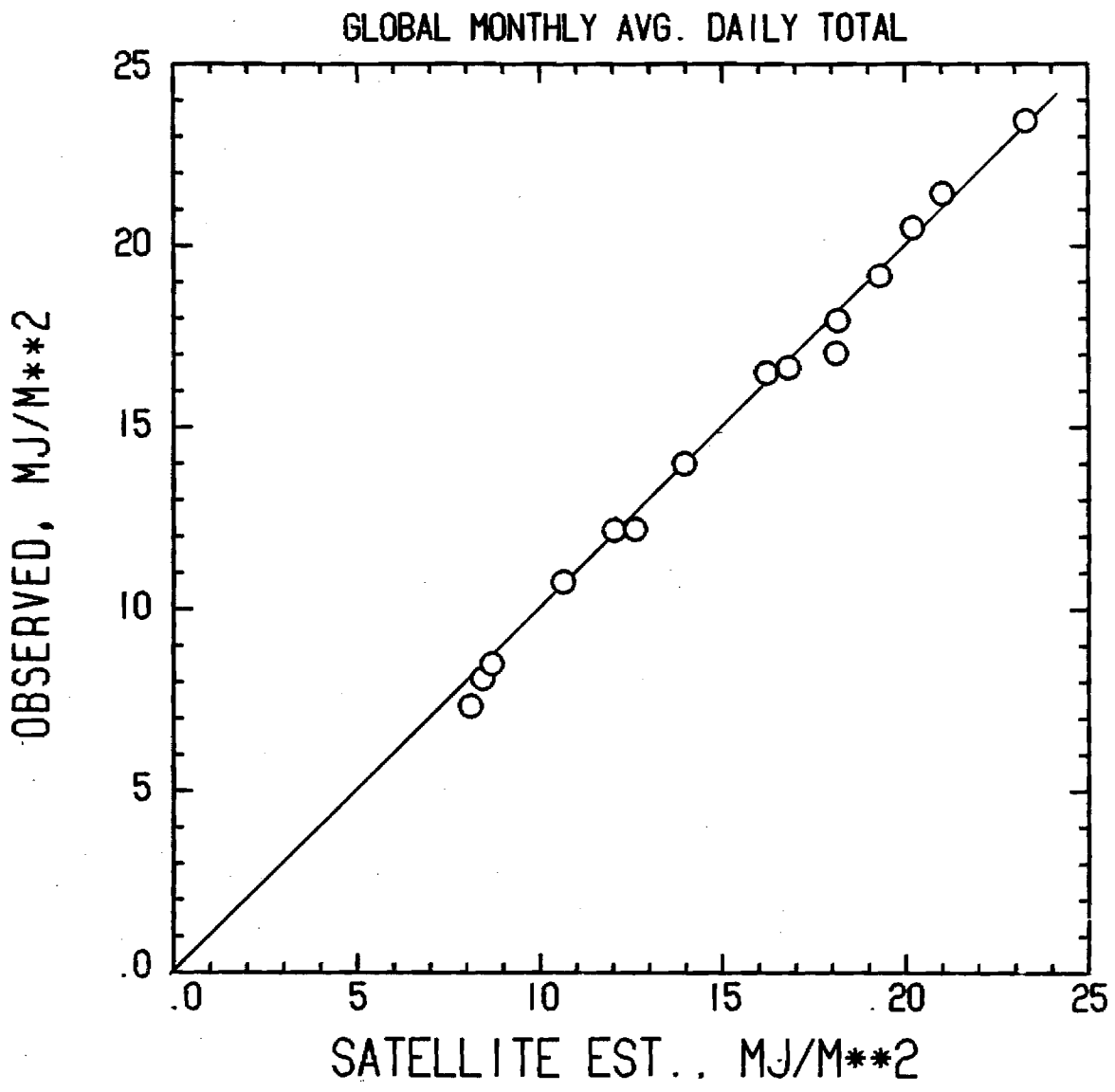


Figure 1 - Monthly averaged daily total global horizontal irradiance observed at Georgia Tech versus that estimated from the GOES satellite.

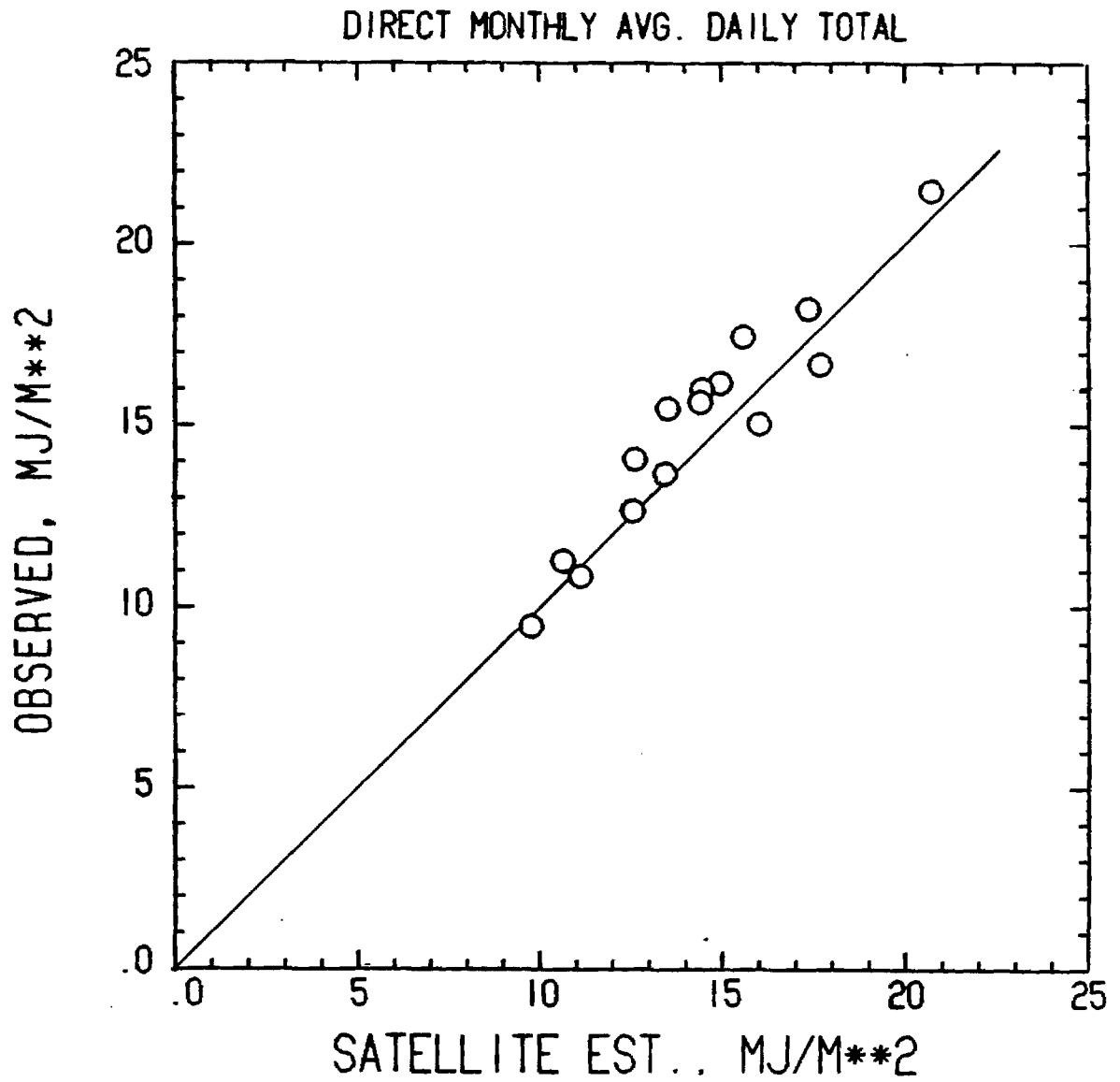


Figure 2 - Monthly averaged daily total direct normal irradiance observed at Georgia Tech versus that estimated from the GOES satellite.

Global Horizontal vs Counts

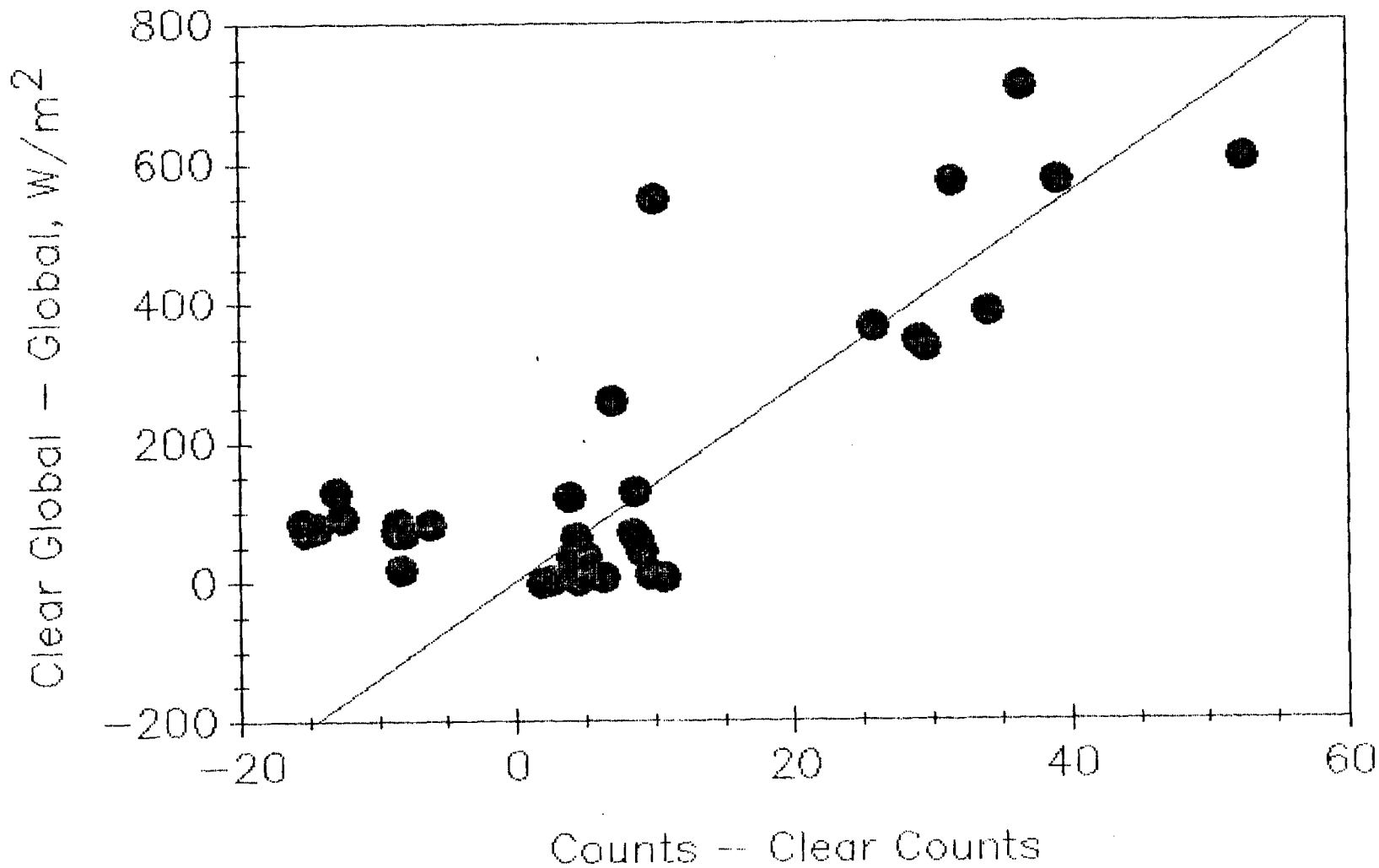


Figure 3 - Observed hourly global horizontal irradiance, relative to clear global, versus the observed METEOSAT radiance counts, relative to the counts expected under cloud-free conditions.

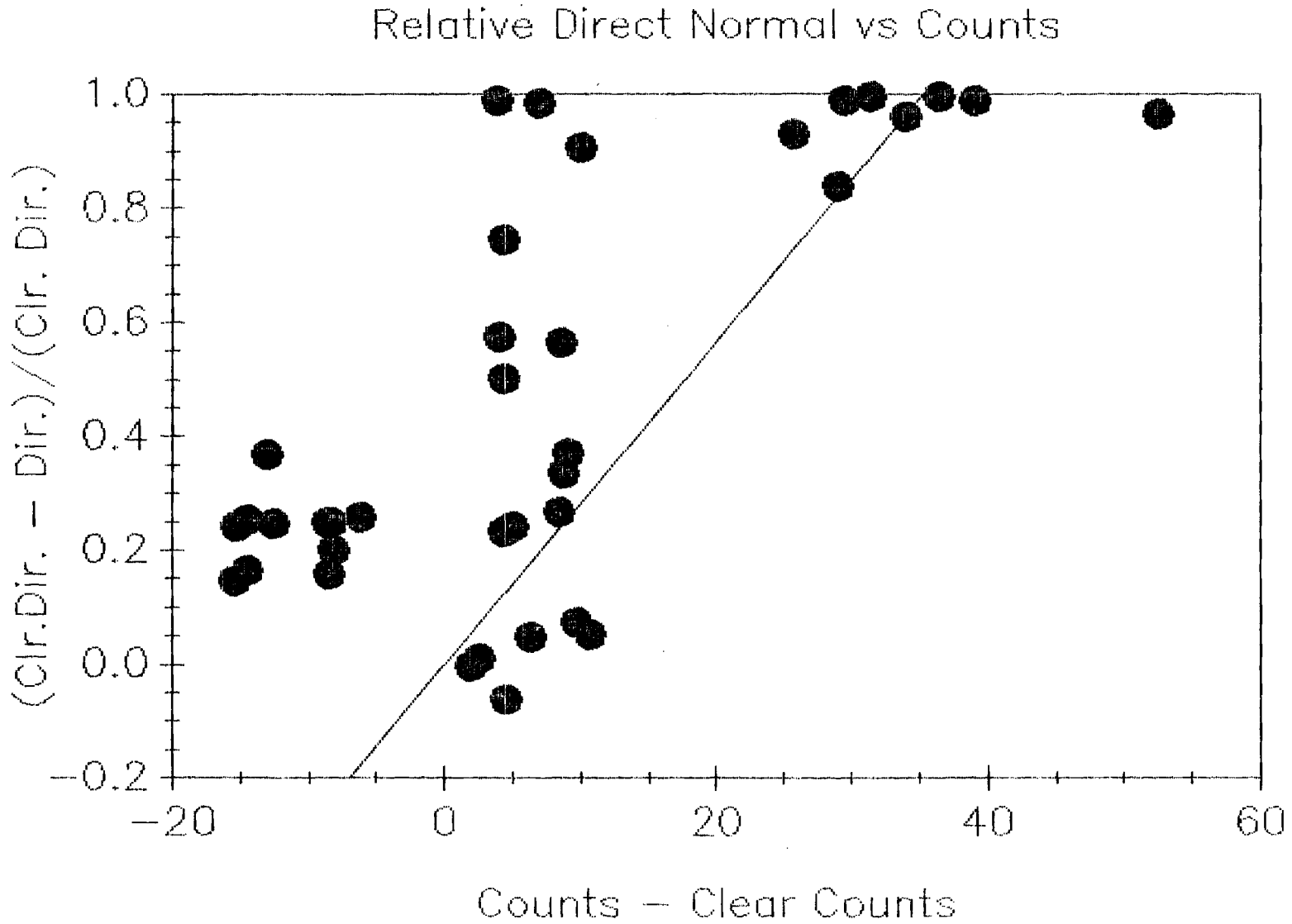


Figure 4 - Observed hourly direct normal irradiance, relative to clear direct, versus the observed METEOSAT radiance counts, relative to the counts expected under cloud-free conditions.

Global Horizontal, Day 348, 1982

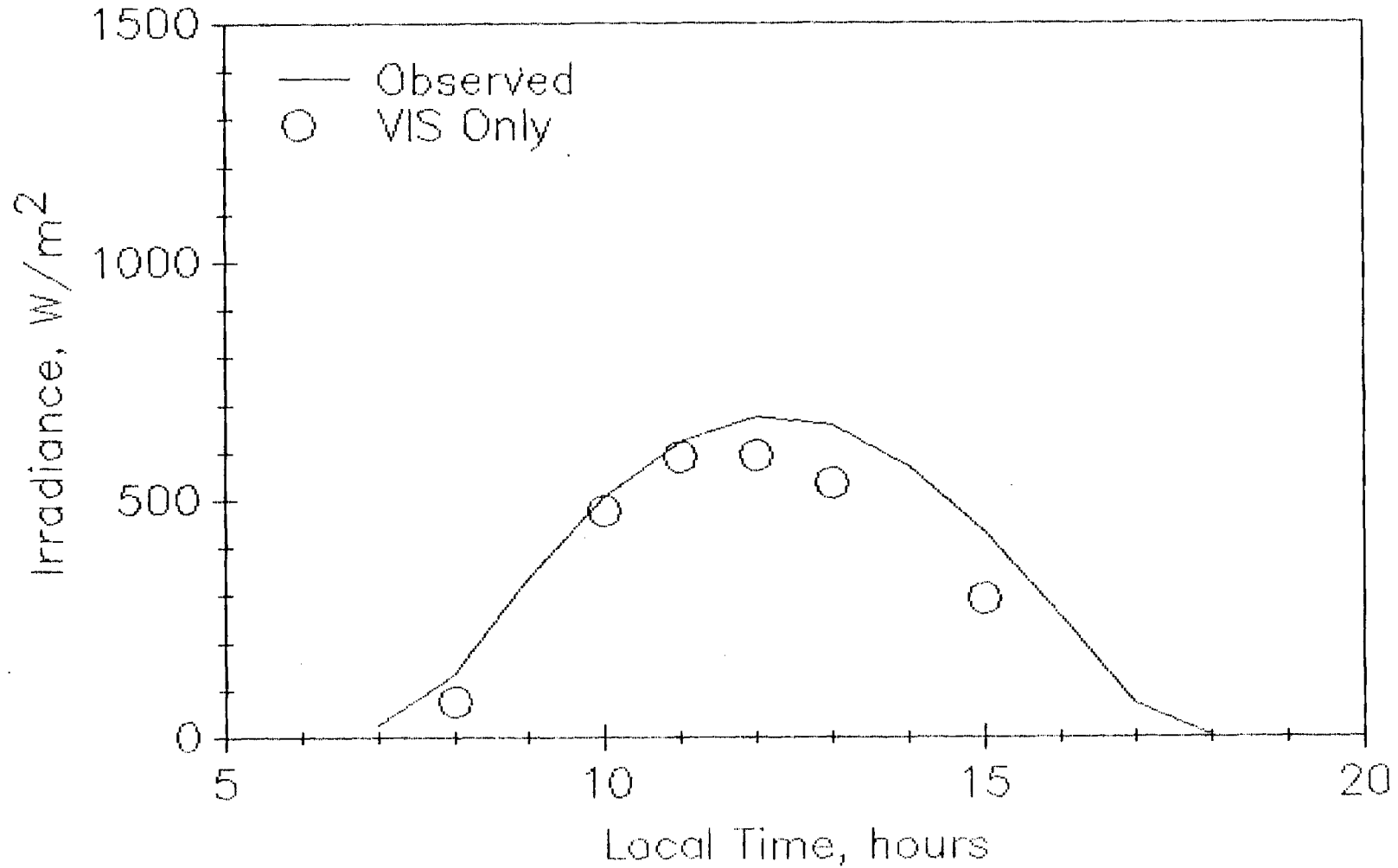


Figure 5 - Time series plot of hourly satellite-estimated global horizontal irradiance compared with observed values, for Day 348, 1982, using the VIS-only technique.

Direct Normal, Day 348, 1982

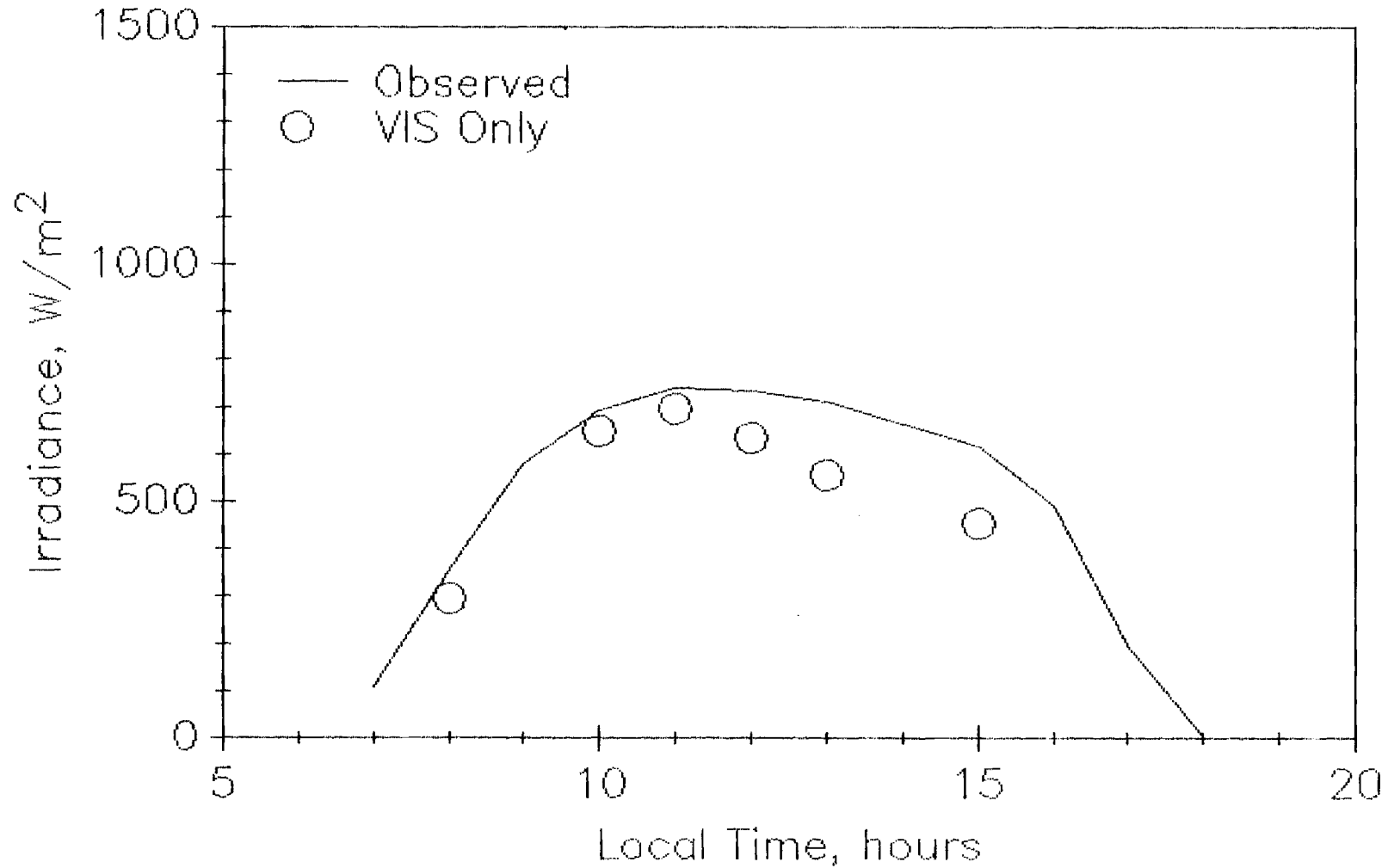


Figure 6 - Time series plot of hourly satellite-estimated direct normal irradiance compared with observed values, for Day 348, 1982, using the VIS-only technique.

Global Horizontal, Day 53, 1982

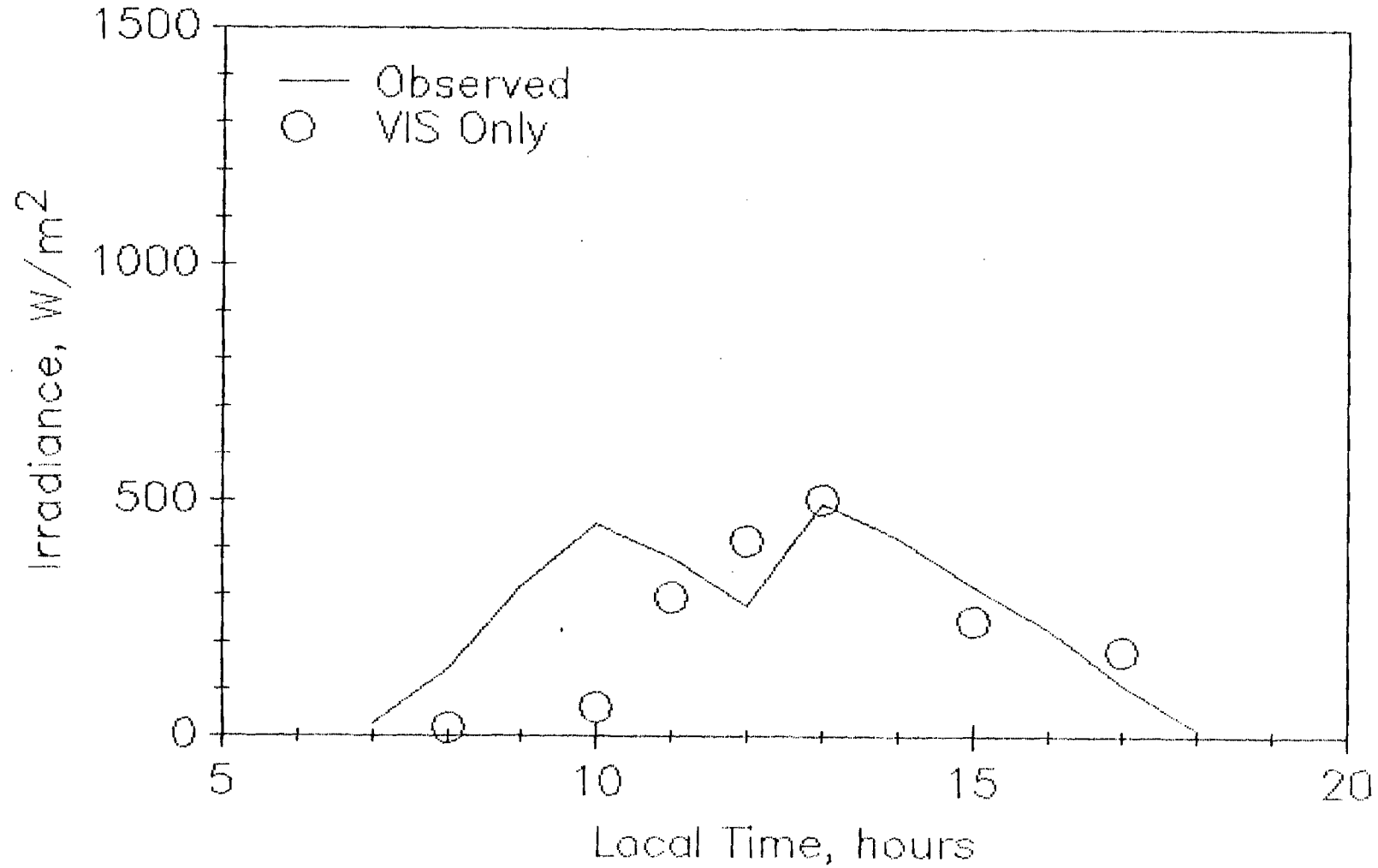


Figure 7 - Time series plot of hourly satellite-estimated global horizontal irradiance compared with observed values, for Day 53, 1982, using the VIS-only technique.

Direct Normal, Day 53, 1982

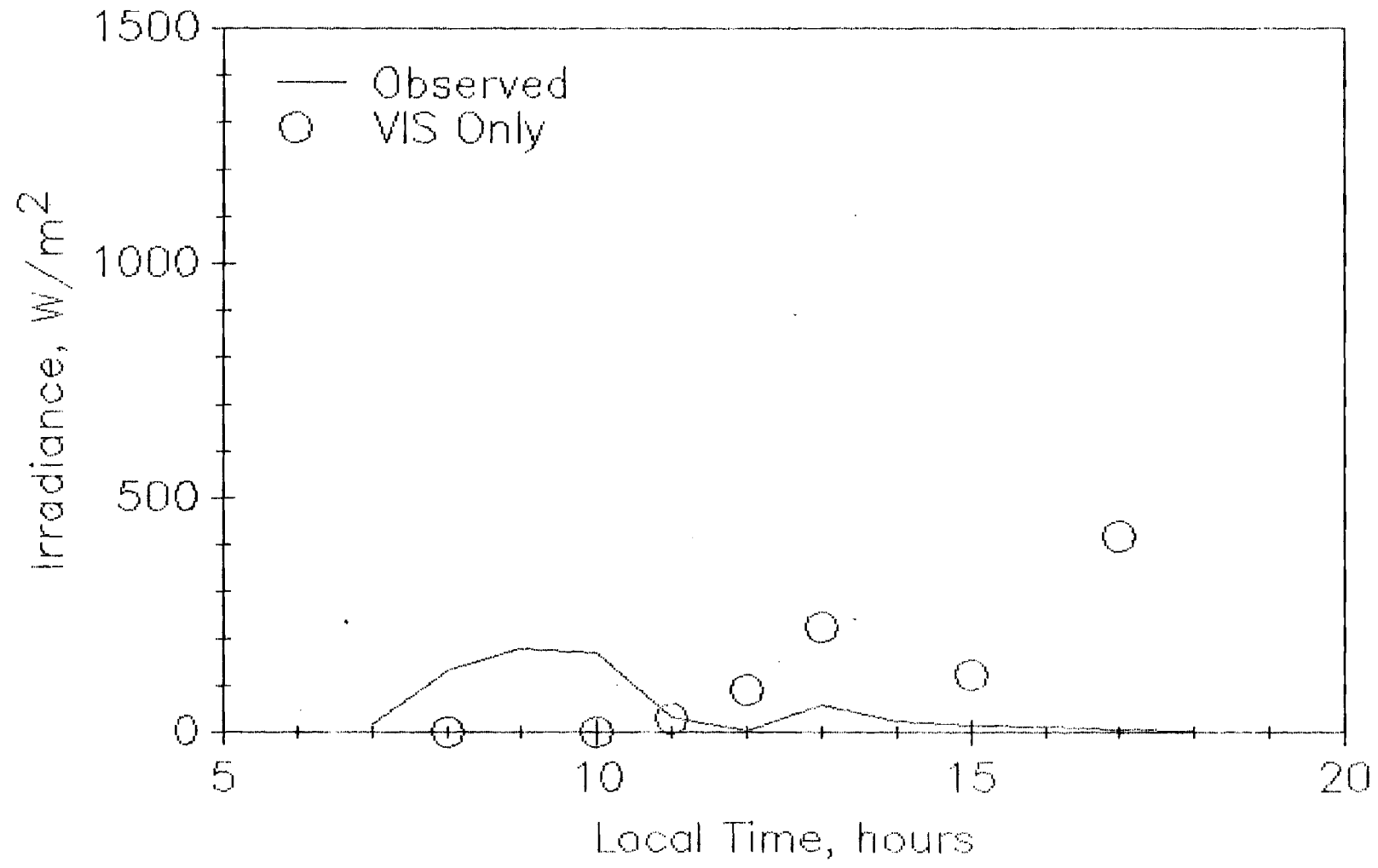


Figure 8 - Time series plot of hourly satellite-estimated direct normal irradiance compared with observed values, for Day 53, 1982, using the VIS-only technique.

Global Horizontal, Day 105, 1984

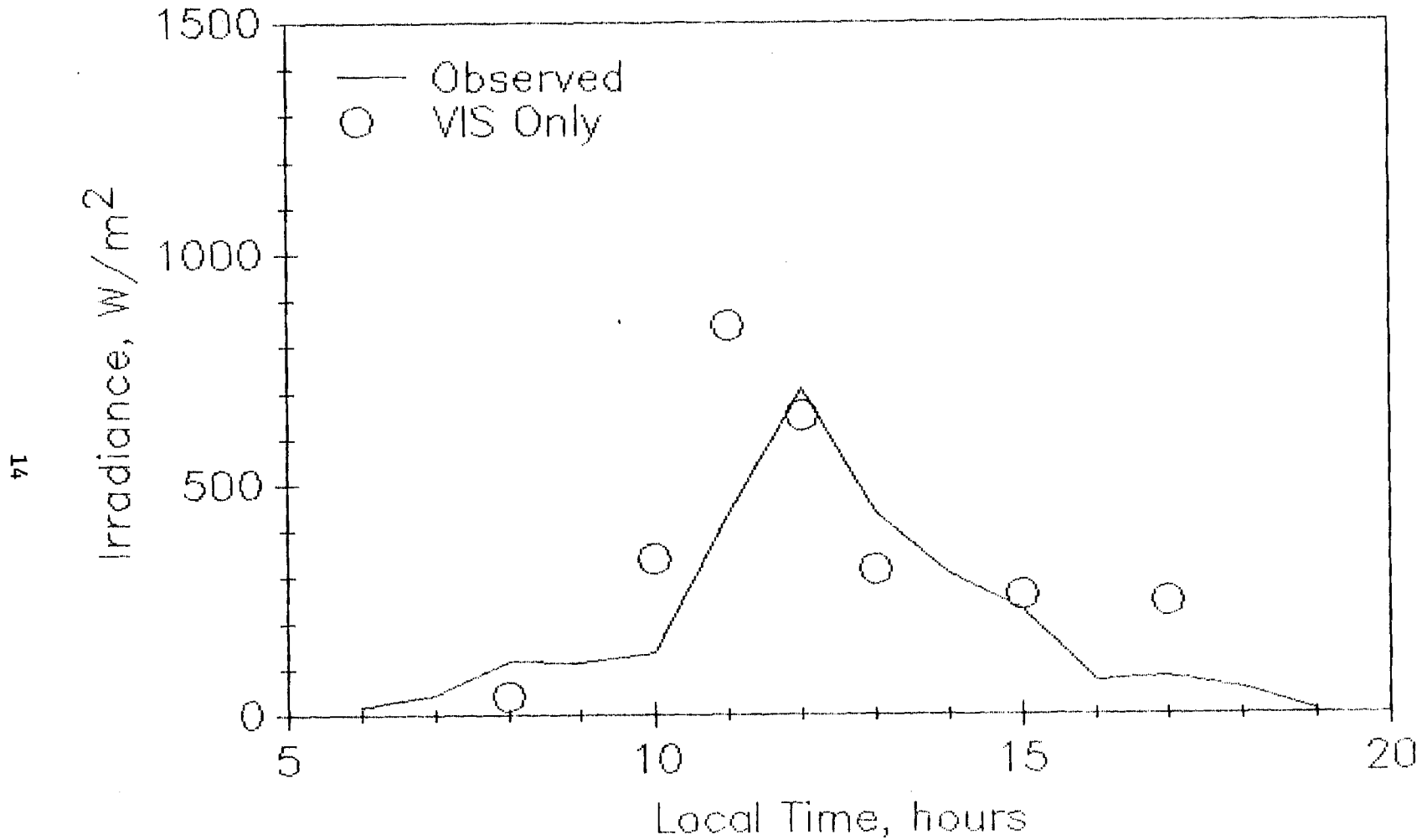


Figure 9 - Time series plot of hourly satellite-estimated global horizontal irradiance compared with observed values, for Day 105, 1984, using the VIS-only technique.

Direct Normal, Day 105, 1984

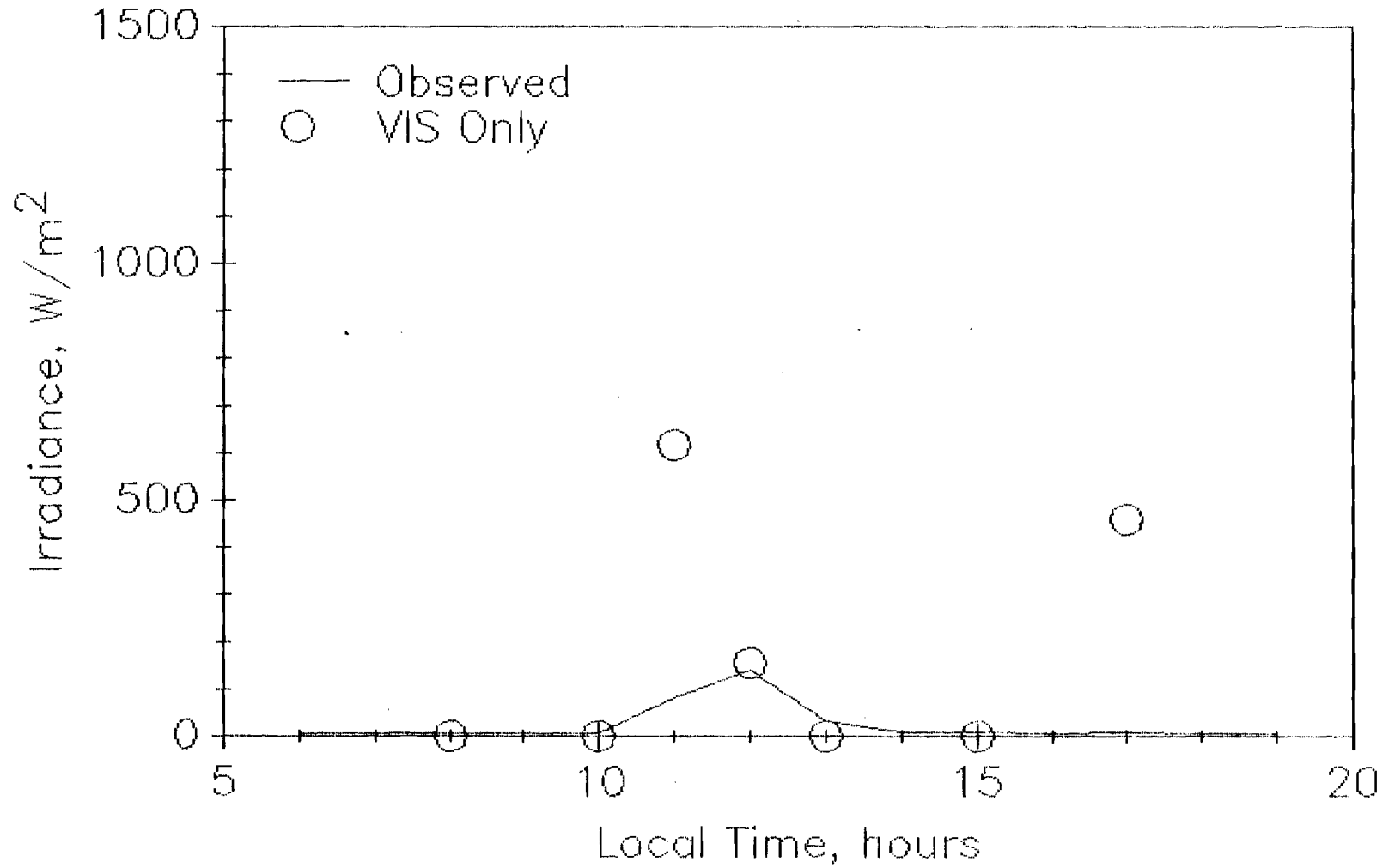


Figure 10 - Time series plot of hourly satellite-estimated direct normal irradiance compared with observed values, for Day 105, 1984, using the VIS-only technique.

Global Horizontal, Day 167, 1982

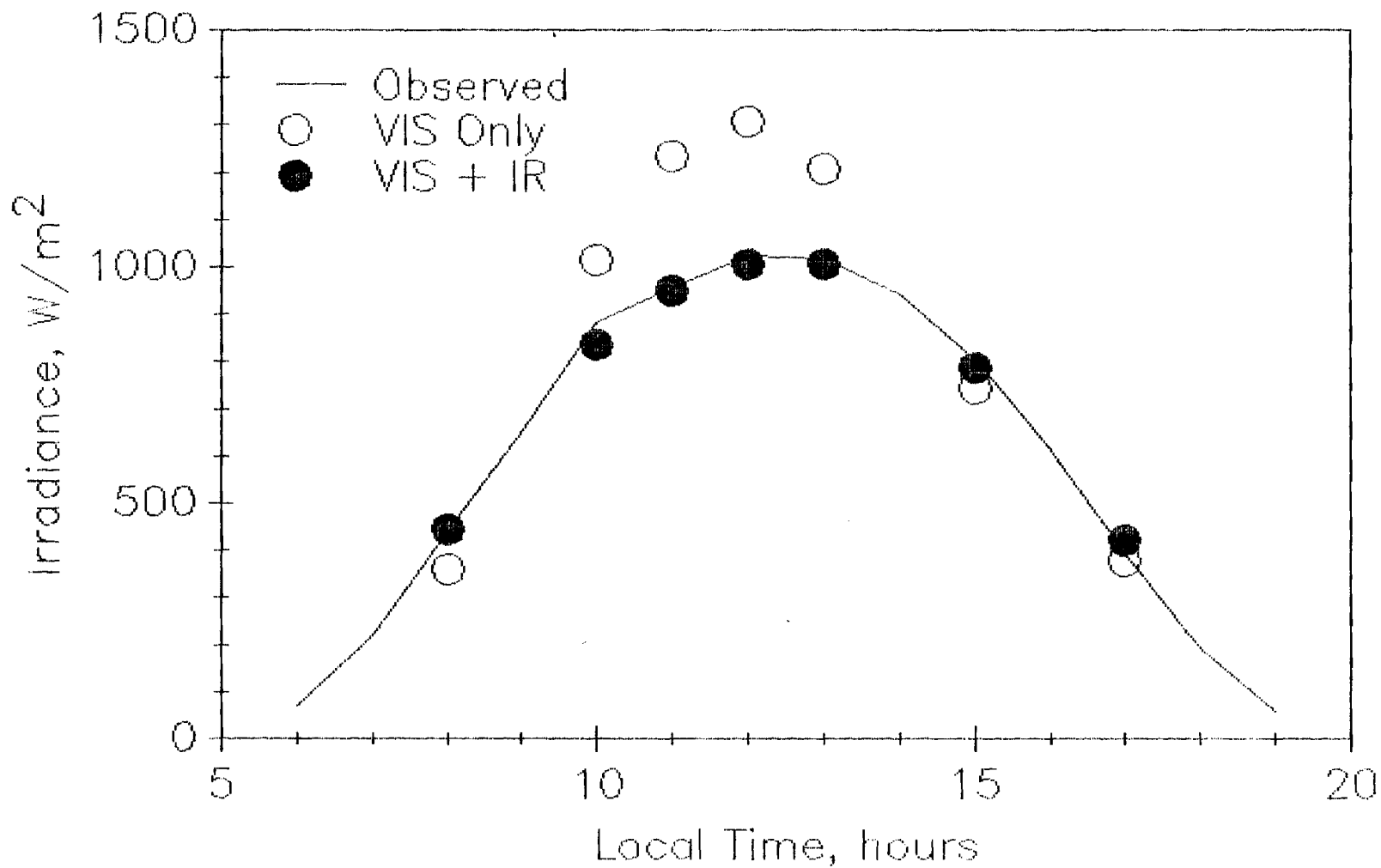


Figure 11 - Time series plot of hourly satellite-estimated global horizontal irradiance compared with observed values, for Day 167, 1982, using the VIS-only and the VIS+IR techniques.

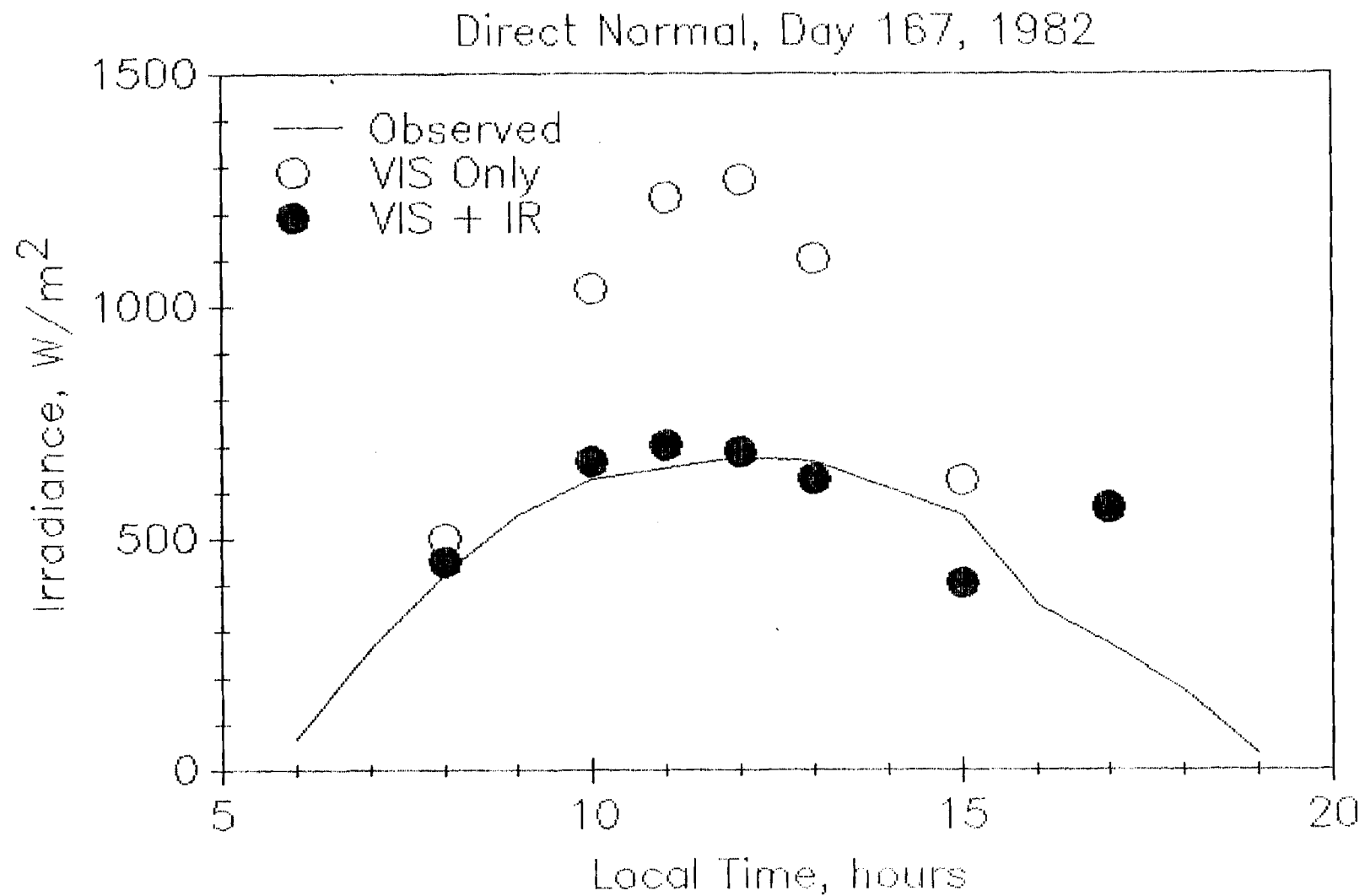


Figure 12 - Time series plot of hourly satellite-estimated direct normal irradiance compared with observed values, for Day 167, 1982, using the VIS-only and the VIS+IR techniques.

Global Horizontal, Day 167, 1983

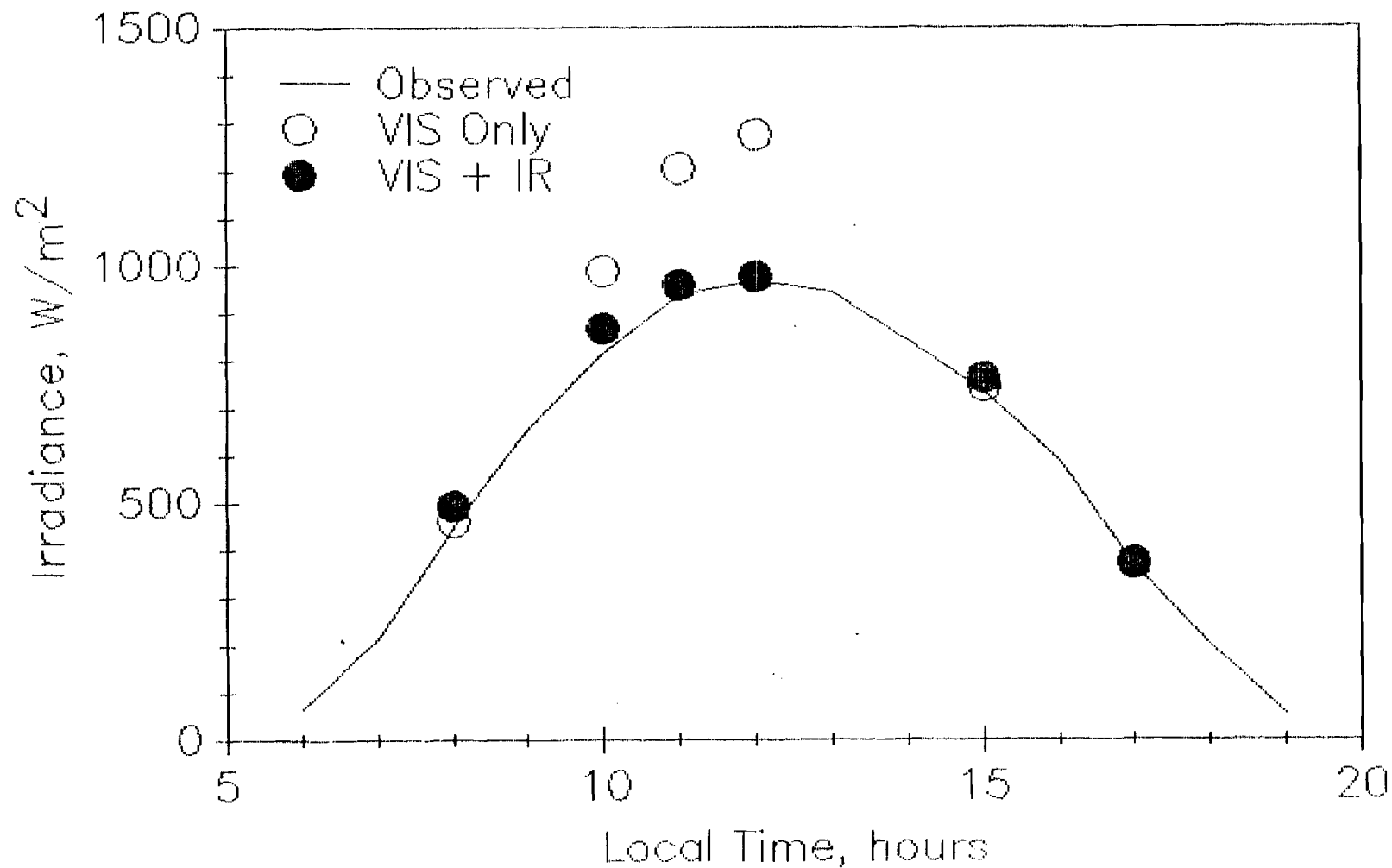


Figure 13 - Time series plot of hourly satellite-estimated global horizontal irradiance compared with observed values, for Day 167, 1983, using the VIS-only and the VIS+IR techniques.

Direct Normal, Day 167, 1983

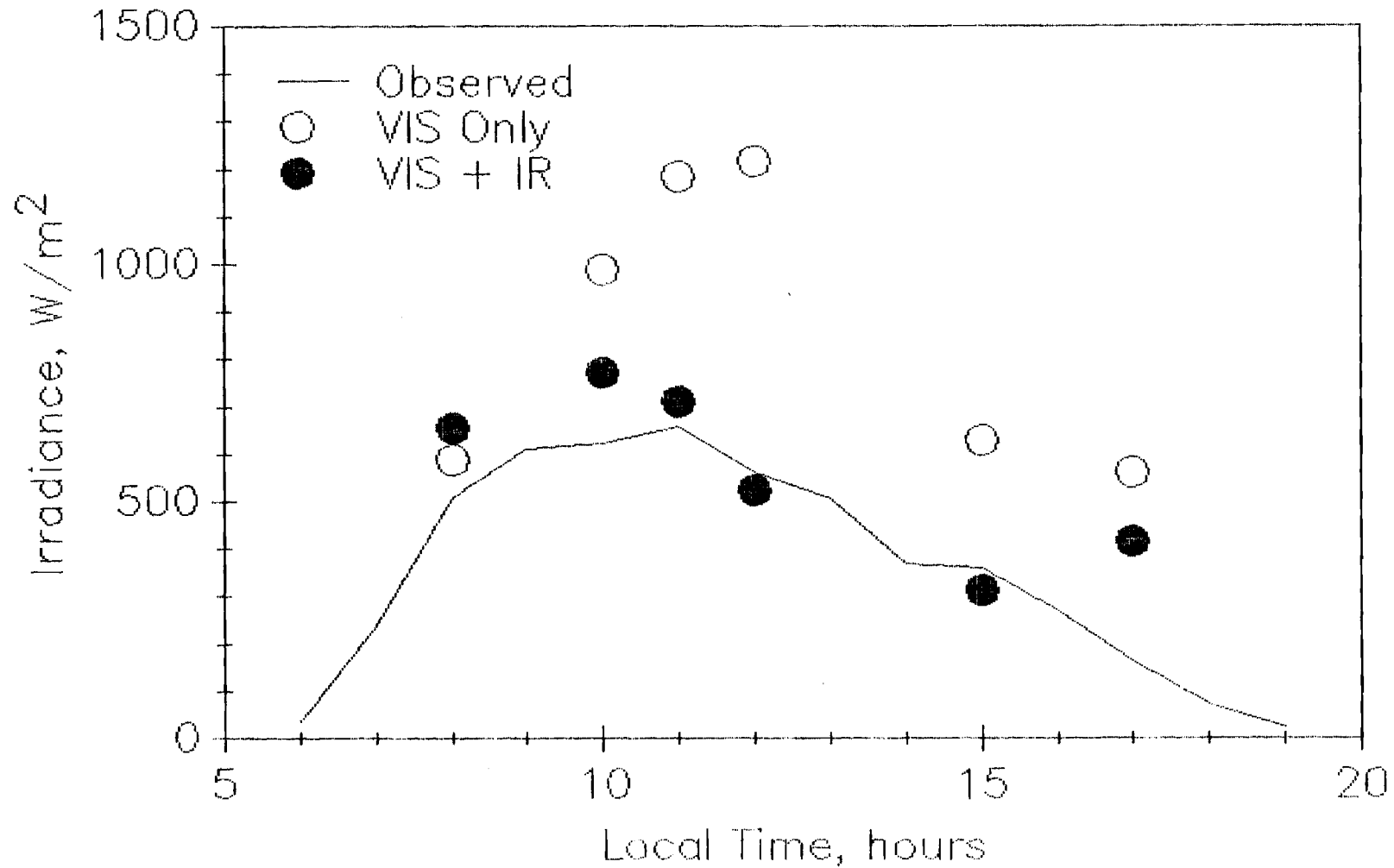


Figure 14 - Time series plot of hourly satellite-estimated direct normal irradiance compared with observed values, for Day 167, 1983, using the VIS-only and the VIS+IR techniques.

Global Horizontal, Day 167, 1984

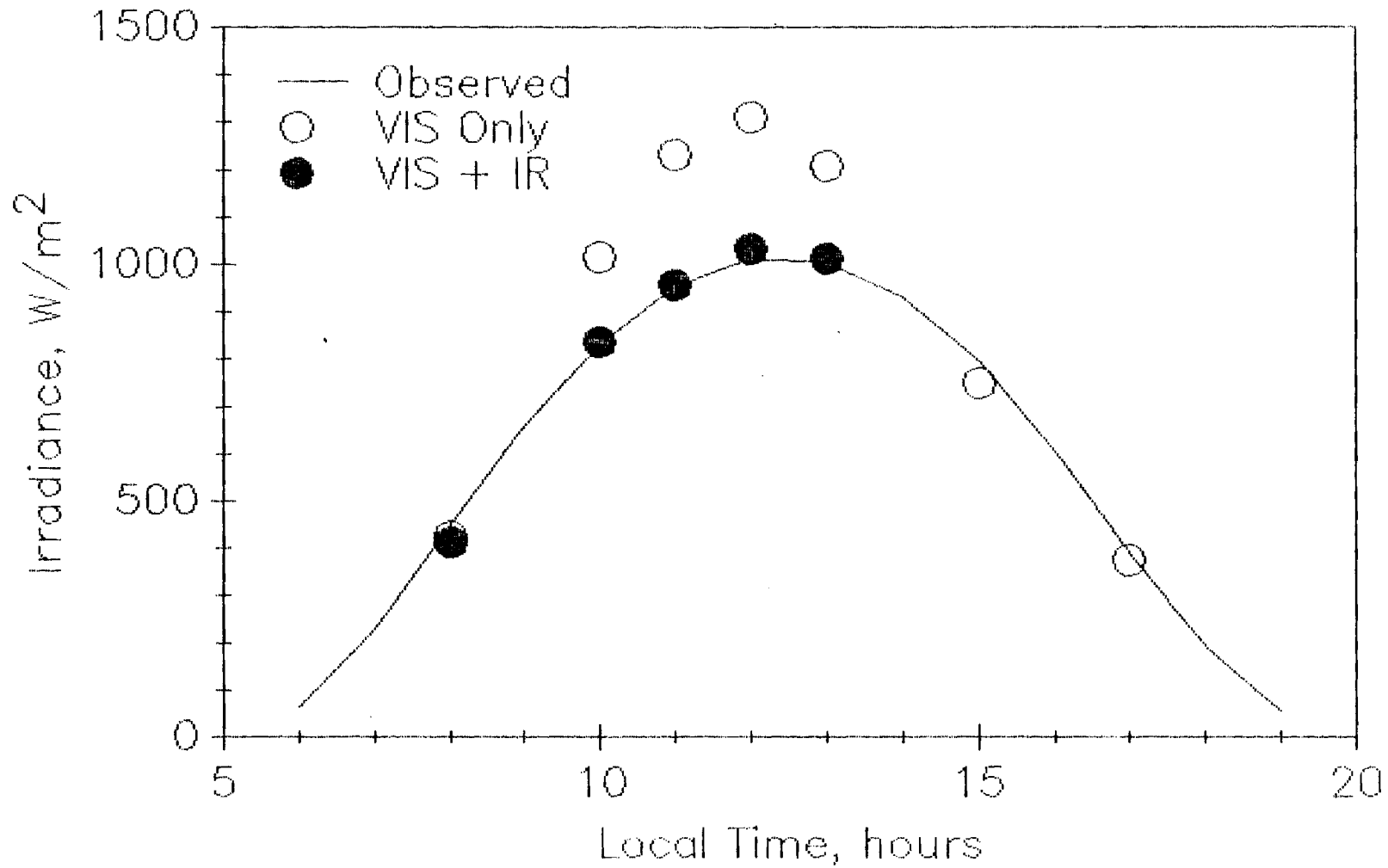


Figure 15 - Time series plot of hourly satellite-estimated global horizontal irradiance compared with observed values, for Day 167, 1984, using the VIS-only and the VIS+IR techniques.

Direct Normal, Day 167, 1984

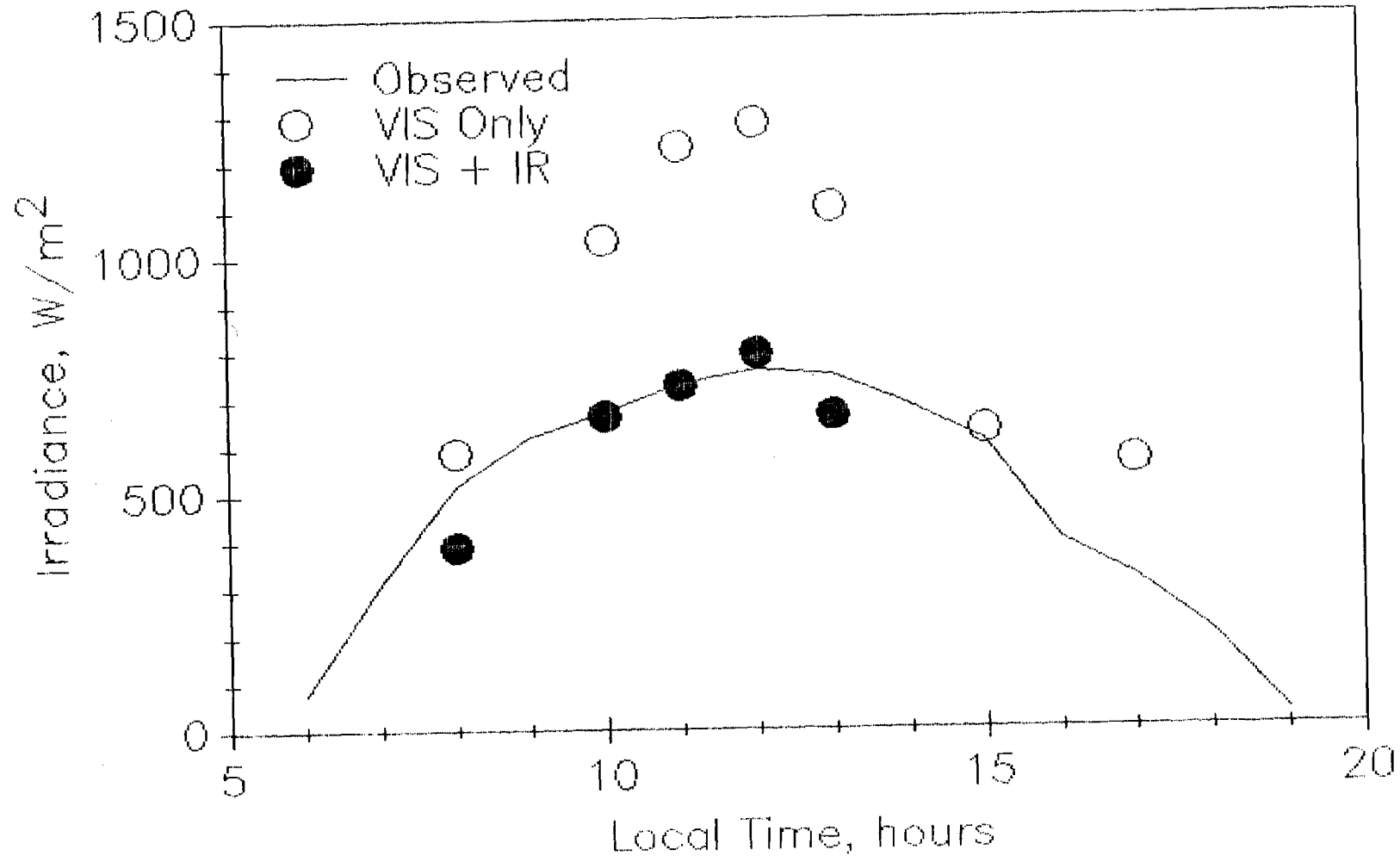


Figure 16 - Time series plot of hourly satellite-estimated direct normal irradiance compared with observed values, for Day 167, 1984, using the VIS-only and the VIS+IR techniques.